INSTITUTE FOR DEFENSE ANALYSES

Manufacturing for Quantum Systems

(Presentation)

Jessica G. Swallow
Lance G. Joneckis

December 2020

Approved for public release;
distribution is unlimited.

IDA Document NS D-20438

Log: H 20-000457

INSTITUTE FOR DEFENSE ANALYSES
4850 Mark Center Drive
Alexandria, Virginia 22311-1882

About This Publication

This work was conducted by the Institute for Defense Analyses Central Research Program, Project C2258 "Manufacturing Challenges for Quantum Sensing." The views, opinions, and findings should not be construed as representing the official position of either the Department of Defense or the sponsoring organization.

For More Information

Jessica G. Swallow, Project Leader
jswallow@ida.org, 703-845-2490

Leonard J. Buckley, Director, Science and Technology Division
lbuckley@ida.org, 703-578-2800

Copyright Notice

Executive Summary

Background

The U.S. Department of Defense (DoD) lists quantum science among its 11 modernization priorities for research and development. Quantum science includes the use of controllable quantum systems (e.g., cold atoms, solid-state color centers) to sense, communicate, and process information. Of these three functions, quantum sensing is the nearest term application for quantum science, some types of quantum sensors being already commercially available. The DoD desires novel and improved quantum sensors for applications such as position, navigation, and timing; miniaturized high-contrast field sensing; and wideband, small-scale antennas. Solid-state devices are of particular interest because of their potential to be compact, robust to extreme environmental conditions, and low maintenance. However, manufacturing and fabrication challenges have limited the reliable production of high-performance solid-state quantum sensors at scale. Quantum information processing (QIP) is still in a very early stage of development, but of critical interest to DoD because of its potential disruptive impact. Manufacturing challenges will only be exacerbated when attempting to fabricate QIP systems that may need millions of controllable quantum bits (qubits) integrated with supporting technologies.

Objective

This central research project had three goals:

- Understand manufacturing and fabrication challenges, including for supporting technologies, that limit the performance of a few representative quantum systems of interest to DoD.
- Link manufacturing approaches to potential manufacturing yield and reliability characteristics.
- Identify areas for DoD-supported research in quantum manufacturing.

Quantum sensing and QIP rely on many of the same technologies and materials, including the substrate containing the controllable quantum system of interest, and the technologies used to control, isolate, and interact with that system, such as photonics, lasers, and vacuum pumps. This work aims to identify research areas that will not only have an impact on the manufacturability of quantum sensors today but also increase the viability of scaled-up quantum computing in the future. Doing so helps the DoD focus resources, accelerate the development of quantum technology, and connect quantum technology to DoD applications and capabilities of interest.

Representative Systems

We limited our scope to a few representative examples from a variety of possible quantum-sensing and -computing platforms. Representative systems were selected based on potential value for the DoD-relevant sensing application of position, navigation, and timing or for overlap with potential scaled-up QIP. Specifically, we focused our analysis on atom chips, nitrogen vacancy (NV) color centers in diamond, and entanglable phosphorus dopants in silicon. Both atom-chip and NV-center technologies have a path to transition into tactical gyroscopes, if enabled by improvements in manufacturing, either by miniaturizing and integrating supporting systems (for atom chips) or by improving sensitivity at lower cost (for NV). NV-center technologies have also been proposed as single-photon sources and as a type of qubit for QIP. Entangled phosphorus dopants in silicon would be mainly intended for QIP rather than sensing. Second-generation QIP platforms (NV-centers, P-doped Si) show advantages for scalability compared with today's most advanced first-generation QIP platforms (superconducting qubits and trapped ions), in particular the potential for high density and integration with other supporting technologies such as photonics or Si electronics.

In general, it is easier to fabricate quantum sensors than quantum computers, because of the lower scale of integration for the quantum systems and because quantum sensors take advantage of the isolation of the quantum system, while quantum computers need more direct interaction among a large number of distinct controlled quantum systems. But both sets of applications rely on the same supporting technologies, such as lasers, photonics, vacuum systems, and cryogenics. Therefore, improvements in manufacturing of quantum sensors are expected to have secondary benefits for QIP.

Results

Our discussion is guided by several general concepts for manufacturing, including that it is beneficial to keep the number of fabrication steps low (flow consolidation), that techniques developed for one material may not easily transfer to another, that parallelization saves time and cost, that thoughtful in-line testing improves device yield and saves resources, and that upstream steps limit downstream options.

Focusing first on atom chips, where the goal is miniaturization and integration of supporting systems (e.g., optics, vacuum), several critical manufacturing challenges need to be addressed. These include 3D magneto-optical trap fabrication and integration of ferromagnetic materials, laser sources, and vacuum pumps. These challenges require innovation in the fabrication of multi-material chips. Such innovation may include novel or improved methods of wafer bonding, layer lift-off, layer transfer, and high-aspect-ratio etching, as well as via fabrication. Furthermore, investment into lithography, etching, and material-growth methods for non-Si substrates, particularly those that can also accommodate photonic structures, would enable integration of laser, vacuum, and sensing systems into atom chips. Using the example of atom chips, we conducted a first-order quantitative analysis of expected cost-yield tradeoffs, showing that heterogeneous integration has clear advantages over monolithic fabrication approaches.

Moving on to NV-centers, where the goal is lower cost and increased sensitivity, we note that NV-centers are a workhorse example of a solid-state quantum-sensing system that can operate at room temperature. Fabrication methods that are effective for NV are likely to be applicable to other types of color centers as well. Improving the sensitivity of NV-based sensors relies on a few characteristic fabrication challenges, including improving the purity (isotopic and chemical) and crystalline quality of the diamond substrate to reduce noise and increasing the density of NV-centers and/or improving the efficiency of photon collection to improve signal strength. It is challenging to balance the desire for increased NV density against the need to minimize crystal strain and impurity concentrations. Chemical vapor deposition (CVD), ion implantation, laser irradiation and annealing, geometrically constrained heteroepitaxy, and lift-off and transfer processes are all of interest for fabricating these systems. Lift-off and transfer, in particular, is attractive because it allows for reuse of the expensive bulk diamond substrate for CVD growth while enabling heterogeneous integration with other substrates that may be preferred over diamond for certain system components (e.g., photonic structures).

Because NV-centers are of interest for QIP as well as quantum sensing, and because integrating photonics with NV can be a component of either application, we also investigated methods of precise NV placement alongside photonic structures such as waveguides. The most interesting method identified was femtosecond-laser fabrication, a flexible technique that can fabricate 3D structures in diamond, including precise placement (to within 50 nm) of NV and direct fabrication of waveguides. This technique and a method of precision dopant placement in Si (hydrogen depassivation lithography) were used as examples from which to construct a model of yield tradeoffs for different types of direct-write qubit fabrication. This model illustrates several important considerations, in particular, the importance of very high yields for individual write steps (and metrology to confirm qubit formation) and the influence of annealing steps on placement precision.

From this analysis, we derive key comparisons between manufacturing for sensing and computing. For quantum sensing, less precision in the placement of controllable quantum systems may be tolerable, which allows for higher temperature downstream fabrication steps including annealing. Because quantum sensors are more likely to be fabricated at lower scales of integration, they can also be manufactured more slowly, meaning that direct-write methods may be tolerable. Sensors can also use post-fabrication calibration to accommodate placement uncertainty. In contrast, for QIP, the scale of manufacturing complexity is greater and the precision required is higher. Therefore, QIP requires manufacturing methods that are both *more precise* and *faster* than the ones used for manufacturing sensors. However, both applications rely on much of the same supporting technology, using similar substrates (e.g., diamond, Si, aluminum nitride, etc.) and similar methods to connect (e.g., using photonics or wiring), control (e.g., using photonics or CMOS), and isolate (e.g., using cryogenics) qubits. Therefore, advancements made in the manufacturing of quantum sensors (e.g., methods of heterogeneous integration, increased manufacturing speed or yield, increased substrate purity, etc.) are likely to benefit the application of QIP.

Finally, we consider scale-up for solid state QIP. Potential research that could increase the speed of fabricating dense arrays of quantum systems includes multiplexing of femtosecond-laser fabrication and hydrogen depassivation lithography, use of advanced optical lithography coupled to directed assembly for placing qubits, and application of nanoimprint lithography to quantum-system component fabrication.

Heterogeneous integration is a second area that must be developed further for quantum science, having applications for both quantum sensing and QIP. With heterogeneous integration, individual components optimized for particular functions can be combined to achieve a more successful system than would be possible through a monolithic approach. Furthermore, heterogeneous integration methods enable tiled approaches to qubit integration, which can help overcome yield problems that are currently common with solid-state qubit fabrication methods.

Conclusion and Outlook

Our findings indicate that the sweet spot for quantum sensing and eventually quantum-information processing is manufacturing that has very low fixed costs and that achieves high yields at relatively low throughput. Manufacturing throughput is not as important for quantum systems as it is to today's integrated circuit industry, because of the lack of demand at scale. Therefore, manufacturers of quantum systems should try to capitalize on less expensive manufacturing methods or equipment that can be used for multiple purposes. Similarly, heterogeneous integration will be an important strategy for manufacturing QIP systems. Because demand for these devices is likely to remain limited, the key to lowering their cost will be to capitalize on those technologies that have been developed and optimized for each component of the system, rather than seeking a specialized monolithic approach.

We recommend several areas for further research, including advanced processing with non-silicon substrates; in-line measurement, monitoring, and testing tools for photonic and quantum circuits and elements; approaches to enable heterogeneous integration (e.g., lift-off and layer transfer, wafer bonding, high-temperature superconducting single photon detectors); methods to decrease reliance on direct-write approaches; and adaptation of fabrication approaches with multifunctional potential. We also note the need for increased reporting of manufacturing-relevant parameters in literature, such as defect types, distributions, and effects on functional structures, as well as speed and yield. We hope that advancements in manufacturing and fabrication of quantum sensors and their supporting technologies will not only advance these technologies towards commercial availability but also support future scale-up of solid-state quantum-computing architectures.

Contents

Manufacturing for Quantum Systems

Jessica Swallow
Lance Joneckis

IDA 1

Central Research Project Focus

- Understand the manufacturing and fabrication challenges that limit the performance of quantum systems of interest to DoD, particularly quantum sensors, *by focusing on a few representative systems.*
- Link manufacturing and fabrication technologies, including for supporting technologies, to performance outcomes in devices.
- Map manufacturing/fabrication methods, including for supporting technologies, to critical manufacturing parameters (yield, reliability, etc.).
- Identify areas for further DoD-supported research.

This Central Research Project (CRP) is aimed at understanding manufacturing and fabrication challenges for quantum systems, in particular quantum sensors of interest to DoD, and identifying paths for further research and development that will benefit DoD in this space. This study is motivated by the recent interest by the United States and others in investing in quantum technology and quantum research. For example, in 2019 the Defense Science Board released a report stating that the DoD must vigorously pursue quantum technology having particular military potential, and it identified quantum sensing as the nearest term technology of interest.

In this CRP we have a few main goals. First, we seek to understand the manufacturing and fabrication challenges that limit the performance of quantum systems of interest to DoD, particularly quantum sensors, by focusing on a few example systems. We sought to connect challenges and performance issues associated with manufacturing and fabrication technologies, including supporting technologies that are outside the quantum sensor itself (i.e., the "physics package") to performance outcomes in devices. Next, we sought to map manufacturing and fabrication methods being used today at the research scale to their potential critical manufacturing parameters, such as yield and reliability. Finally, we sought to identify areas for further research supported by DoD. To date, most of the research in quantum science has focused on performance challenges. Research into manufacturing and production challenges is equally important for select prototype systems when they are candidates for advance capabilities.

Why Manufacturing Matters: Photovoltaics

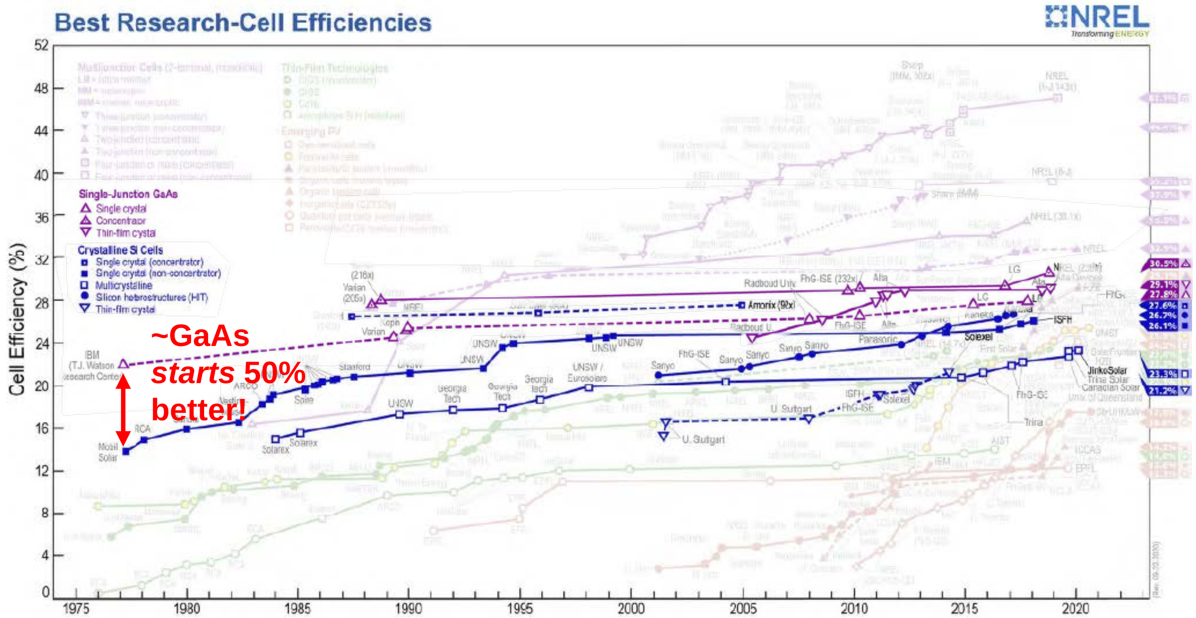

https://www.nrel.gov/pv/cell-efficiency.html

Si modules can be manufactured less expensively than other options with comparable or better efficiency; as a result, Si modules dominate the commercial market despite their material disadvantages.

IDA | 3

We begin our analysis of manufacturing considerations for quantum systems with an example pulled from the area of photovoltaics (PV).

This is the National Renewable Energy Laboratory (NREL) Chart of best research-cell efficiencies for photovoltaics, which shows the best efficiencies established by various types of solar cells as a function of time based on a rigorous, well-defined set of tests established by NREL. This chart is updated continually and can be found at https://www.nrel.gov/pv/cell-efficiency.html.

Looking closely at this chart, we see that Si-based solar cells (those shown in blue) are *not* the best performing cells. In fact, Si is an odd choice of feedstock material for a semiconductor solar cell—it has an indirect bandgap, which means that it is naturally inefficient at converting light into electricity, at least relative to direct-bandgap materials like GaAs.

During the early days of photovoltaic research, it was quickly discovered that GaAs had much better inherent photovoltaic conversion efficiency than Si. But unlike Si, GaAs did not have a strong industry surrounding its purification, single-crystal growth, interface and surface engineering, and patterning. So, in 40 years of research, GaAs-based solar cells improved from about 22% efficiency to about 28% efficiency (only a 25% improvement in performance), while Si solar cells, which benefit from a thriving microelectronics industry, have seen performance gains from an underwhelming start of 14% efficiency to today's performance of about 26% efficiency—almost a factor of 2. *But they are still not better than GaAs*. Even so, Si solar cells dominate the global market for photovoltaics, as shown on the next slide.

Meanwhile, competing technologies based on thin crystalline films, organic photovoltaics, and other concepts continue to be researched. But, with the exception of CdTe, none of these have made a substantial inroad to the global PV market, despite some rapid performance gains and other interesting advantages (e.g., light weight, flexibility, inexpensive starting materials). Note that many of the "emerging PV" and thin-film technologies also benefited from the microelectronics industry, if indirectly, by using methods of film growth, deposition, or patterning that were initially developed in that industry or by forming hybrid "tandem" solutions with Si.

Solar Cells: Why Does Si Predominate?

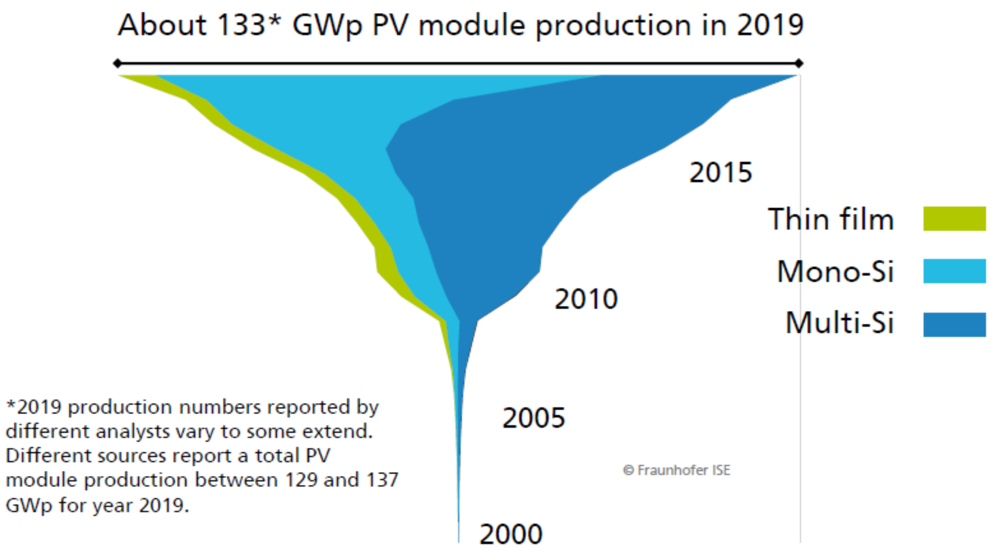

Source: Photovoltaics Report, Fraunhofer Institute for Solar Energy Systems, ISE, June 23, 2020.

Preexistent manufacturing and fabrication technologies matter!

IDA | 4

This figure shows the share of global PV module production occupied by thin-film, single-crystal Si, and polycrystalline Si, from 2000 to 2019. The two forms of Si dominate this market compared to thin film solar cells.

This story illustrates the importance of manufacturing and fabrication in the commercial success of novel technologies. A higher performing system from a physical standpoint may not be the option that wins in the commercial market because it may be too expensive to manufacture, too difficult to scale, or use source materials that are too rare or difficult to purify. Also, if an alternative technology benefits from a thriving supporting industry (i.e., if it relies on a dual-use manufacturing technology), then it can be very difficult for new, less established material systems to penetrate the market, even if they have interesting advantages that distinguish them. Those technologies may be forced to seek out niche markets (such as the defense industry) that place a different value on features like weight, flexibility, and ruggedization.

In this briefing, we discuss manufacturing and fabrication technologies for quantum systems, with a particular focus on quantum sensing. These technologies have some things in common with photovoltaics (indeed, some photovoltaics use "quantum dots," an example of a quantum sensor), but they are not subject to the same constraints and performance goals that the photovoltaic industry sees. Differences include the following:

- Demand scale / Target market
- Performance goals
- Diversity of applications

We will see that Si plays a role in quantum sensors as it does in the photovoltaics world. We will also see that the advantages of Si are diminished in the face of the lower demand for quantum sensors and the niche associated markets, but not necessarily in the context of larger scale integration associated with quantum computing.

Non-market Considerations and Production Volumes in DoD

Light Interferometric Gravitational Observatory

Nuclear Weapons

Chip-scale atomic clock

Examples:
- Manhattan Project for nuclear weapons
- Quantum computing for cryptanalysis, in principle

Unique capabilities for science, proof of concept, or knowledge generation—manufacturing is not a consideration.

Examples:
- Nuclear weapons as a deterrent
- Missile defense
- **Quantum computing** for quantum simulation and applied cryptanalysis

Unique capabilities w/ small volume production—DoD must subsidize development—limited manufacturing consideration.

Examples:
- LIDAR (possible adoption in self-driving cars)
- **PNT technologies** (e.g., for GPS-denied environments)

Non-unique capability with larger volume (though small compared to commercial) demand, cost-sensitive to manufacturing because of competing technologies.

Manufacturing research needed

Singular production & unique capability

Higher production volumes & competing technologies

Manufacturing considerations must balance the uniqueness of a capability and the needed production volume.

IDA | 5

While the DoD has a strong desire to use commercial technologies when possible, it is often the uniqueness of a capability and its role in the DoD that may be more important to producibility than such large-scale issues of manufacturability discussed previously. This can be broken down into three reasonably distinct areas:

1. Systems that offer a unique capability not achievable with conventional technologies, where the emphasis is on either proving that such systems are in fact technologically possible or that the demand is for only one system.
2. Systems that offer a unique capability where low-volume producibility is acceptable.
3. Systems with larger demand where a new technology offers a distinct benefit over conventional technologies.

Systems in the first class are often about pushing emerging technologies to their limits with minimal considerations about producing more than one system. Often these are used to demonstrate that such systems are possible or because there simply isn't demand for more than a very small fixed number. Many big-science projects fall into this category, such as the light interferometric gravitational observatory (LIGO) project. Quantum computing in general—and specifically its potential use for cryptanalysis—also falls into this category, mostly because we are unsure of the scalability of quantum computing and its ability to have an advantage for computational problems of interest.

Systems in the second class are mostly defined by the need for a small number of such systems where there is no practical alternative to the capability they provide. Here, issues of manufacturability and research into manufacturability are critical to cost effectively producing the number of system needed. The best example of this is the production of nuclear weapons used as a deterrent, where a much larger number of weapons are needed than were needed for the Manhattan project. Quantum computing also falls into this class for applications such as quantum simulation and possibly future cryptanalysis if the promise of the technology is proven. Quantum sensors used in strategic applications can also fall into this class, though these will likely be limited to the highest performing sensors.

Systems in the third class are those where there are viable alternatives based on conventional technologies, but the new technology offers a distinct advantage. These also tend to be cost-sensitive applications, especially when the novel technology is a subsystem and therefore the cost of the subsystem is relative to the cost of the system. These technologies are also well positioned to break out from their niche applications and become commercial products. If LIDAR breaks out from a niche role and becomes standard on self-driving cars and robotic platforms, then its production cost will fall precipitously. This will largely be driven by innovation in design and manufacturability, funded by revenue from product sales. A number of position, navigation, and timing (PNT) technologies, especially those used in tactical applications (specifically, timekeeping and rotation- and acceleration-sensing technologies) could also become more mainstream.

This report focuses on the last two classes of applications because these are the applications where issues of manufacturability and specifically the need for manufacturability research are critical to the establishment of the capability in the volumes required.

Outline

- Background on Quantum Information Sciences
  - Gyroscope Case Study
  - Quantum Computing and Manufacturing at Scale
- Manufacturing Considerations for Representative Quantum Systems
  - Atom Chips and Heterogeneous Manufacturing
  - Nitrogen Vacancies in Diamond
  - Phosphorus Dopants in Silicon
  - Case Study: Fabrication Precision and Yield
  - Enabling Scale-Up
- Outlook

Quantum Information Sciences — Quantum Mechanics + Information

- ***Representation*** and ***processing*** of ***information*** via a ***controllable quantum system***

- Systems that can
  - **Sense** — acquire information from the environment via a quantum interaction
  - **Communicate** — move quantum information in space and time
  - **Compute** — process quantum information (includes quantum simulation)

- Quantum systems exploit non-classical properties
  - **Discrete states** — Finite number of states that can be measured
  - **Superposition** — Ability of a quantum system to be in two or more (observable) states at the same time
  - **Entanglement** — Non-classical correlations on measurements of interacting quantum systems

IDA | 7

Quantum information science is a broad field of study that covers the intersection of quantum mechanics and information, particularly the representation and processing of information via a controlled quantum system. Systems encompassed by quantum information include those that can sense via quantum interactions, communicate quantum information through space and time, and compute by processing quantum information. Some of the non-classical properties that quantum systems exploit include discrete states (as opposed to continuous), superposition, and entanglement.

Production Scale for Quantum Systems

- Sensors
  - High-volume applications need low cost
    - ➢ PNT for tactical weapons
  - High (sensitivity, accuracy, and precision) has a cost
    - ➢ Controlling sources of noise
  - Some applications have need for only a small number of units, often with extreme requirements
    - ➢ PNT for ICBMs
  - Golf-ball-sized to refrigerator-sized systems

- Quantum Computing
  - Millions of controlled quantum systems (i.e., qubits)
  - Analog quantum systems—higher manufacturing quality generally means fewer units will be needed
  - Data-center sized systems

This report will focus on a few representative technologies that span a range of applications and scale. A primary role for quantum sensors in the DoD is for position, navigation, and timing (PNT) in GPS-denied environments. This includes navigation and guidance for platforms (e.g., submarines) and weapons (e.g., tactical and strategic missiles). We will also look at quantum computing, with a specific focus on quantum computing approaches offering a computational advantage over classical computation for problems of likely interest to the DoD.

Platforms and weapons can use PNT modules that provide sensing of rotation, acceleration, and timekeeping. Tactical weapons systems are potentially high-volume applications where cost is an issue. Strategic weapon systems are low-volume applications where cost is a secondary issue compared with the primary issues of higher precision and long-term reliability over decades of dormancy.

In general, higher precision systems are more complex and costly, in large part owing to enhanced isolation from noise sources and more extreme techniques for stabilization and measurement protocols. Sensor modules are typically comprised of a few sensors, for example, to sense rotation, which requires a sensor for each axis, and to sense the different modalities. Sensors also have application-specific SWaP requirements. Packaged sensor sizes vary from the size of a golf ball to a refrigerator, depending on the application and sensing modality. As we will see shortly, these sensors have significant components beyond the basic sensor, which include optical sources, detectors, actuators, vacuum pumps, and cooling systems.

Quantum computing is at the opposite extreme with a practical quantum computer being composed of millions of controllable quantum systems (e.g., physical qubits) operating in an analog manner (in contrast to digital operation for classical computation) throughout the duration of the computation. Systems of this size will be housed in the controlled environment of a data center and accessed remotely. It is not clear that the current first-generation approaches of trapped-ion and superconducting qubits will be able to reach this scale. These platforms are a focus of commercial interest, including from IBM, Microsoft, Intel, and Google. Rather than focus on these more mature platforms, we have chosen to focus on novel second-generation quantum computing platforms that show promise for scalability, specifically, phosphorous-doped silicon and NV-centers in diamond.

Quantum Sensors Have Been Around for a While: SQUIDs

- The superconducting quantum interference device (SQUID): an extremely sensitive magnetometer
  - Invented in 1964
  - Cryogenic temperatures
  - Based on the Josephson junction: two superconductors coupled weakly together and separated by a thin (nanometer-scale) normal conducting or isolating barrier
- Just because it is “quantum” doesn’t mean it is hard to manufacture
  - Fabricated using conventional deposition, etching, oxidation, and photolithography methods

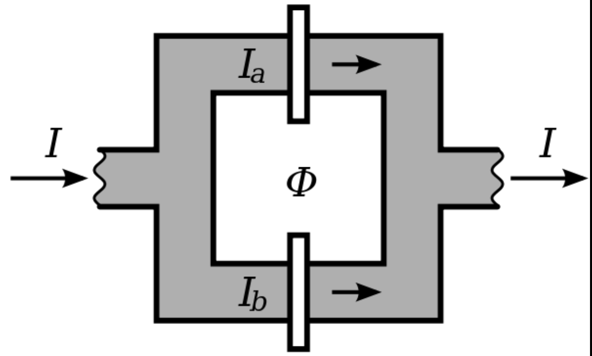

Source: Miraceti, own work, CC BY-SA 3.0, https://commons.wikimedia.org/w/index.php?curid=13302041.

Device scale: ~1–2 μm
Junction scale: ~100 nm

What are the manufacturing hurdles that currently limit adoption of novel quantum sensors of relevance to DoD?

IDA | 9

Quantum sensors are not as new as one might think. The superconducting quantum interference device, or SQUID, is an extremely sensitive form of magnetometer that was invented in 1964 and remains in wide use. This device is based on the Josephson junction, which is a type of quantum device in which two superconducting regions are separated by a thin barrier that is either insulating or conducts normally, creating a tunneling barrier. The magnetic flux passing through the enclosed loop is quantized and comprises the field being sensed and the magnetic field produced by the current flowing through the device. This current will change in response to the applied magnetic field to keep the flux quantized. SQUIDs are widely used today in diverse applications, including biomedical imaging, measuring the magnetic properties of material samples, scanning microscopes, and geological surveying and sensing.

From a fabrication perspective, SQUIDs are fairly easy to make: all that is required is conventional metal deposition (sputtering, evaporation, or other methods can work), photolithography, etching, and oxidation technology, and one can fabricate very small sensors (on the scale of micrometers, the junction itself on the scale of nanometers).

A key limitation of the SQUID is its operating temperature range. The SQUID needs to be held at cryogenic temperatures (4K), which can be inconvenient. For this reason, alternative magnetic sensors, such as atomic vapor sensors (another type of quantum device) are of interest.

In fact, the designation “quantum sensor” or “quantum system” is a broad and imprecise term that may encompass a wide range of devices and systems. In this CRP, we focus on a few representative examples of quantum sensors but do not attempt to cover the entire range of these technologies.

References:

Liu et al. (2015).

Robbes (2006).

DoD Applications for Quantum Systems

- PNT — Position, Navigation, and Timing
  - Magnetometers — Atomic vapor, and nitrogen vacancy in diamond (NV-D)
  - Gyroscopes — Atomic vapor, NV-D, and matter wave

  } Deep dive into manufacturing issues

- Quantum Computing
  - Qubits — Placed phosphorous dopants in silicon, placed NV centers in diamond
  - Quantum Clusters — Optically entangled qubits

  } Scale-up challenges considered

https://www.gpssource.com/pages/assured-pnt

https://www.nytimes.com/2019/10/21/science/quantum-computer-physics-qubits.html

IDA 10

Quantum systems have a wide range of DoD applications. For sensing, perhaps the most notable of the military applications is position, navigation, and timing (PNT), which includes the ability to navigate in GPS denied, intermittent, and limited (DIL) access environments and to accurately measure time. Quantum sensors that detect changes in magnetic field, acceleration, rotation, and gravity have been proposed as means toward enhanced DIL PNT. Some examples of these types of sensors include atomic vapor sensors (which rely on the motion of atoms in highly controlled environments) and nitrogen vacancies in diamond, which are excellent solid-state magnetic field sensors. Diamond NVs can also be used in gyroscopes by sensing changes in magnetic field that result from accelerations and rotations.

Quantum computing is more often heard about in the news, but we will touch only briefly on quantum computing in this briefing. We will focus in particular on difficulties surrounding the scale-up of qubit manufacturing. Some systems that can be used as quantum sensors can also be used as qubits in a quantum computer. Diamond NVs are an example of this, where information is typically read in and read out by optical means. Another option is precisely placed phosphorus dopants in silicon. We will discuss both of these types of systems in this briefing. Although there are many types of qubits, including trapped ions and superconducting qubits, we choose to focus on the NV and P-Si examples because they are more scalable, even though they are currently less technically mature.

Quantum Sensing for DoD: Gyroscope Case Study

IDA 11

Gyroscopes

- Gyroscopes sense rotation about a fixed frame of reference.
- Critical component for PNT in DoD systems for GPS-denied environments.
- Sensitivity and stability (i.e., drift) are application-dependent.
- Requirements depend on application (in order of increasing sensitivity and stability)
  - Consumer – Motion inference
  - Industrial – Robotics
  - Tactical – Missile guidance
  - Navigation – Platform guidance
  - Strategic – Nuclear platform and missile guidance
- Wide range of technologies, maturities, other properties.
  - Many gyroscopes rely on magnetometry

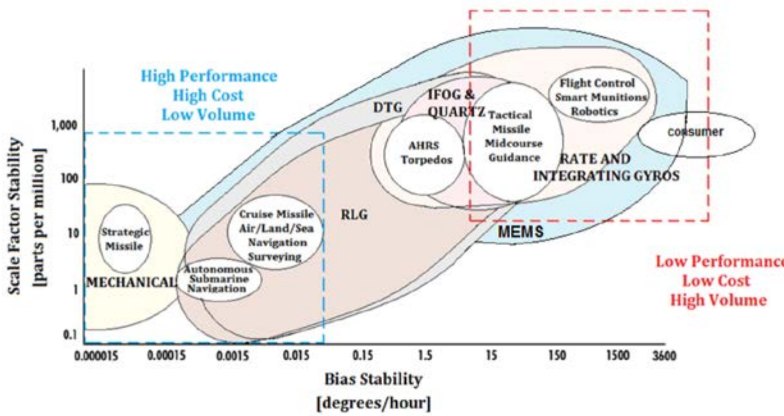

Source: Passaro et al. 2017).

IDA | 12

Gyroscopes sense rotation about a fixed frame of reference. They can be characterized most basically by the smallest rotation that can be sensed and the duration over which gyroscopes can track rotation from a reference frame. These two characteristics are more commonly known as sensitivity and stability or drift. Gyroscopes are critical components for PNT capabilities in DoD systems, especially in the GPS-denied environments. They are also used in consumer and industrial applications.

Requirements depend on the application and can be categorized into the following five classes:

1. Consumer: having a sensitivity of 30–3,000 degree/√hour and minimal requirements on drift.
2. Industrial: having a sensitivity of 1–30 degree/√hr and minimal requirement on drift.
3. Tactical: having a sensitivity of 0.1–30 degree/√hr and stability of tens of minutes.
4. Navigation: having a sensitivity of 0.01–0.1 degree/√hr and stability of hours, mostly for aeronautic navigation.
5. Strategic: having a sensitivity of 0.0001–0.01 deg/√hr with stability of hours (for missiles) and days to months (for platforms such as submarines).

In our analysis of gyroscope technologies, we start with a short discussion of magnetometers, and in particular atomic vapor magnetometers, which form the basis for tactical rotation sensing. The operation of magnetometers is easier to understand than that of gyroscopes. We will then discuss a number of approaches, both classical and quantum, for rotation sensing for PNT applications.

Magnetometers

Many gyroscopes sense rotation by sensing changes in the orientation of a magnetic field.

Example magnetic field sources and strengths

Source	Approximate Magnetic Field Strength
Neuron depolarization (imaged by MEG)	0.5 pT (5 x 10^{-13} T)
Earth's magnetic field	0.5 G (50 µT)
Refrigerator magnet	50 G (5 mT)
Junkyard electromagnet	1 T
Clinical MRI scanners	0.5 - 3.0 T (typical)
Research MRI scanners (human)	7.0 T – 11.7 T
Laboratory NMR spectrometers	6 - 23 T
Largest pulsed field created in lab nondestructively	97 T
Largest pulsed field created in lab (destroying equipment but not the lab)	730 T

A. D. Elster, "Relative Field Strength." *Questions and Answers in MRI*. Elster LLC, accessed December 4, 2020, mriquestions.com/how-strong-is-30t.html.

Magnetic field strength and frequency by application

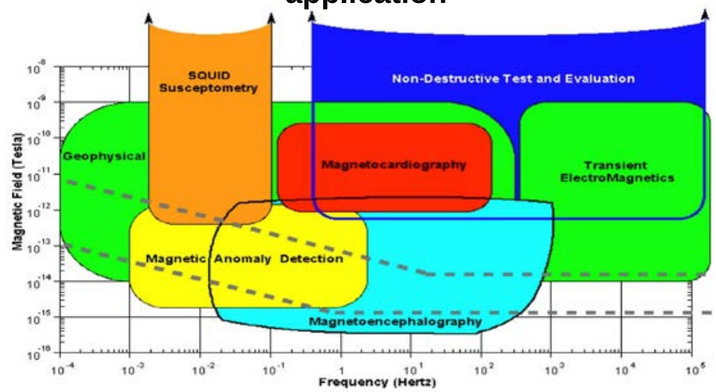

Fagaly et al. 2006.

Many types of quantum sensors can be used as magnetometers (e.g., SQUIDs, diamond NV, atomic vapor).

IDA 13

Magnetometers are the fundamental sensor contained in many gyroscopes. These gyroscopes sense rotation by sensing changes in the orientation of a magnetic field. These figures provide some examples of magnetic field strengths of some common benchmarks, as well as the magnetic field strengths and frequencies for several applications of magnetometry. Many types of quantum sensor can be used as magnetometers, including SQUIDs, diamond NV, and atomic vapor sensors.

Atomic Vapor Magnetometers

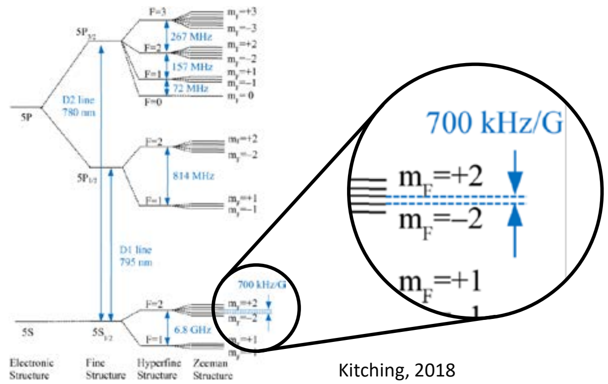

Kitching, 2018

Energy level spectrum of ^{87}Rb

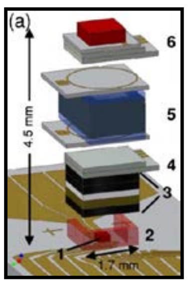

1. Laser (for spin polarizing)
2. Spacer
3. Optics package
4. ITO Heater
5. Rb87 Vapor Cell
6. ITO Heater and Photodiode
7. Voltage controlled oscillator
8. Magnetic coils

Schwindt et al. 2007.

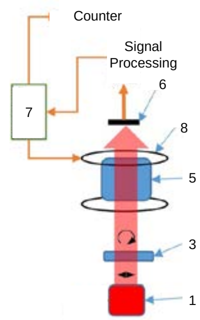

- Several types of atomic magnetometers
- Free-spin precession
  - Energy splitting perturbed by magnetic field
  - Electrons in these states are spin-polarized
  - Applied magnetic field caused Larmor spin-precession
  - Measure spin precession
- Sensitivity is not as good as SQUID
- Common technology base with chip-scale atomic clocks
- Miniaturized discrete systems

Larmor Precession

$$\omega_{rotation} \propto B_{measured}$$

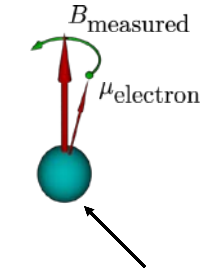

Much of the technology used in atomic vapor magnetometers is similar to the technology used in chip-scale atomic clocks. Atomic vapor magnetometers also form the basis for tactical rotation sensing.

The magnetic field being sensed perturbs the energy levels of the atoms in the atomic vapor via the Zeeman effect. Sensing proceeds by optically spin polarizing the electrons, which will cause their magnetic moment to precess about the applied magnetic field, as shown in the diagram in the upper right corner. This is known as Larmor precession. The frequency of this precession can be sensed, from which the level of the applied magnetic field is determined. Alternatively, the precession is equivalent to a coherent oscillatory change in occupancy probabilities of the two energy levels, the frequency of oscillation being determined by the energy difference. This mechanism, and the means for sensing it, is very similar to the techniques used for nuclear magnetic resonance sensing.

An example magnetometer is shown in the lower left. Rubidium atoms are confined in a heated vapor cell, and the laser is used to spin polarize the electrons. Magnetic coils are used to sense the precession of the magnetic field along the axis of the cavity. As discussed in the next slide, the sensitivity of atomic vapor magnetometers is not as high as that of a SQUID magnetometer.

References:

Kitching (2018).

Schwindt et al. (2007).

Comparison of Sensitivity for Several Types of Magnetometers

Technology	Typical DC Sensitivity	Notes
SQUID (Ref 1)	1 fT/√Hz	4.2 K Operation
Atomic Vapor - SERF (Ref 2)	1 fT/√Hz	RT operation; resonant modification of spin polarization; requires extremely homogenous, near-zero magnetic field for operations, which is often not practical
Atomic Vapor - Free spin (Ref 2)	100 fT/√Hz	RT operation; Free precession of spin-polarized; Magnetic field perturbs oscillation
NV Centers (Ref 4)	1 pT/√Hz	High spatial resolution; Limited by fluorescence collection efficiency and high-density spin coherence times

- Sensitivity measures the ability of the device to limit the effects of noise.
- Improving sensitivity depends on controlling sources of the noise.

IDA 15

The sensitivity of a sensor is a measure of the effect of noise on sensor performance. Because noise is random and measurements of magnetic field are typically the result of multiple samples taken over a period of time, measurement error decreases with the square root of the measurement time, assuming other sources of error, such as drift, are also controlled. Measurement error is (sensitivity) / (√measurement time).

For atomic magnetometers (and other quantum sensors), major sources of error include projection error and limited quantum coherence (see Degen, Reinhard, and Cappallerro 2017). Projection noise results from a quantum system's inability to produce a fractional measurement, owing to the discrete nature of the quantum states. Projection noise is reduced by making many measurements, which stems from having a large number of quantum systems (e.g., atoms) in the sensor. Errors from decoherence result from the relaxation of the quantum system from its prepared state because of external influences. For example, collisions of an atom with the wall of a microcavity can depolarize the atom. The decoherence time of quantum systems sets an upper limit to the measurement time.

SQUID magnetometers have a very high sensitivity because of the quantization of magnetic flux confined in the superconducting loop. The major source of noise is the shot-noise of the current, which is essentially a projection noise. The disadvantage of SQUIDs is that they require cryogenic temperature to operate.

There are several types of atomic vapor magnetometer (see Weis, Bison, and Grujić 2017), including spin exchange relaxation-free (SERF, not discussed in this report) and free-spin (discussed on the previous slide). The SERF magnetometer removes the limitations of spin relaxation by forcing the atoms to rapidly exchange spins. Applied magnetic field is measured by passing a light beam through the atomic vapor. SERF magnetometers are theoretically orders of magnitude more sensitive than SQUIDs, but all SERF magnetometers require careful compensation of stray fields, making them impractical for many applications.

Free-spin magnetometers overcome many of the practical limitations of the SERF magnetometer but have lower sensitivity. The sensitivity is predominantly limited by the coherence time of the atom, which is reduced by inelastic collisions with the sidewalls of the cavity. Proper coating of the cavity can preserve spin and increase the coherence time. There is a balance between atomic density, coherence time, and other deleterious effects associated with increasing density that also limits sensitivity.

Free-spin magnetometers can also be based on NV-centers in diamond. NV-centers act like artificial atoms that can be polarized. While they don't suffer from collision-based depolarization, decoherence effects originating primarily from nuclear spins in the diamond host limit sensitivity. At present, sensitivity is about an order of magnitude worse than free-spin atomic vapor magnetometers, but there is room for improvement. One key advantage of NV-based magnetometers is the spatially fixed location of the NV centers, which affords better spatial resolution.

We next discuss a number of approaches, both classical and quantum, for rotation sensing for PNT applications, some of which rely on magnetometry.

References

Schmelz and Stolz (2017).

Weis, Bison, and Grujić (2017).

Wolf et al. 2015).

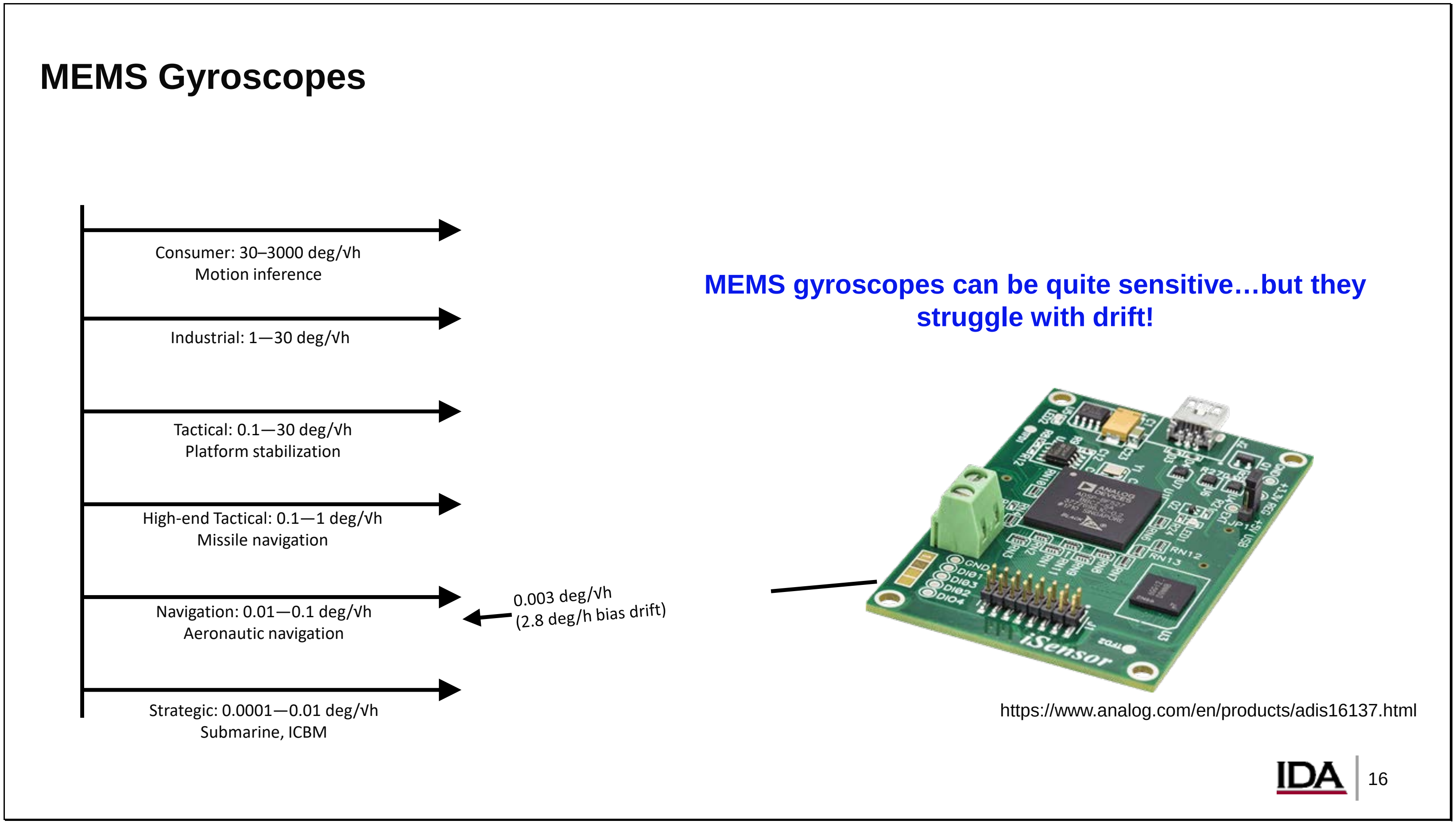

The most cost-effective gyroscopes are those based on microelectromechanical systems (MEMS) technology, which can exhibit sensitivities suitable for navigation, but lack the necessary stability. This figure shows a commercially available device produced by Analog Devices (ADIS16137) and selling for roughly $1,000. While the sensitivity at 0.003 degree/√hr is fine for many applications, the bias drift of 2.8 degree/hr limits its applicability. The intrinsic reason for these drifts stem from the formation of charged surfaces and is endemic to MEMS, making them unsuitable for PNT applications.

Atomic Vapor (NMR) Gyroscopes

Consumer: 30–3000 deg/√h
Motion inference

Industrial: 1—30 deg/√h

Tactical: 0.1—30 deg/√h
Platform stabilization

High-end Tactical: 0.1—1 deg/√h
Missile navigation

Navigation: 0.01—0.1 deg/√h
Aeronautic navigation

Strategic: 0.0001—0.01 deg/√h
Submarine, ICBM

0.1 deg/√h

0.005 deg/√h
(0.02 deg/h bias drift)

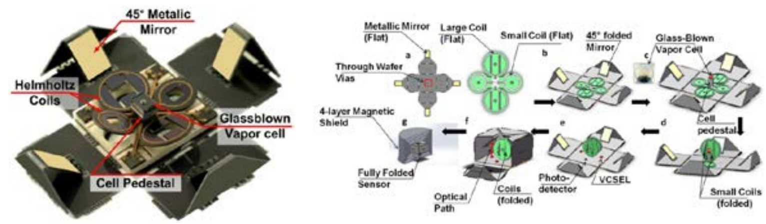

Noor (2018)

This

Atomic vapor-based gyroscopes show trade-offs between performance and manufacturability!

Easier to manufacture, poor sensitivity

Individually made, excellent sensitivity

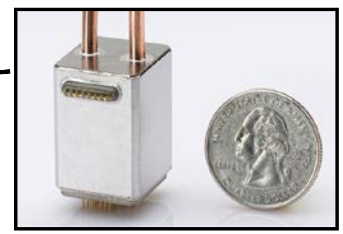

Walker (2016)

IDA | 17

This slide shows two approaches to using atomic vapors for gyroscopes. Both of these use the free-spin decay mechanism described earlier for magnetometers described previously. The extension of a magnetometer into a gyroscope involves replacing the sensed magnetic field of the magnetometer with one fixed to a frame of reference and sensing the change in the magnetic field with rotation.

The lower image shows a discrete system similar to the one for the magnetometer shown on slide 14. The upper image is an attempt to make the gyroscope more manufacturable using planar manufacturing techniques and limiting the number of discrete components. It failed to achieve the sensitivity required for DoD PNT tactical applications, but as this was only the first attempt, there is likely room for significant improvement.

One possible innovation is to replace the atomic vapor with NV-center in diamond (Walker and Larsen 2016).

References

Noor and Shkel (2018).

Walker and Larsen (2016).

Ajoy and Cappellaro (2012).

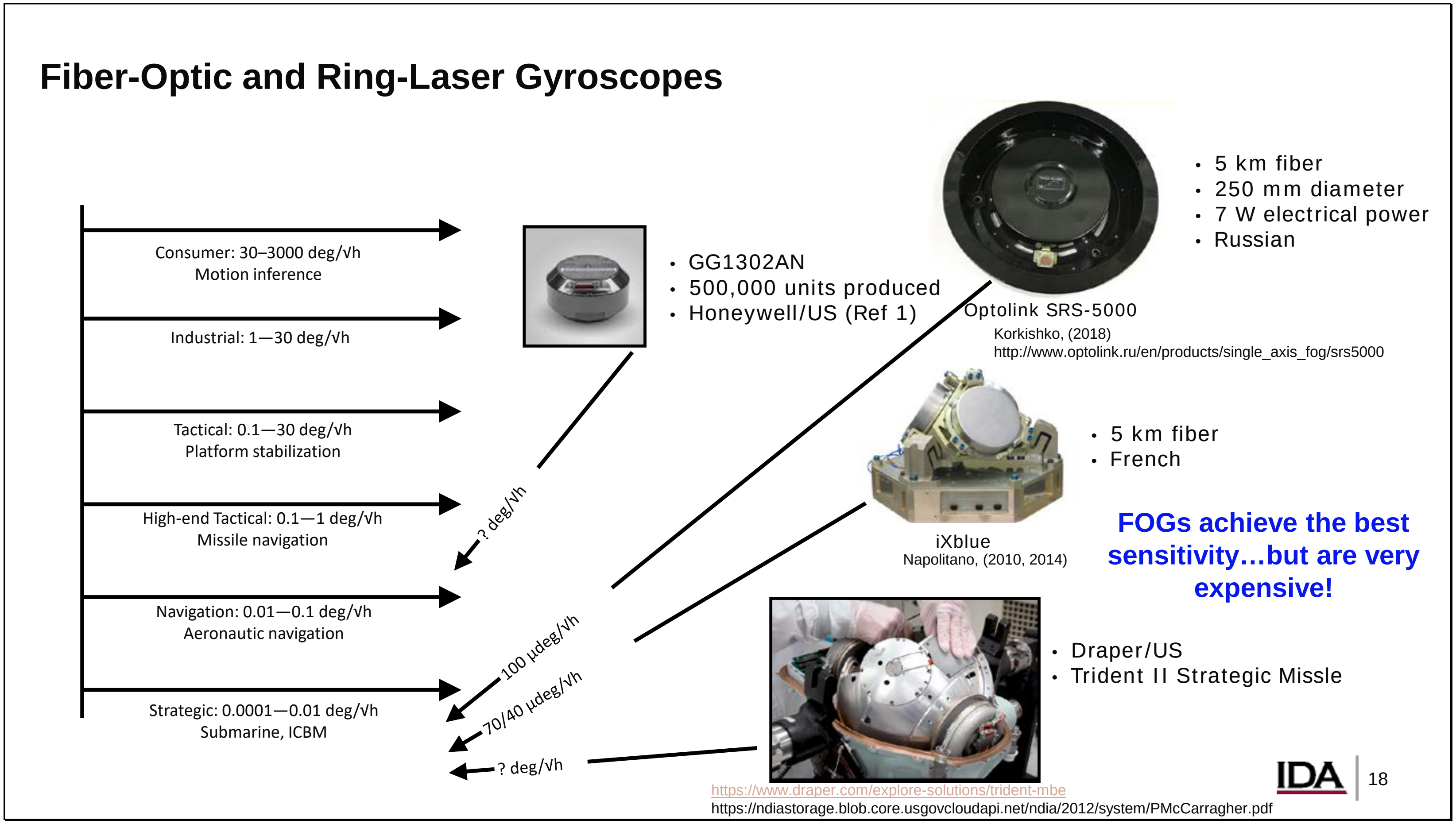
Fiber-Optic and Ring-Laser Gyroscopes
Consumer: 30–3000 deg/√h
Motion inference
Industrial: 1—30 deg/√h
Tactical: 0.1—30 deg/√h
Platform stabilization
High-end Tactical: 0.1—1 deg/√h
Missile navigation
Navigation: 0.01—0.1 deg/√h
Aeronautic navigation
Strategic: 0.0001—0.01 deg/√h
Submarine, ICBM
? deg/√h
100 μdeg/√h
70/40 μdeg/√h
? deg/√h
• GG1302AN
• 500,000 units produced
• Honeywell/US (Ref 1)
• 5 km fiber
• 250 mm diameter
• 7 W electrical power
• Russian
Optolink SRS-5000
Korkishko, (2018)
http://www.optolink.ru/en/products/single_axis_fog/srs5000
• 5 km fiber
• French
iXblue
Napolitano, (2010, 2014)
FOGs achieve the best sensitivity…but are very expensive!
• Draper/US
• Trident II Strategic Missle
https://www.draper.com/explore-solutions/trident-mbe
https://ndiastorage.blob.core.usgovcloudapi.net/ndia/2012/system/PMcCarragher.pdf
IDA
18

The highest precision and most stable gyroscopes have been dominated by the technically mature ring laser gyroscope and more recently by the fiber-optic gyro (see next slide for a description of their operation). Ring laser gyros use a cavity laser and sense a phase shift. Gyros suitable for aeronautic navigation cost on the order of $10,000 to $25,000 (not verified) and have been used for decades.

Sensitivity for a ring laser gyroscope is limited by pinning of the lasing mode to the cavity. More recent variations have moved the laser outside of the Sagnac interferometer. This configuration is known as a fiber-optic gyro (FOG) and has been able to achieve 1 nautical mile accuracy per month in an inertial navigation system (Paturel et al. 2014).

The most recent upgrade to the Trident II strategic missile system upgraded the gyroscope from a mechanical version to a FOG (https://www.draper.com/explore-solutions/trident-mbe). One of the most demanding requirements for the FOG to satisfy was the ability to work with the required precision and stability after years and potentially decades of dormancy.

References

Honeywell (2020).

Menéndez (2019).

Korkishko et al. (2018).

Napolitano (2010.

Paturel et al. (2014).

Interferometric Gyroscopes

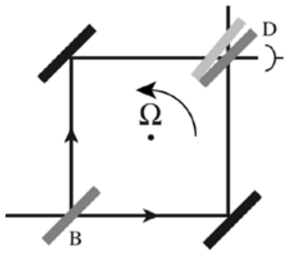

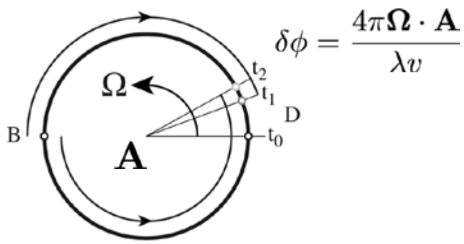

- Rotation is measured from the phase shift of an interferometer undergoing rotation:

$$\delta\phi = \frac{4\pi \mathbf{\Omega} \cdot \mathbf{A}}{\lambda v}$$

  Most interferometers use photons, but recently matter interferometers used neutral atoms.

- For a matter interferometer:
  - The wavelength is the DeBroglie wavelength

$$\lambda_{\text{atom}} = \frac{h}{p}$$

  which is much smaller than the wavelength of an optical photon.

- For interferometers having the same area, phase shift scales with energy:

$$\frac{mc^2}{h\nu} = 6 \times 10^{10}$$ (for Cs atoms)

IDA 19

Because the interferometric concept can be used for both matter-based and photon-based interferometry, we here include a brief explanation of the working mechanism of interferometric gyroscopes. This figure presents the basic operating principle of interferometric gyroscopes. This includes the ring laser gyroscope and the fiber-optic gyroscope discussed previously as well as matter-based gyroscopes, which use matter waves instead of optical waves (Gustavson 2000).

The key element is the Sagnac interferometer, as shown on the image in the upper left. The light (or matter wave) is split by beam splitter B into a clockwise and counterclockwise propagating wave. The two waves are recombined at beam splitter D. A rotation of the interferometer causes a phase shift between the two counter-propagating waves. The phase shift is proportional to the rotation rate and the area enclosed by the counter-propagating beams.

Matter wave interferometers enclosing the same area and with the same number of particles have the advantage that the phase shift scales with energy (Gustavson 2000). Using cesium atoms, this results in 10^{10} improvement in sensitivity. The challenge is that it is difficult to practically realize matter interferometers that enclose the same area and have similar particle fluxes as photon-based interferometers.

The area of FOGs is increased simply by wrapping more loops of fiber around a common spool, which is not possible for matter interferometers. In addition, it is much easier to get a large flux of photons than it is to get a similarly sized flux of matter particles. The net result of these two factors removes practically all intrinsic advantages of matter-wave interferometers over optical interferometers.

References

Gustavson (2000).

Gustavson, Landragin, and Kasevich (2000).

Matter-Wave Interferometers

Consumer: 30–3000 deg/√h
Motion inference

Industrial: 1—30 deg/√h

Tactical: 0.1—30 deg/√h
Platform stabilization

High-end Tactical: 0.1—1 deg/√h
Missile navigation

Navigation: 0.01—0.1 deg/√h
Aeronautic navigation

Strategic: 0.0001—0.01 deg/√h
Submarine, ICBM

0.03 deg/√s

600 μdeg/√h
w/Area reversal
(2005)

10 μdeg/√s

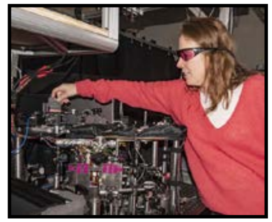

Chen (NIST 2018)

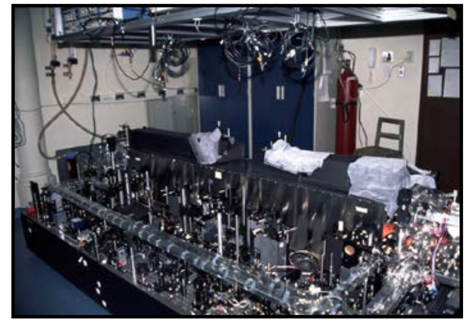

Gustavson (Stanford 2000)
Durfee (Stanford 2005)

Matter-wave interferometers face a miniaturization challenge with integrated technologies (laser tables, vacuum systems).

IDA | 20

While matter-wave interferometers have intrinsic advantages over fiber-based interferometers, when similarly configured (see previous slide), the miniaturization challenges are formidable. The first matter-wave gyroscope was developed at Stanford in 2000 (Gustavson, Landragin, and Kasevich 2000). While the short-term stability was on par with optical interferometers, the gyroscope suffered from stability problems. In an optical gyroscope based on the Sagnac interferometers, the two paths are identical (CW and CCW) in the fiber; consequently, common-mode sources of error (such as thermally induced change in the fiber's length) cancel out. Matter-wave-based interferometer have used spatially disjoint paths for the two beams.

In 2005 a technique called "area reversal" was used to remove much of the drift (Durfee, Shaham, and Kasevich 2006); consequently, the resulting performance was on par with the best optical gyroscopes.

Attempts in 2018 to make the gyroscope more compact also reduced its sensitivity and left the device with excessive drift (Chen et al. 2018).

Given all these factors and the inherent complexity of matter-wave interferometers, it is not likely that they will ever be competitive with fiber-optic gyroscopes.

References

(1) Chen et al. (2018).

(2) Gustavson, Landragin, and Kasevich (2000).

(3) Durfee, Shaham, and Kasevich (2006).

Quantum Sensor Gyroscope

- Strategic high precision
  - Optical — Fiber-optic gyroscope (FOG)
  - Atomic — Atom Interferometer (AI)
  - Tough for AI to outperform FOG
    - Area advantage for FOG (coiled fiber)
    - Quanta number advantage for photons
- Tactical medium precision (low cost)
  - MEMS — has sensitivity, but high drift (electrical charging)
    - manufacturing challenges, sensitivity is limited
  - Atomic vapor NMR gyroscopes
    - Glass cell, discrete — good sensitivity, acceptable drift
  - NV-diamond ???

There may be a niche for *tactical* quantum sensor gyroscopes if:
(a) the cost of compact NV-based systems can be lowered and sensitivity improved, or
(b) atomic vapor-based systems can be miniaturized.
Supporting technology, especially laser integration, is critical in both cases.

IDA 21

Fiber-optic gyroscopes (FOGs) will be increasingly used for strategic systems. It is not clear that FOGs are at their practical limits, should higher sensitivity be need. It is exceedingly unlikely that FOGs will ever be replaced by matter-wave gyroscopes, especially given the latter's significant increase in complexity.

There is likely a need for low-cost tactical gyroscopes for use in missiles and possibly other applications. It remains an open question if NV-centers in diamond (or other material) could have a practical advantage over atomic vapors. Either type of system requires a significant amount of supporting technology, such as lasers, optical detectors, and other components. Regardless, this is a cost-sensitive application, and cost should be on the order of a chip-scale atomic clock (about $1,000).

Quantum Computing and Manufacturing at Scale

Quantum Computing

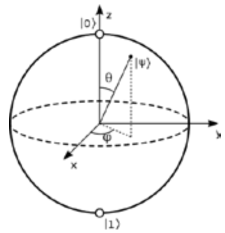

Block sphere representation of a qubit

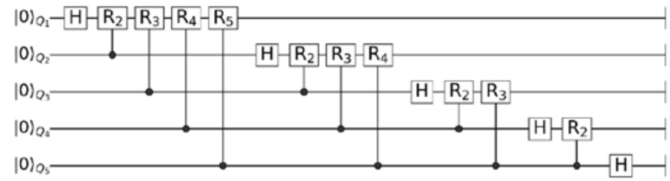

Quantum Computation as a series of gate operations on qubits

- Qubits: A collection of (mostly) isolated and controllable quantum systems
  - Atoms, superconducting circuits, photons, …
  - Special quantum states, similar to classical bit states of 0 and 1
  - Continuum of uniquely quantum states that are a superposition of 0 and 1 and can be entangled with other qubits
- Quantum (logic) gates
  - Discrete manipulation of quantum state of qubits
  - Computation is a sequence of quantum gates applied to addressable qubits

IDA 23

There are many excellent introductions to quantum computing, covering the basic concepts (Nielsen and Chuang 2010; Preskill 2018; Ladd et al. 2010), physical platforms (Clarke and Wilhelm 2008; Blatt and Wineland 2008), and algorithms (Montanaro 2016; Childs and Van Dam 2010). In particular, we highly recommend the recent National Academy of Science report *Quantum Computing: Progress and Prospects* (2019). This report should be noted for its fair (unbiased), complete, and up-to-date discussion of quantum computing.

For the purpose of this effort, a quantum computer is a large collection of (mostly) isolated and controllable quantum systems. These are the qubits. Running a quantum computation consists of applying an ordered sequence of gate operations. More details can be found in the references included with this slide. The two most mature platforms are trapped ions and superconducting qubits. Much effort is being put into the development of a quantum computer based on these first-generation platforms by the U.S. government and commercial companies. It is not clear that they are scalable to the sized needed for practical computations, that is, computations having a significant advantage over classical computation.

References

Blatt and Wineland (2008).

Childs and Van Dam (2010).

Clarke and Wilhelm (2008).

Ladd et al. (2010).

Montanaro (2016).

National Academies of Sciences, Engineering, and Medicine (2019).

Nielsen and Chuang (2010).

Preskill (2018).

Quantum Computers — Trapped ions

- States are atomic energy levels of an ion
- Ions are trapped on an atom chip
- More sophisticated traps allow for the ions to be moved on the chip
- Highly stable lasers, optical cooling, vacuum systems, optics, RF generators to stabilize and move the ions, …

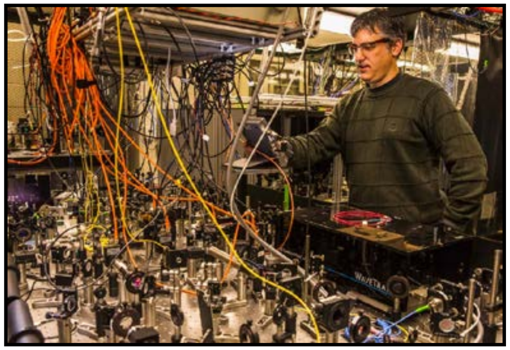

https://physicsworld.com/a/quantum-computing-from-the-ground-up/

U of MD, circa 2014 — ~11 bits

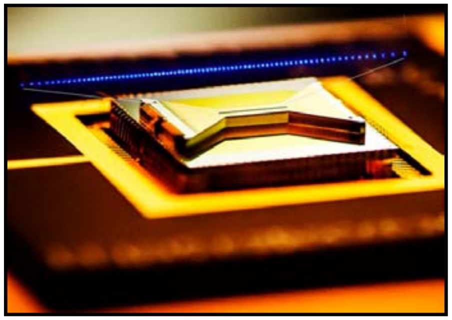

https://physicsworld.com/a/ion-based-commercial-quantum-computer-is-a-first/

Linear ion trap

https://phys.org/news/2020-10-ionq-next-generation-quantum.html

IonQ, circa 2020 — 32 bits

IDA | 24

Trapped ions are negatively charged ions held in an electrostatic trap. Linear traps are surface traps fabricated using silicon technology. The ions are levitated above the surface of the trap and are positioned about 1 mm apart. Traps are maintained at 4K to reduce heating of the ions. Each trapped ion is a qubit (though additional ions are inserted to aid in cooling the computational ions, i.e., sympathetic cooling). An example of a trap is shown in the lower left figure (note that the ions are much closer to the chip than they are depicted in this picture.) More sophisticated traps allow for shuttling and rearranging the positions of the ions.

Current traps hold about 30 ions and have been engineered for operation in a data center. The figure in the lower right shows an operational system having 32 ions. Functionally, what was on the optical table in the upper right is now in the box. The size of the packaged quantum computer is estimated to be about 4 × 8 × 6 feet. Such systems can be accessed through Amazon Web Services.

Quantum Computers — Superconducting Qubits

- Integrated circuit — Josephson junctions, microwave waveguides, capacitors, and inductors
- Gigahertz clock speeds
- Nano-Kelvin operating temperature
- Silicon-chip fabrication, dilution refrigeration, microwave signal networks, electrical noise isolation, control systems

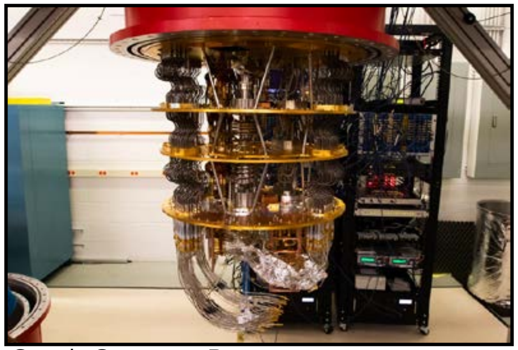

Google Sycamore Processor
https://www.nytimes.com/2019/10/23/technology/quantum-computing-google.html

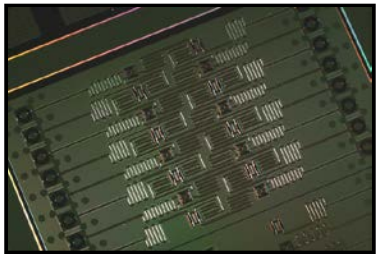

IBM 16 qubit processor
https://www.ibm.com/blogs/research/2018/09/next-gen-qubits/

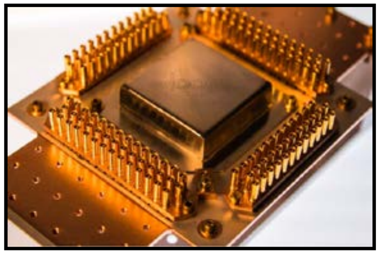

Google 54 qubit Sycamore (Ref 1)

IBM Quantum Processor
https://www.youtube.com/watch?v=o-FyH2A7Ed0

IDA 25

This slide shows the key components in a superconducting quantum computer. All the qubits are fabricated on a planar circuit, as shown in the 16-qubit processor from IBM. Larger chips are available such as the 54-bit Sycamore chip from Google. The chip has to be cooled with a dilution refrigerator to 10 nK or so. This is accomplished with a cryostat such as the one shown in the upper right corner of the slide. In the bottom of this picture, one can clearly see all the signal lines that are necessary to control the quantum processor and connect to the Sycamore chip via the connectors.

Google's Sycamore quantum computer was able to perform a "computation" that would have taken thousands of hours on the largest existing supercomputers in several minutes (Arute et al. 2019), achieving the milestone of "quantum supremacy." While this was an impressive feat, the implication for using a quantum computer to solve practical problems of interest remains an open question.

References

Arute et al. (2019).

Quantum Bits are Expensive

Bit Type		Cost in 2020 Dollars		
		Now	In 10 years	In > 30 years
Bit Type	Classical Bit	$\$10^{-8}$	$\$10^{-10}$	$\$10^{-11}$
	Physical Qubit	$10,000	$1,000	$1.00
	Logical Qubit	$100 million	$100,000	$100.00

- Classical bits cost $\$10^{-8}$/bit today
- Currently, physical qubits are $10,000/bit, logical qubits are 1,000 to 100,000 times more expensive
- Even accounting for technical progress, qubits will always be many orders of magnitude more expensive

IDA | 26

The key takeaway of this slide is that qubits are expensive and, relative to classical bits, will likely always remain so. Much of this cost comes from the fact that the qubit is a controllable quantum system and needs a significant amount of supporting equipment, as discussed on the previous two slides. At present there is a difference of about 12 orders of magnitude in the cost of a classical bit compared with a physical qubit. Logical qubits are fault tolerant and comprise between 1,000 and 100,000 physical qubits, bringing the cost of a logical qubit to over $1 million, if one could be made today.

While the cost of a qubit will certainly decrease, it will always be many orders of magnitude more expensive than a classical bit. Consequently, the computational efficiency of a quantum computation must be *exponentially more* than the classical computation. This places a severe limitation on the computations that can run on a quantum computer and be cost effective.

How Many Qubits Do You Need?

- **Quantum Advantage:** A quantum computer is most viable for computations that are classically intractable
- Hence, quantum algorithms need an *exponential speedup* (over classical computations) to have a practical quantum advantage
  - *Quantum Fourier Transform* (QFT)
  - *Quantum Walk* (QW)
  - NP-complete problems have sub-exponential speedup

IDA | 27

This need for an exponential speedup in a quantum computation, as argued in the previous slide, places severe restrictions on practical quantum algorithms. Basically, only algorithms that rely on the quantum Fourier transform (QFT) or the quantum walk are viable at present. This includes Shor's algorithm for factoring integers and quantum simulation, both of which rely on the QFT. Quantum walks could be useful for select problems, but they are likely to have more computational resource requirements than either Shor's algorithm or quantum simulation.

Examples: How Many Qubits Do You need?

- Shor's algorithm (for ***N***-bit number)
  - ~5 ***N*** (logical) qubits and N^3 (logical) gates
- Quantum simulation (ground-state energy level of molecule)
  - ~100 (logical) qubits and ~10^{15} gates (nitrogen fixation)
- Logical qubits are fault-tolerant; physical qubits are not
  - 1,000 to 100,000 physical qubits are needed for a logical qubit

Quantum computers need to have ~1,000,000 (physical) qubits to have quantum advantage for practical applications

IDA | 28

This slide offers some numerical examples to estimate the number of qubits needed for quantum advantage. At present, approximately 100 to 10,000 logical qubits are needed for computations ranging between 10^9 and 10^{15} gate operations. These are logical qubits and logical gate operations. Realistically, quantum computers will need on the order of several million high-quality physical qubits to solve practical problems of interest.

Why Alternative Platforms?

- Trapped-ion and superconducting are the most mature platforms
- Qubits are large, typically 1– 4 mm^2 for the physical qubit
- More “stuff” around them
- Superconducting
  - Microwave plumbing
  - Tunable elements (for isolation)
- Trapped-ion
  - Ion sources
  - Lasers for atomic cooling (often with sympathetic cooling)
  - High NA optical access (for gates and readout)
- Large surface area (several square meters, in all likelihood, distributed over many chips)

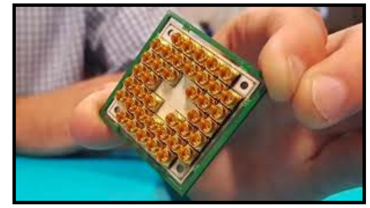

Intel 17-qubit chip, 2017 (Ref 1)

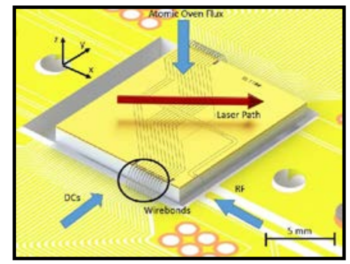

Diagram showing parts
of a trapped-ion chip (Ref 2)

IDA 29

As we have previously mentioned, the two most mature quantum computing platforms, trapped-ion qubits and superconducting qubits, are receiving significant attention from the U.S. government and commercial corporations, and we see no need to consider manufacturing issues related to these two platforms in this report. Rather, our concern is that neither of these platforms is scalable to the number of qubits needed for many—possibly all—computations of interest.

This is in large part owing to the physical size of qubits for both these two platforms. Superconducting qubits are from 1 to 4 mm^2, and while ions themselves are small, the physical volume allocated to an ion is about the same as that for a superconducting qubit. Planar ion traps that hold 10–100 qubits are a few square millimeters. Unlike the (nearly) ever-shrinking transistor, qubits are not likely to become more dense in either of these technologies, and the only alternative is to use more or possibly larger chips for the qubits. Overall, quantum computers containing 1 million physical qubits will need several square meters of chip area to hold the qubits.

In addition, as mentioned in previous slides, there is lot of "stuff" around these qubits. This includes microwave components and circuitry, control systems, and dilution refrigeration for superconducting qubits. For trapped-ion qubits, it includes ion sources, additional ion species for sympathetic cooling, RF circuitry for trapping and moving ions, access paths for optical signals, and more. We fully appreciate that this additional stuff or something equivalent is need for any quantum computing platform, but higher densities of qubits can provide a way forward for reducing the overall volume of these ancillary components.

The best way to improve the scalability of quantum computing platforms is to increase the density of qubits, thereby reducing the overall number of chips in the system and the need for cooling. Because neither of these approaches is possible with the trapped-ion or the superconducting platform, we have chosen in this report to explore second-generation platforms that, while less mature, still show promise.

References

Intel Newsroom (2018).

Romaszko et al. (2020).

Alternative Platforms

- Phosphorous-doped silicon (or other host)
- NV-center
- Photonic quantum computers
  - Not qubit-based; have potential to be significantly smaller overall

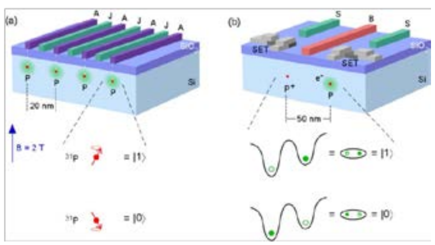

P-doped Si (Ref 1,2)

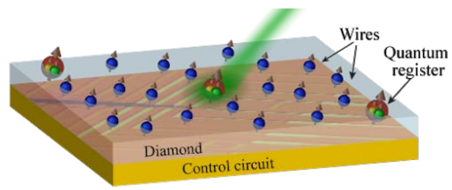

NV center in diamond (Ref 3,4)

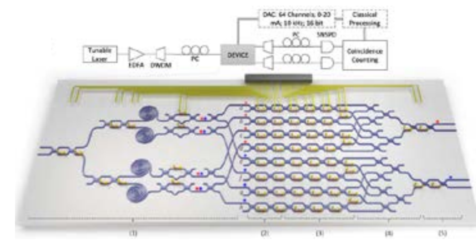

Photonic computer (Ref 5,6,7)

All these quantum computing platforms still require significant support beyond the physical qubit.

IDA | 30

This report explores manufacturing issues associated with three alternative second-generation computing platforms: phosphorous doped silicon and NV-centers in diamond. Photonic quantum computing is an additional second-generation platform of interest; however, in this project it was only covered to the extent that we discuss photonics manufacturing also of interest to the other platforms.

Phosphorous doped silicon (Dzurak et al. 2003; Veldhorst et al. 2015) uses energy levels in the phosphorous dopant for a qubit. Fabrication requires that these P-dopants be placed in precise positions approximately 13-14 nm apart to allow two-qubit interactions. This could significantly increase the density of qubits, although they would still require cooling in the nanoKelvin range for operation. By moving to optical energy levels, the need for cooling could be reduced, although likely not eliminated. A good choice for this are NV-centers in diamond or some other substrate (Childress and Hanson 2013; image source: http://qeg.mit.edu/research.php). The final approach is the photonic quantum computer where the computational states are photon states (e.g., polarization) and the optical circuitry is linear optics. This last form of computing has the potential for a significantly reduced number of cluster states (a cluster state is the equivalent to a logical qubit, see (Rudolph 2017 in particular) and can operate at room temperature with the possible exception of needing cooled detectors to improve the quantum efficiency of detecting single photons.

All three of these second-generation platforms are less technically mature than either the superconducting or trapped-ion platform, especially the NV-center approach. Nevertheless, all have received significant attention and are viable candidates for second-generation platforms for quantum computing that offer significant advantage over the first generation platforms. Our intent in this report is to focus on issues of manufacturability and the need for research into manufacturability that may accelerate the development of these second-generation platforms.

References

1. Dzurak et al. (2003).
2. Veldhorst et al. (2015).
3. Childress and Hanson (2013).
4. Image source: http://qeg.mit.edu/research.php
5. Qiang et al. (2018).

6. Rudolph (2017).
7. O’brien, Furusawa, and Vučković (2009).

Manufacturing Considerations for Representative Quantum Systems

IDA | 31

Sensor Manufacturing Goals

- Sensors are easier to manufacture than quantum computers:
  - Quantum sensing takes advantage of isolated quantum systems.
  - Quantum computing relies on interacting quantum systems.
  - *Quantum systems work better in isolation.*
- Quantum sensors and computers rely on the same supporting technologies (e.g., lasers, photonics, vacuum systems, cryogenics).

Improved integration and miniaturization of quantum sensors and supporting technologies will have secondary benefits for quantum computing.

IDA 32

In general, manufacturing quantum sensors is easier than manufacturing quantum computers. Not only is the scale of the manufacturing smaller in terms of the number of controlled quantum systems, but sensors also take advantage of isolated quantum systems. In contrast, quantum computing relies on interacting quantum systems. Since quantum systems work better in isolation, quantum sensors are usually easier to manufacture. However, both quantum sensors and quantum computers rely on the same supporting technologies, as shown in the prior charts. Improving integration and miniaturization of quantum sensors and supporting technologies is expected to have secondary benefits for quantum computing.

Quantum Sensor Performance Metrics and Manufacturing Goals

- Key performance metrics:
  - Sensitivity
  - Decoherence time
  - Dynamic range
  - Sampling rate
  - Operating temperature
- Other goals:
  - Compact form factor / high density of quantum sites
  - Reliability / repeatability
  - Better performance / cost trade than competing classical sensors

This slide lists several key performance metrics for evaluating the performance of quantum sensors, some of which have been discussed on the previous slides. These include sensitivity, decoherence time, dynamic range, sampling rate, and operating temperature. In addition, it is often desirable to decrease the size of a sensor or make the density of quantum sites greater, to have high reliability and repeatability in manufacturing the device, and to have a better performance vs. cost trade than competing classical sensors (e.g., MEMS-based gyros).

General Manufacturing Considerations

- **Flow consolidation:** More steps typically increase cost and decrease yield.
  - In a many-step process, yields for individual steps need to be *very* high.
- **Substrate-specific chemistry:** Use of multiple substrate materials requires specialized chemistry for etching or reactive techniques.
  - *Just because you can do something with silicon doesn't mean you can do it with another substrate.*
- **Step–by–step integration efficiency:** Parallelization saves time and cost.
  - *You are only as fast as your slowest step.*
- **Continuous monitoring**: Thoughtful in-line testing improves device yield and saves resources.
- **Order of operations:** Upstream steps limit downstream options.
  - *Temperature, vacuum, vibration, chemical compatibility.*

IDA 34

This slide summarizes some general manufacturing considerations that guide our analysis of quantum system fabrication approaches.

First, additional steps typically increase the overall cost and decrease the overall yield of a manufacturing process. To combat the yield problem, individual steps must have very high yields in multi-step processes.

Second, many quantum-sensing schemes rely on multiple substrate materials to support different components of the package. The same processes for etching, film growth, or cleaning that work for one substrate may not work for another, and one cannot assume that the same resolution or reliability that is seen for a process applied to silicon will apply when that same process is used on a different substrate. There are many advantages to heterogeneous integration approaches, however; therefore, the trick is to choose the right substrates for the right job and to identify areas where further R&D is needed in the processing of that material to enhance performance, lower cost, or improve repeatability.

Following from the above point, parallelization in manufacturing saves time and cost. This is one potential advantage of heterogeneous integration, where multiple components can be processed simultaneously and combined only after determining that each individual component meets quality requirements. The idea here is to prevent bottlenecks in manufacturing, and keep yield high.

Along the same lines, conducting in-line testing of components and process monitoring during fabrication can help improve device yields and saves resources, for example by quickly identifying problems in the fabrication line, by rejecting wafers early that have defects that cannot be fixed (preventing those wafers from continuing through the processing line), or by identifying places where an error-correction step may be taken.

Finally, a key consideration in process engineering is the effect of upstream steps on available downstream options. Structures fabricated earlier in a manufacturing process need to be protected from damage by later processing steps. A simple example of this is temperature stability—high-temperature annealing steps can cause diffusion or reactivity and are sometimes used to smooth out defects introduced into a crystal from intense processes such as ion implantation. Structures fabricated early in a process need to be able to withstand all subsequent annealing steps. Other environmental conditions that can damage various types of structures include vacuum, vibration, and chemical exposure (e.g., wet etches).

Atom Chips and Heterogeneous Manufacturing

IDA | 35

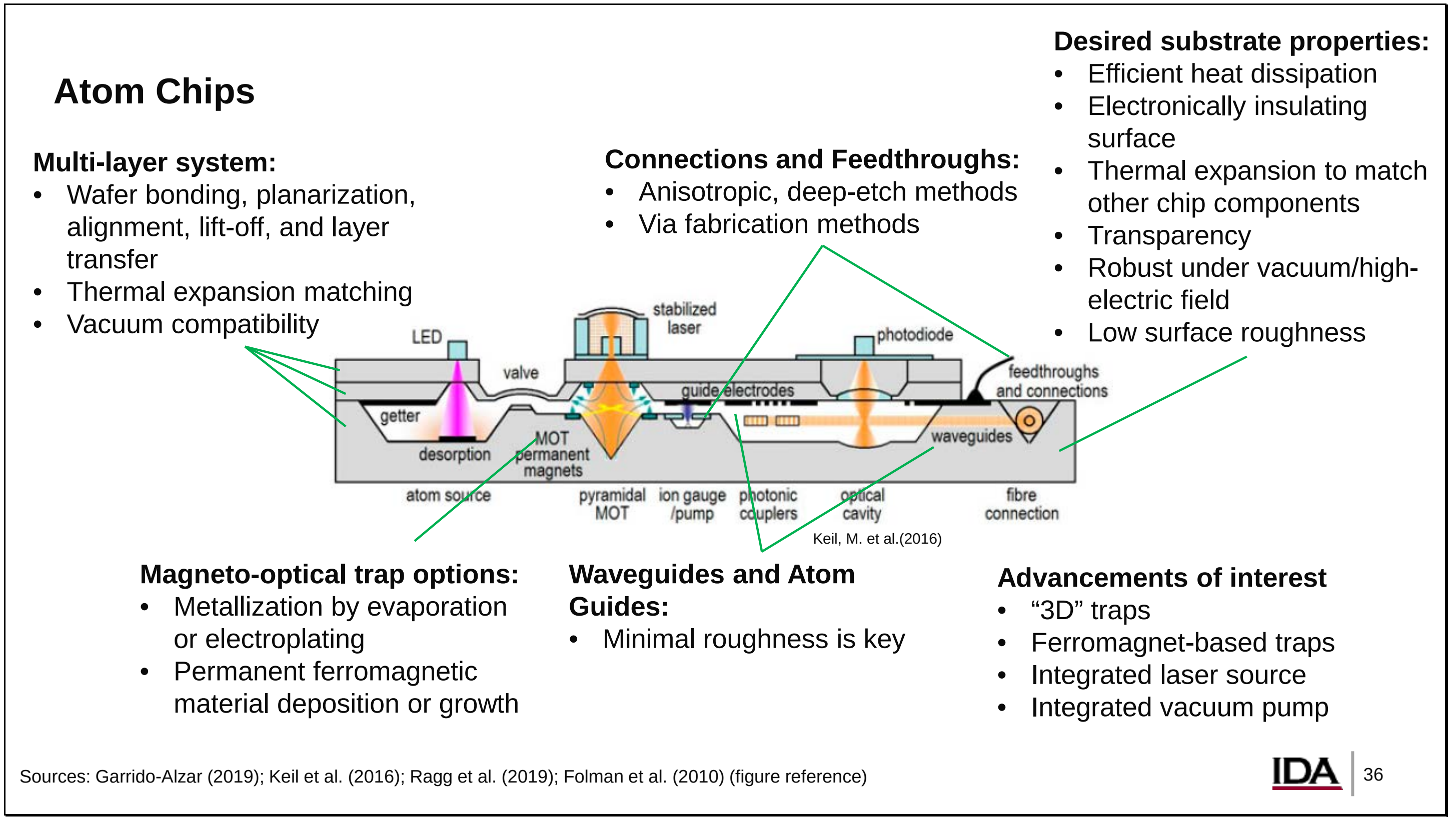

Atom chips are complicated systems. They include many components that have different roles, but must work together and remain compatible through the life of the chip. For example, a typical atom chip incorporates some form of magneto optical trap (MOT) (where atoms are captured); waveguides and beam splitters to guide the atoms to their measurement location or guide read-in/read-out optical stimuli to the desired location; and connections and feed-throughs (vias) that allow atom access, laser access, and electronic access to the chip.

With these components in mind, we have several considerations. First, consider the substrate, which needs to have a number of properties listed on the slide, including high thermal conductivity (for efficient heat management from the current that is typically pushed through the MOT), an electronically insulating surface (that can handle high electric fields), thermal expansion that matches the interfaces the substrate may need to withstand with MOT layers or other layers (e.g., glass, metallization), transparency (to enable optical access from outside the chip), and robustness under vacuum and high electric field. Silicon is not an ideal substrate for atom chips because of its low transparency and semiconducting character; however, SiO2 can be grown on Si to provide a thin insulating barrier on its surfaces. Some alternatives include aluminum oxide (sapphire), aluminum nitride (surface roughness is a problem), silica, and GaAs. Yttria-stabilized zirconia has been used as a substrate on rare occasions. Diamond might be a good option as well; however, it does not appear to have been widely explored as an atom-chip substrate. Overall, the substrate's thermal and electronic properties need to be carefully controlled because MOTs are critical to device function and must act as expected.

One important performance metric for the chip is the distance between the atoms (or ions) and the chip surface—smaller distances provide better control of matter propagation and lower power operation, but atoms too close to the surface tend to lose lifetime by heating too much. Also, atoms that are closer to the surface are more susceptible to potential variation caused by fabrication defects. From a fabrication standpoint, bringing the atom closer to the chip surface would make fabrication of wells and cavities easier because it would demand less etch time, less precision of anisotropic processes, and less concern about shadowing effects during fabrication. Also, fabrication of 3D ion traps can avoid asymmetries in the potential field, which also facilitates more efficient atom shuttling. Therefore, 3D trap fabrication is of interest.

The MOT on a chip may be fabricated in a number of ways, such as using metallization layers (through either evaporation or electroplating) to create magnetic-field traps or by using permanent magnets for the same purpose. Permanent magnets have lower noise and can sustain high fields easily, but are not dynamically programmable as electromagnetic-based traps are (Keil et al. 2016). For electromagnetic-based traps, there are multiple fabrication options, including evaporation (which is highly controllable but slow and expensive) and electroplating (lower cost, with acceptable control of roughness possible and able to produce highly anisotropic wire geometries) (Garrido-Alzar 2019). More exploration of methods for precise-composition-controlled deposition or growth of metal alloys on substrates of interest for atom chips (including sapphire) could be beneficial for producing extremely low-noise traps.

In addition, today's atom chips have external systems associated with them, such as a laser source and a vacuum system. Although the atom chip itself may be on the scale of centimeters, these other systems can cause the whole package to increase to liter-scale volumes. Moving parts, particularly for the vacuum system, can also reduce reliability. One important goal is to miniaturize and incorporate solid-state vacuum pumps (e.g., the Knudsen pump on the next slide) into the chip to further miniaturize the package, reduce power demand, and (possibly) improve reliability.

Atom Chip: Anodic Bonding and Deep Anisotropic Etching

Fabrication of Through-Si Vias

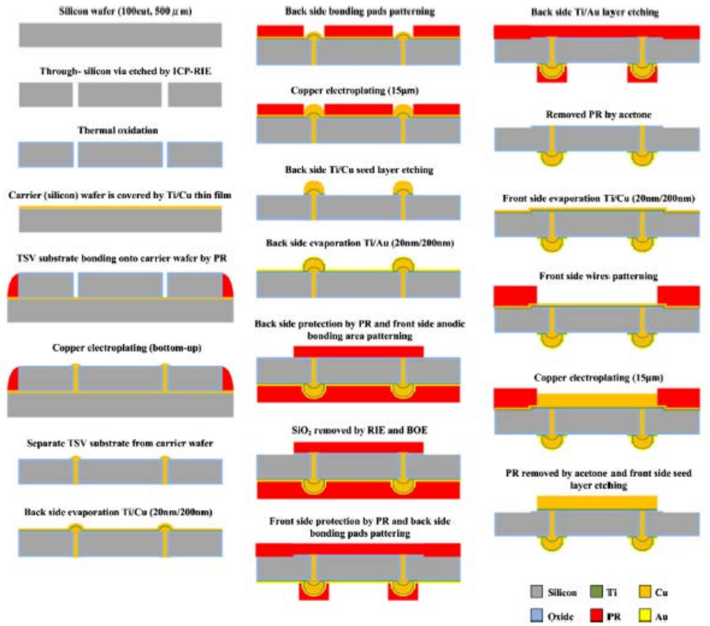

Chuang et al. (2013)

Knudsen pump microfabrication

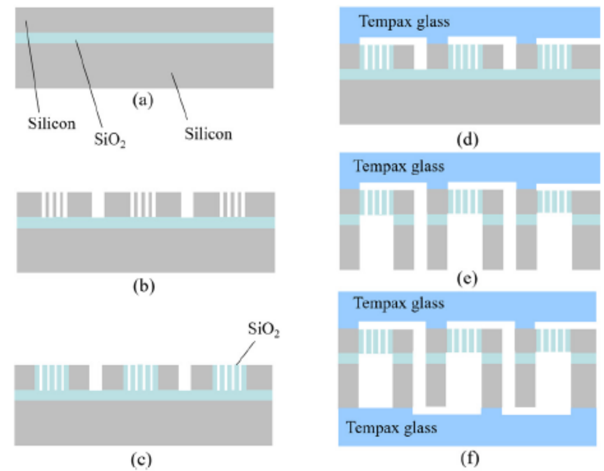

Figure 2. Fabrication process. (a) SOI wafer (7 μm/1 μm/300 μm). (b) Photolithography, RIE, and deep RIE. (c) Wet thermal oxidation and RIE. (d) 1st anodic bonding. (e) Backside photolithography, deep RIE, and RIE. (f) 2nd anodic bonding.

Van Toan et al. (2018)

IDA 37

Atom chips use features on different scales from typical microelectronic platforms—wells on the order of tens of microns are not unusual, because maintaining a cold atom temperature requires substantial separation from the atom chip surface. Atom chips also often use multiple materials and may rely on alternative substrates from Si to ensure adequate heat management and needed electronic and surface properties. Manufacturing technologies of interest for the atom chip therefore include the ability to etch deeply into unusual substrates in a controlled fashion (deep, robust, anisotropic etch capability). Furthermore, atom chips benefit from optically transparent substrates (which can permit photons to travel to the atom of interest from outside the chip). Finally, wafer bonding of dissimilar substrate materials, which has a prerequisite for high-quality planarization, is also important.

This chart illustrates some example process diagrams pulled from literature of (left) fabrication of through-Si copper vias for an ultra-high-vacuum atom chip and (right) deep etches and wafer bonding used to produce a Knudsen pump with a silicon-on-insulator wafer and glass. The diagram on the left shows extensive detail, including patterning and removal of photoresists, as well as deposition of adhesion layers. In contrast, the diagram on the right is somewhat simplified. It does not include photoresist patterning and removal for the various photolithography steps, nor does it show the etching process applied to the Tempax glass components. In general, photolithography proceeds by (1) cleaning the surface, (2) depositing photoresist, (3) patterning the photoresist with exposure to light through a mask, (4) developing photoresist, (5) the reaction of interest (typically an etch or a deposition), and (6) removing the photoresist. Individual photolithography "steps" are therefore really multistep processes themselves. Note also that the etch depths of the first step (a to b) shown in the Knudsen pump fabrication is 7 μm for openings of 1 μm diameter (aspect ratio of 7:1) and that the deep reactive ion etch used to fabricate these trenches proceeds by a series of etching and passivation cycles. These diagrams illustrate how complex such via and well microfabrication processes can be.

There are also some important details to keep in mind for fabricating structures containing features at many length scales (tens of nanometers to hundreds of micrometers). Some techniques designed for microfabrication don't work well for thick structures. These include various etching and film-growth techniques. Challenges arise because of stress effects at interfaces (e.g., thick films form dislocations and cracks when grown on non-lattice-matched substrates), thermal-expansion effects (see previous mention), polycrystallinity, etc. Also, many precise methods have slow growth rates (e.g., ALD, CVD, PLD) such that micron-scale growth can be prohibitive. Finally, surface reconstructions, faceting, and other thermodynamically favorable processes may produce undesired roughness in deep trenches.

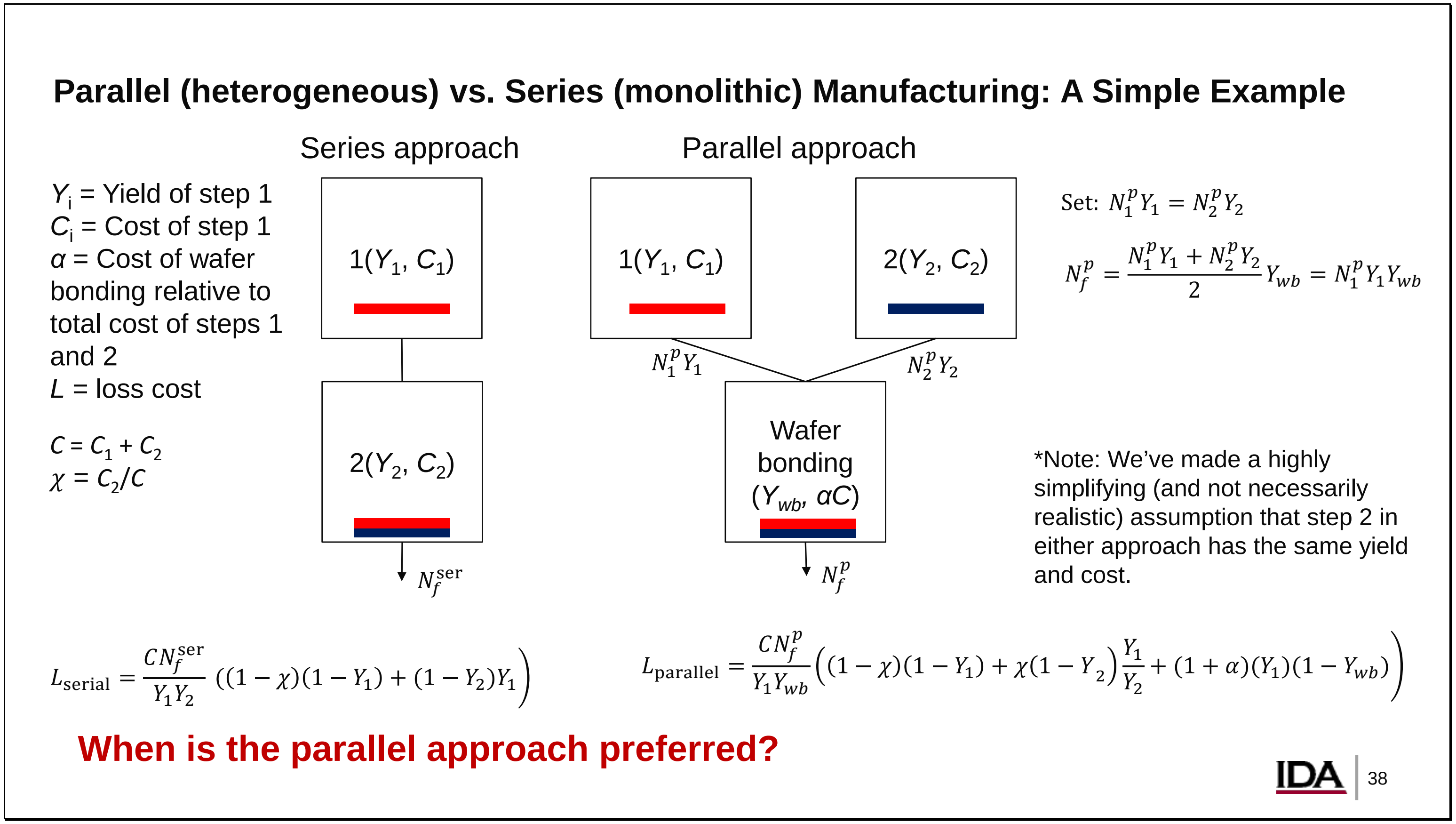

An important manufacturing strategy that has the potential to improve device performance and reduce manufacturing waste is the idea of "heterogeneous" or "parallel" manufacturing. In this approach, rather than trying to fabricate all components of a device into a monolithic substrate (e.g., silicon), different device components are fabricated separately, potentially on different substrate materials, and then the components are combined to form the final system. This slide schematically illustrates these two approaches with a very simplified model.

Here, we consider a multi-layer chip system that can be made in one of two ways. In one approach ("series" or "monolithic"), we attempt to build the system monolithically. In the other ("parallel" or "heterogeneous"), we attempt a wafer-bonding approach after having built two “subsystems” or “sublayers.”

Note that this is overly simplified. There are additional costs associated with attempting monolithic fabrication, such as the need to include protection steps or adapt processes to prevent damage of preexisting structures. At the same time, you might save on other costs associated with needing to have separate deposition systems (equipment) or additional supplies for handling multiple substrate types. If most of the cost of the processing is the substrate material (rather than the processing itself), C_2 could be quite different for the parallel approach than it is in the series approach, because it would need to cover the cost of additional supplies.

The diagram shows that each layer has a fixed yield and cost associated with that manufacturing step and that there is also an additional yield and cost associated with wafer bonding. Here, we define alpha as the cost of wafer bonding relative to the combined costs of fabrication of two layers. The total loss cost of these processes is shown in the equations, where we have required that the total number of wafers successfully manufactured from steps 1 and 2 in the parallel approach is equal, and where we have accounted for the wafer bonding step effectively halving the number of wafers (by combining two wafers into one). By comparing the loss costs of the two approaches as a function of the parameters χ and α, we can understand the conditions under which it makes sense to use either the parallel or series approach.

To put this in context, consider a process in which the yield of step 1 is 90%, the yield of step 2 is 80%, and the yield of the wafer bonding step is 100%. We want to produce 10 final wafers.

For the series process, we will lose one out of every five wafers in step 2. Therefore, we need, on average, 12.5 wafers to go into step 2. We will also lose one out of every 10 wafers in step 1. Therefore, we will need 13.9 wafers in total to begin our process. The expected cost of losses of this approach is given by the sum over lost wafers and associated cost at each step. Since 2.5 wafers are lost in step 2, each of those wafers costs C because they have already gone through the full process. Also, the ~1.4 wafers lost in step 1 each cost $(1-\chi)*C$. So, the total lost cost for the series approach is $C * (2.5 + 1.4\ (1-\chi)) = C*(3.9 - 1.4\chi)$.

For the parallel process, we will lose no wafers in wafer bonding, but we will again lose 1/10 in step 1 and 2/10 in step 2. So, step 1 must begin with 11.1 wafers on average and step 2 must begin with 12.5 wafers on average. Losing 1.1 wafer at step 1 costs $(1 - \chi) * C * 1.1$. Losing 2.5 wafers at step 2 costs $\chi\, C * 2.5$. So, our total lost cost for the parallel process is: $((1-\chi) * C * 1.1 + \chi C * 2.5) = \mathrm{C}\ (1.1 - 1.4\chi)$. So, to produce 10 final wafers, the parallel process will cost 2.8C less than the series process.

When Is the Parallel Approach Preferred?

Steps 1 and 2 are equally expensive

- Low wafer bonding cost
- High wafer bonding yield
- Low individual step yield
- High individual step cost disparity

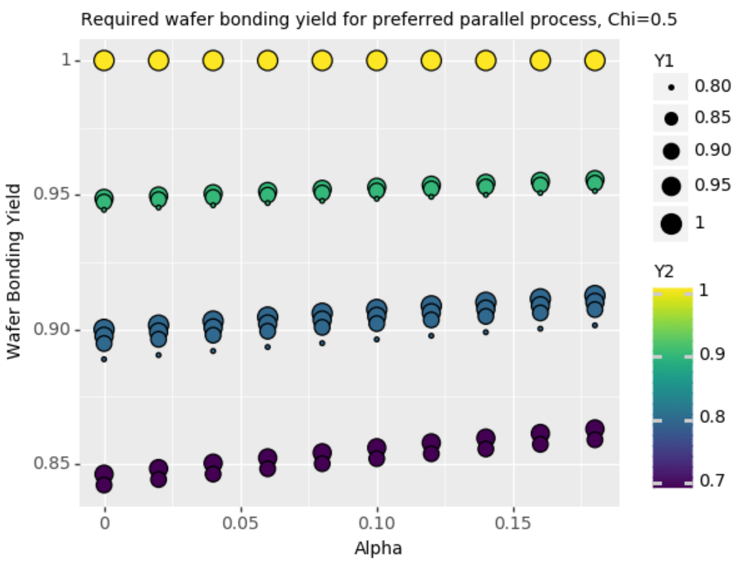

General manufacturing considerations:

- Flow consolidation
- Substrate-specific chemistry
- Parallelization saves time and cost
- Continuous monitoring
- Order of operations

IDA | 39

We can plot the conditions required to ensure that parallel processing will cost less than series processing. Of course, this is all subject to the significant simplifying assumption—not likely in reality—that the yields and costs of subprocesses 1 and 2 are not affected by whether we take the wafer bonding or the monolithic approach.

In general, we see that increased wafer bonding yield and decreased α, as expected, will lead to greater favorability for the parallel-processing approach. Ultimately, costs are saved in parallel processing when there is adequate understanding of the outcomes of each subprocess. This requires in-line monitoring to prevent wasteful follow-on processing. Otherwise, we may falsely believe our subprocess yields are high and lose the benefit of parallel (wafer-bonding) approaches to producing multi-functional structures.

The plot on this slide shows the required wafer-bonding yield as a function of α to ensure that the parallel (wafer bonding) approach is preferred in the case of $\chi = 0.5$ (i.e., the two subprocesses are of comparable cost). With increased yield for the subprocesses, we must have increased wafer-bonding yield to ensure that the final losses for a parallel (wafer bonding) approach are less than the serial losses. This restriction is also greater for higher α (in other words, if the wafer-bonding step itself is expensive, then it also needs to have a higher yield to be worth using).

To analyze a real-world decision set of this type, it would be necessary to allow Y_1, Y_2, C_1, and C_2 to vary, depending on whether the approach is series or parallel. Furthermore, some measure of the performance of the final product is also important in determining the overall value of different manufacturing approaches. In general, however, this analysis illustrates several general facts:

1. De-serialized (non-monolithic) manufacturing of multifunctional components can substantially increase overall processing yield and save manufacturing costs, particularly when:
    a. Wafer bonding (component-combination) steps have high yield and/or low cost.
    b. Subsystems struggle with yield individually and can be manufactured separately.
    c. There are additional savings associated with manufacturing subsystems separately (e.g., fewer processing steps required, less strict requirements on subcomponent starting materials (e.g., purity, roughness, temperature tolerance) or fabrication steps (e.g., resolution), less exquisite/specialized machinery needed, etc.).
2. Taking advantage of de-serialization requires the ability to judge the performance of subprocesses through in-line testing. Costs are saved by detecting fatal defects early in a multistep manufacturing process. With early defect

detection, one can discard partly processed wafers at intermediate steps and avoid wasting cost, time, or materials on later fabrication steps on an already defunct wafer. This requires:

   a. Understanding of fatal defects (what types of defects are fatal in which locations on a die or wafer).
   b. Available methods to detect defects or test device functional performance at intermediate processing steps. For example, one can test the connectivity of electrical components through simple probe tests. Ideally, these methods are *nondestructive, fast,* and can be integrated *in-line.* If in-line and/or nondestructive methods are unavailable, a lot-sampling approach can be used. Such methods will not be infallible.

3. Understanding cost and yield of individual fabrication steps is critical when selecting an overall fabrication approach.

Finally, although this study was inspired by atom chips, it also applies to ideas for heterogeneous quantum chips (Wan et al. 2020)—in that paper, quantum "microchiplets" are fabricated with only a few emitters and attached to larger scale photonic chips produced by more standard and scalable fabrication methods. The idea of "microchiplets" is discussed elsewhere in the briefing.

Nitrogen Vacancies in Diamond: Purity, Positioning, and Photonic Integration

IDA | 40

The Nitrogen Vacancy Color Center

- Workhorse system for solid-state spin qubit type
- Uses:
  - Sensing
  - Ensemble and single spin
  - Quantum information processing
  - Single-photon sources
- Sensitive to:
  - Magnetic field
  - Electric field
  - Temperature
  - Pressure
  - Rotation
- Spin-to-optical and spin-to-photocurrent readout compatible

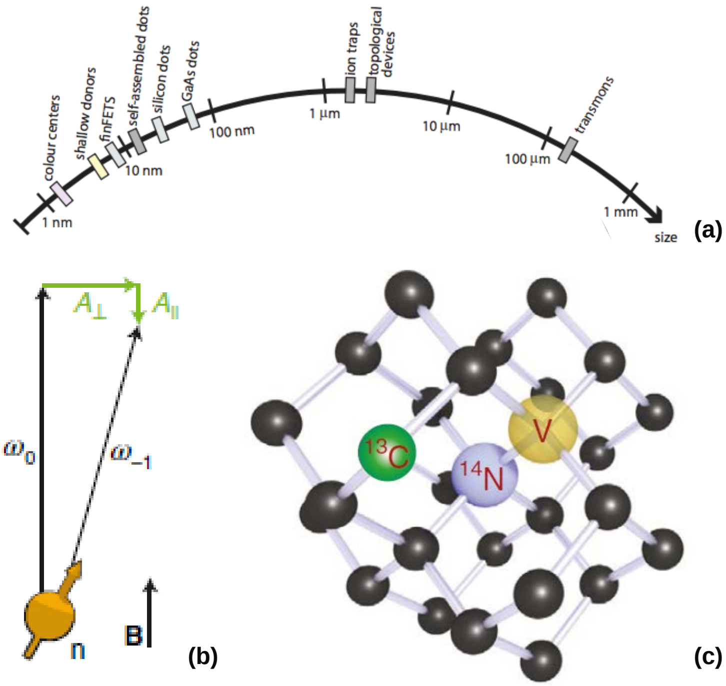

Sources:
Degen, Reinhard, and Cappellaro (2017)
Figure (a) from Acosta (2013)
Figures (b) and (c) from Awschalom et al. (2018)

The nitrogen vacancy color center is a workhorse system for studying solid-state-spin-based qubits. NV centers are of interest for a wide range of quantum-sensing applications, including sensing electric and magnetic fields, temperature, pressure, and rotation. They can be prepared as ensembles or as single-spin systems for applications such as scanning-probe imaging, vector-field sensing, or even quantum information processing. They can also act as reliable single-photon sources, and they are compatible with multiple types of qubit readout (spin-to-optical or spin-to-photocurrent).

The images on this slide illustrate the NV color center, which is a negatively charged defect in diamond in which a vacancy and a nitrogen impurity are in close association within the diamond lattice. The color center will couple with nearby nuclear spins, such as intrinsic ^{14}N and lattice ^{13}C. The sensitivity of the color center arises from hyperfine coupling between a nuclear spin and an external magnetic field. This coupling is a direct sensor of magnetic field, but can also be applied to sensing temperature, rotation, electric field, and pressure. Color centers are very small in size relative to other types of qubits.

The Nitrogen Vacancy Color Center

- Advantages:
  - **Room temperature (RT) operation**
  - Long coherence times (up to a few milliseconds at RT)
  - Optical read/write of spin state
  - Stable in nanostructures
  - Spatial resolution
- Disadvantages
  - Expensive substrates (~$2000 for 0.5 mm x 5 mm x 5 mm)
  - Competing color centers
  - Fluorescence signal collection is difficult
- Fabrication approaches:
  - Direct growth (including delta-doping)
  - Ion implantation
  - Femtosecond laser
  - NV complexes typically formed with combination of irradiation and annealing

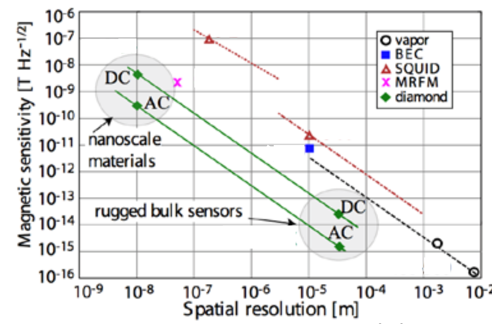

Acosta, V. M. *UC Berkeley*, 2011
*Diamond points are projections

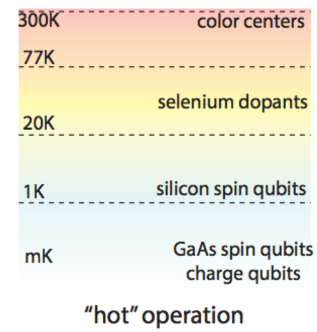

Chatterjee et al. (2020)

Sources:
Degen, Reinhard, and Cappellaro (2017)
Achard, Jacques, and Tallaire (2020)
Awschalom et al. (2018)

IDA 42

NVs have several key advantages, including long coherence times, optical read and write of spin states, and room-temperature operation. NVs can also be fabricated and remain stable inside of nanostructured systems, which further facilitates their integration with photonic read-in and read-out.

NVs do have some key disadvantages, including the cost of fabricating substrates of adequate purity and crystalline quality with required N densities, and associated challenges related to competing color centers in the material. The desired color center is the negatively charged NV- complex; however, neutral defects and substitutional nitrogen defects can add noise to the material.

There are a number of fabrication approaches for making this color center, including direct homoepitaxial growth of doped diamond by chemical vapor deposition, ion implantation, and femtosecond-laser approaches. Direct growth is typically the gentlest method, but without the assistance of irradiation or implantation, it can be difficult to obtain the desired density of NV- defects. Ion implantation, on the other hand, can damage the crystal and has challenging dependencies relating to implantation conversion yield, implantation depth, and spatial resolution. Some of these issues can be mitigated by overgrowth of diamond on shallowly implanted materials and through the use of post-implantation annealing steps. Another option, however, is the femtosecond-laser approach, which can be gentler than ion implantation while still causing NV formation with 3D positioning. It also has the added advantage of easy integration with preparing photonic waveguide structures.

All these approaches are typically followed by irradiation or annealing steps (or both) to either create vacancies or cause vacancies to migrate to the sites of N and form the NV- complex.

Nitrogen Vacancy Ensemble Magnetometers

Spin-projection-noise-limited sensitivity — $\eta_e \propto \dfrac{1}{C_e \sqrt{NRT_2^*}}$ — Spin dephasing time

$T_2^* \sim \dfrac{1}{[^{13}C]}$ (Dilute limit of $^{13}C/^{12}C$ << 0.01)

$T_2^* \sim \dfrac{1}{[N_S^0]}$ (unirradiated N-rich diamond)

Spin readout contrast → Degraded for large ensembles – manage by:
(a) Controlling orientation of spins
(b) Minimizing competing nitrogen defects

Number of non-interacting spins → Option 1: Increase spin density (higher NV-defect density)

Number of detected photons → Option 2: Improve photon collection efficiency (better engineering of geometry and interfaces)

Spin dephasing time → Option 3: Improve substrate quality (purity, crystallinity, isotopic enrichment)

Excellent crystalline quality and high defect density are conflicting goals!

Sources:
Achard, Jacques, and Tallaire (2020)
Barry et al. (2020)

IDA 43

This slide shows that the spin-projection-noise-limited sensitivity of NV ensemble magnetometers is affected by several factors, including spin readout contrast, number of non-interacting spins, number of detected photons, and the dephasing time of spins. One can increase the number of spins in the ensemble by increasing the density of NV defects. Or, one might attempt to improve photon-collection efficiency by engineering the geometry or photonic interfaces of the device. One might also try to lengthen the spin dephasing time by improving substrate quality, which might involve increasing chemical or isotopic purity or obtaining a crystal of higher quality (e.g., fewer strain or dislocation-type defects). A final option is to consider improving the contrast of the system by fabricating a device with a higher proportion of spins in a particular orientation (which will detract from any goals of vector-field sensitivity) or by biasing the material toward a higher probability of N forming the NV- complex as opposed to other color centers (such as the neutral NV defect).

Methods exist to achieve each of these different goals, but they have trade-offs. For example, simply increasing the concentration of nitrogen in the crystal can significantly degrade crystalline quality, such that it may be difficult to grow single crystals, or there may be many strain and dislocation-type defects left in the structure. Also, increasing NV defect density tends to degrade the spin-readout contrast for the device. Engineering a good NV ensemble magnetometer is closely tied to both diamond-substrate engineering (to improve coherence time) and photonics engineering (to improve the collection efficiency).

From Barry et al. (2020), the neutral substitutional nitrogen defect is the primary contributor to the electronic spin bath in unirradiated N-rich diamonds, and the decoherence time is inversely proportional to the concentration of these defects. However, Hahn echo pulse sequences can mitigate contributions to NV- spin dephasing time due to N effects and allow the decay time of the NV- spin state to approach the coherence time T_2, which is longer than the inhomogeneous dephasing time T_2* by orders of magnitude.

It is also worth mentioning that alternative sensing schema and approaches, such as AC sensing, spin bath driving, applying a bias magnetic field, and double-quantum coherence magnetometry can be used to improve coherence times, contrast, and collection efficiencies. (Barry et al. 2020)

In addition to spin-projection-noise, photon shot noise also limits the sensitivity of NV centers. According to Le Sage (2012), photon shot noise limits the sensitivity of NV centers to 0.1 nT/√Hz. When a device is shot-noise limited, the $m_s = 0$ NV center state is tracked with sensitivity $\Gamma/(\gamma\sqrt{N_0})$, where Γ is the full-width half-maximum of the optically detected magnetic resonance peak, γ is the electron's gyromagnetic ratio, and N_0 is the fluorescence intensity of the $m_s = 0$ state.

Diamond NV Device Fabrication—Substrates

- Typical approach: Chemical vapor deposition (CVD) growth of compositionally and isotopically controlled single-crystal diamond on a high-pressure, high-temperature (HPHT) diamond substrate, followed by irradiation and annealing steps to convert N to NV-defect
  - CVD is only practical for thickness less than a few micrometers
- Diamond purity directly affects sensitivity and permissible NV density
- Optimal NV-density range: 10^{15}–10^{17} cm^{-3}
  - Corresponds to a spacing between NV of 21–100 nm.
- Only a few companies produce the necessary diamond quality for NV-center devices

Sensitivity as a function of NV density for different paramagnetic impurity densities

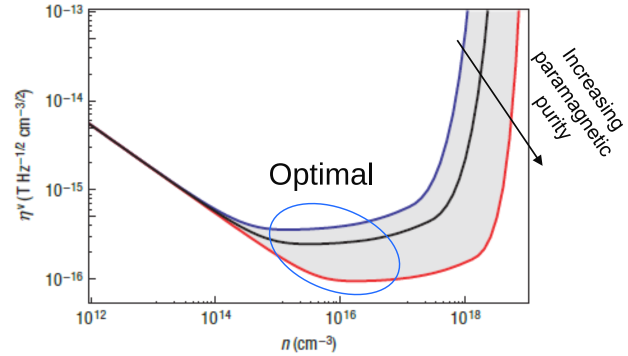

Taylor et al. (2008)

Need: Lower cost methods of fabricating high-purity and isotopically enriched diamond at wafer scales (greater surface area and thickness) + standards defining quantum-grade diamond quality.

Source: Achard, Jacques, and Tallaire (2020)

IDA | 44

Obtaining a high-quality, single-crystal diamond substrate is a requirement for any NV-based quantum sensor. The typical approach for fabricating such substrates is to grow highly controlled films of diamond by chemical vapor deposition on a high-pressure, high-temperature (HPHT) diamond substrate. HPHT diamond can be fabricated near centimeter scale with good crystalline quality; however, it is difficult to achieve this while maintaining the necessary chemical and isotopic purity that permit long coherence times for quantum sensors (Achard, Jacques, and Tallaire 2020). There is an optimal range of impurity density in diamond that maximizes the density of sensors without allowing individual NV to interact; this is shown in the figure on the slide. Notably, increasing paramagnetic purity allows for a higher density of NV sensors for the same coherence time. Note, however, that isotopic noise can be mitigated through dynamic nuclear-polarization methods (Achard, Jacques, and Tallaire 2020).

Since the device layer of most quantum sensors can be quite thin (micrometer-scale) and need not fill the thickness of a wafer, CVD approaches to fabricating the device layer are preferred and less wasteful than direct implantation and annealing of HPHT diamond. CVD allows much better control of the composition (including isotopic purity) of the diamond, which in turn enables longer coherence times. However, it is difficult to obtain NV densities above 100 ppb with CVD-grown diamond. So there is a gap between HPHT diamond (which usually has a too high concentration of N impurities, which degrades coherence times) and CVD diamond (which does not obtain optimal NV density but has long coherence times).

Unfortunately, only a few companies currently fabricate CVD diamond (perhaps the most well-known is Element Six, a component of the De Beers Group), which limits the supply options. This type of diamond is also quite expensive (the going rate at Element 6 is~$2000 for a 0.5 mm × 5 mm × 5 mm sample). Also, HPHT diamond substrates are limited to only centimeter-scale. To enable NV-based quantum sensing to compete with other types of sensors, the cost of these substrates needs to decrease while the size (especially the surface area) needs to increase. Wider area substrates allow for more efficient use of area-exposure fabrication methods and also reduce substrate waste due to edge effects.

Therefore, we require lower cost fabrication methods for quantum-grade diamond, especially at larger areas. Furthermore, standards defining diamond quality are lacking for quantum-sensing purposes; such standards would need to include information on chemical and isotopic purity, microstructural features (strain, dislocation density, etc.), and possibly even information on the concentration of different types of charged point or cluster defects in the diamond.

Research Areas for Improved Diamond Substrate Fabrication

- Geometrically defined epitaxy
- Lift off and transfer (saves the expensive substrate)
- Alternative substrates (heteroepitaxy)
  - Strain management is difficult
- Methods to enhance defect conversion to NV-
  - Limited by difficulty of measuring concentrations of the different types of NV-defect in thin films!

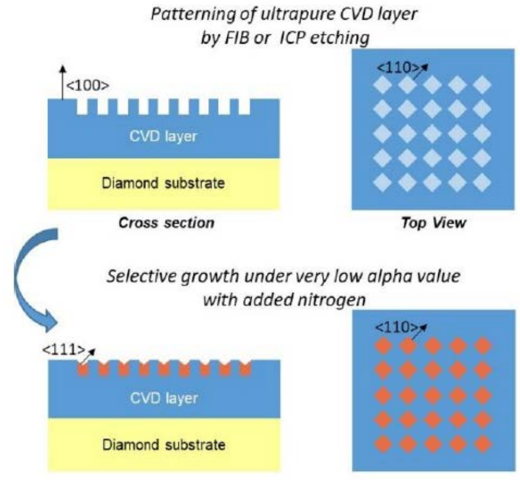

Geometrically-defined epitaxy– holes are about 6 μm in side length

Achard, Jacques, and Tallaire (2020)

Because of this need for less expensive quantum-grade diamonds, some outside-the-box fabrication methods have been proposed, including the use of geometrically defined epitaxy, lift-off and transfer methods, heteroepitaxy on less expensive base substrates, and methods to bias defect conversion to the desired NV- defect. Each of these methods has important limitations. Geometrically defined epitaxy can achieve systematic defect placement, but limited defect density. Lift-off and transfer methods need a way to separate and then attach the device layer to a new substrate without damage. Heteroepitaxy struggles with strain management that produces unwanted defects, and methods for defect conversion are not very advanced because we do not have adequate characterization tools. These suggestions provide several areas for further research.

Ion-Implantation to Form NV-rich Diamond

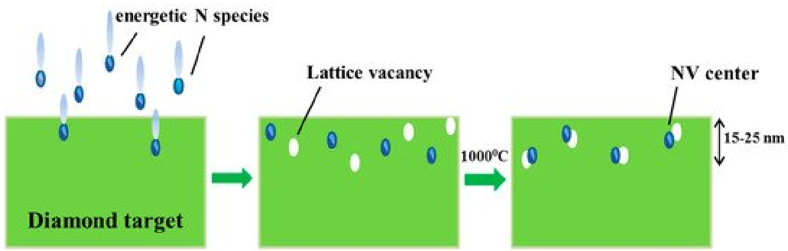

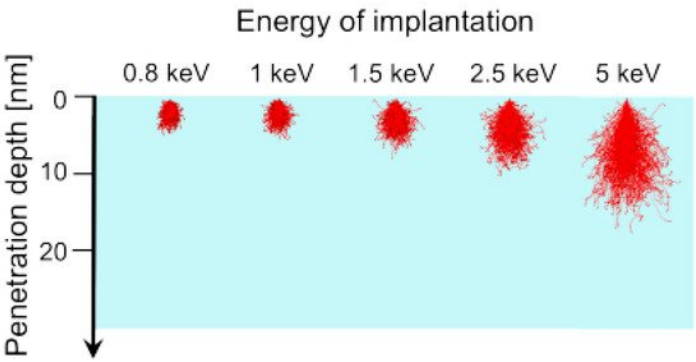

Advantages:
Depth control, well-understood
Works for many ions
Can work with lithography

Drawbacks:
Interdependent depth, straggle, spread, and NV- yield
Crystal damage degrades coherence times—high-temperature annealing required to heal crystal
Positional precision may require direct-write approach (slow) and be degraded by annealing steps

Source: Haque and Sumaiya (2017)

IDA 46

Beyond the diamond fabrication itself is the introduction of the desired NV- defect. As mentioned on the prior slides, there are multiple means of doing this. In this analysis we will focus on two: ion implantation and femtosecond-laser fabrication.

This slide shows ion implantation to form NV-rich diamond. Ion implantation has many advantages, including depth control, extremely well-understood kinetics, broad applicability to different types of implanted defects, and compatibility with lithography (which enables precise defect placement). However, it has a few crucial drawbacks, including in particular the inability to independently control the depth, straggle, spread, and NV- conversion yield of defects made by this method. In ion implantation, these variables are closely linked. Furthermore, ion implantation is harshly damaging to the crystal, and annealing is necessary to both convert defects to NV- and heal the crystal after implantation exposure. This high-temperature annealing (typically between 800 and 1000 °C for 1 to 10 hours) can limit the fabrication steps that can be done before the implantation. Finally, to have excellent positional precision with this method, it is necessary to use a direct-write approach. The annealing step also causes additional defect migration that undercuts the effectiveness of direct-written defects.

Precision Ion Implantation in Photonic Structures: A Manufacturing Perspective

(i) Create silica etch mask by e-beam lithography
Slow, direct write process!

(ii) Standard reactive-ion-etching (RIE)
Straightforward step – least concern

(iii) Angled RIE
Standard method, but needs specialized equipment

(iv) Cleaning
May need slight modifications from standard methods to work for diamond substrate

(v) Targeted ion implantation to produce color centers
Crystal damage. Slow, direct write process.

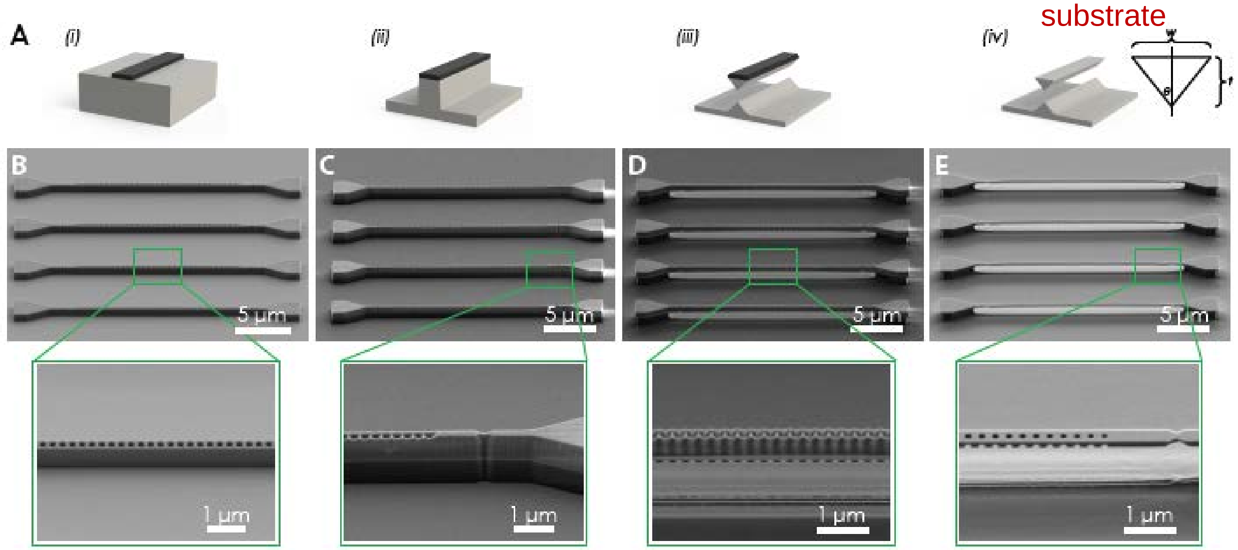

(vi) Annealing up to 1200 °C over 36 h
Low T anneal forms SiV, high T anneal relieves step (v) crystal damage, but hurts positional precision. 1200 °C could damage non-diamond structures.

Sipahigil (2016, Supplementary Material)

IDA 47

This slide gives a bit more of the manufacturing perspective on ion-implantation methods when used for precise positioning. While this example was actually implanting SiVs in diamond, the principle is similar for NVs. What is shown here is a set of fabrication steps where the goal was to precisely place SiVs in photonic waveguides fabricated from diamond. This paper reported on a proof-of-concept from academia that was interesting because of this integration of photonics and ion implantation. However, if this method were to be scaled up for manufacturing of many devices, a number of considerations come into play. These are highlighted in the red text on the slide. For example, there are multiple direct-write processes here—this will be very slow, and the high-temperature-annealing step at the end limits the kind of integrated structures that can be attached to this device before that step. We would like to see increased reporting on these concerns, as well as metrics such as yield and fabrication speed, in academic literature.

Source: Sipahigil et al. (2016).

Femtosecond Laser Fabrication Methods

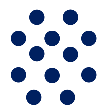

To start, we have an equilibrium structure in a **transparent** material (e.g., diamond, glass)

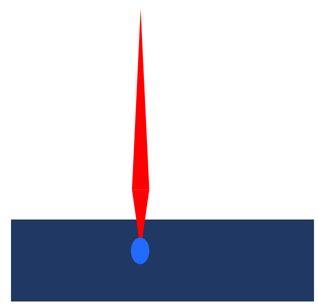

A focused laser pulse introduces **heat**, **stress**, **disorder**, and **defect states**, depending on the selected parameters

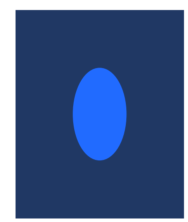

The illuminated region gains **different properties**, such as refractive index, etch rate in solution, diffusion coefficient, etc.

The exact effect depends on the **substrate material** and the **laser pulse parameters**

The laser's resolution is about 1 μm

Possible results:
Waveguides
Diffraction gratings
"Lithography"
Defect (qubit) formation
Controlled diffusion of existing defects
Ablation
Polishing

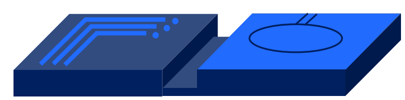

Advantages:
Flexibility
3D and buried structures
In situ monitoring
Error correction

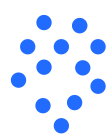

Drawbacks:
Direct write—slow
Rough horizontal surfaces need to be polished

IDA 48

Compare the ion-implantation approach to a femtosecond-laser fabrication approach. This schematic explains the femtosecond-laser approach to NV formation, which is a particularly interesting approach because of its potential to enable integrated fabrication of precisely placed NV defects and photonic structures. The approach is described as follows:

1. Start with an equilibrium structure in a transparent material such as diamond or glass.
2. Irradiate the material with a focused laser pulse. This introduces heat, stress, disorder, and/or defect states in the material. However, the exact effect on the material can be tuned using laser parameters, such as pulse power and duration. The focus of the laser pulse can be at approximately the 1 μm level.
3. Once it has been irradiated (or during irradiation), the illuminated region will have different properties. Depending on the substrate material, these might be slightly different density, which can change refractive index, or a change in the local bonding structure of the material that may change its etch rate in certain solutions. If defects (vacancies) are produced or present, laser pulses can also be used to encourage migration of those defects by activating diffusion. So, for example, you can introduce vacancies with a higher energy laser pulse and encourage diffusion of those vacancies with lower energy laser pulses.
4. Sometimes, this process could be followed by an annealing step to cause such defect migration instead.
5. Many structures can be fabricated this way, including waveguides, diffraction gratings, and precisely placed defects. When coupled to a follow-on etch, lithography can also be facilitated this way for certain substrate materials. Finally, laser pulses with the same laser can also be used for ablation and polishing.

There are a lot of advantages to this approach, including the ability to do all these steps together in one system, which avoids transferring between machines and probably leads to less strict environmental requirements during fabrication. Furthermore, this approach incorporates flexibility in terms of both the substrate in question and the type of defect created (for qubit formation). For example, with diamond, this method should be able to make NVs or SiVs, depending on how the diamond is doped. The advantages of this technique for fabricating nitrogen vacancies are clear, however, relative to ion implantation: the resulting structure should have improved crystalline quality (and therefore better coherence times) than an ion-implanted device; moreover, this approach can allow excellent alignment with photonic structures, which enables efficient photon collection. Both these factors would result in increased sensitivity.

There are also some drawbacks. This is a direct-write method, which can be slow, and the resulting horizontal surfaces from lithography of glass with this approach may need to be polished in an additional step if photonic devices are the goal. Next, we will consider direct-write approaches for a different type of defect, specifically, phosphorus dopants in silicon.

References

Bharadwaj et al. (2019).

Hadden et al. (2018).

Wu et al. (2019).

Phosphorus Dopants in Silicon

IDA | 49

Hydrogen Depassivation Lithography (HDL)

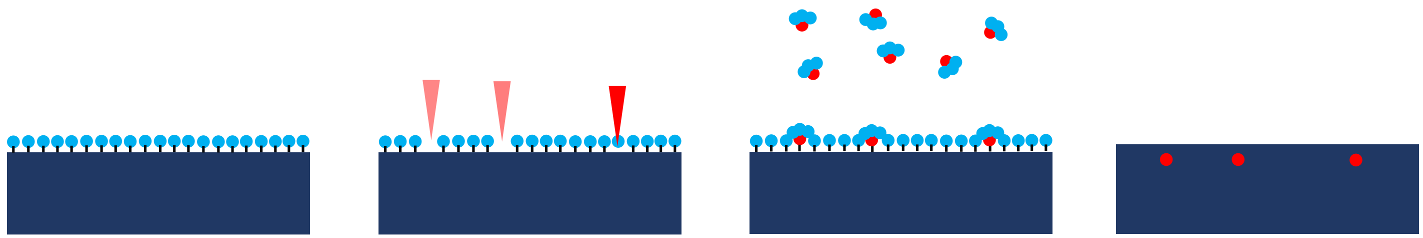

Clean substrate: H-terminated (100) Si substrate, possibly with fiduciary marks, and a 2x1 surface reconstruction

Selectively remove H atoms: Uses a scanning tunneling microscope

Expose to dopant carrier gas: Typically phosphine, which adsorbs to exposed Si sites

Annealing and Si-overgrowth: Dopants incorporated at atomically precise locations and depth

Advantages:
True atomic-scale precision
In situ monitoring
Error correction
Non-damaging to crystal

Drawbacks:
Direct write—slow
Hardly developed for alternative substrates, orientations, or dopants
Instrument drift control is a problem

IDA | 50

This slide introduces the fabrication method known as “hydrogen depassivation lithography.” This method can be used to precisely place P dopants in Si with nanometer-level precision. This slide shows the steps in this method, which is based on integration of a scanning-probe microscope. The method has a number of advantages, including true atomic scale precision, the ability to do in-situ monitoring and error correction of P placement, and minimal damage to the crystal. However, as a direct-write method it is slow, and it has also been developed in particular for this specialized P-doped-Si system. Alternative dopants and substrates remain largely unexplored with this method. Finally, over large areas, instrument drift control for this method is quite challenging; fiduciary marks and instrument isolation are essential to ensuring proper alignment of dopants and structures.

Atomically Precise Doping in Si—A Qubit with Scalable Potential

- Single-phosphorus dopants in Si placed with atomic precision enable controllable two-electron spin correlations
  - Requires inter-donor distance of 13-14 nm, with ~20 nm placement relative to a readout structure
- Potential for scalability for quantum computing
  - Si platform—very small qubits, integration with established CMOS methods*
  - Excellent charge offset drift and stability
- Cryogenic operation
- Remaining manufacturing needs:
  - Low-temperature post-doping steps, such as epitaxial Si overgrowth
  - Accelerated HDL with error correction or an alternative method of P placement
  - Metrology for device layer characteristics (e.g., phase coherence length)

Sources:
Broome et al. (2018)
Wyrick et al. (2019)

*With restricted processing temperature to maintain P positioning accuracy!

IDA | 51

We discuss HDL because it is currently the means by which an interesting type of qubit for quantum computing can be fabricated—single-phosphorus dopant in Si. This type of qubit is actually a two-electron spin-correlated system that relies on precise inter-donor distance (13–14 nm) to allow the qubit to be at the right level of controllability and stability. This type of qubit is interesting because it is built into Si and shows excellent stability characteristics, at least in cryogenic operation. These qubits have the potential to be very small (on the scale of square micrometer, rather than on the scale of square-millimeter like for trapped ion or superconducting qubits) and to be manufactured in conjunction with conventional integrated-circuit manufacturing methods. Single phosphorus atoms in Si have demonstrated a noise floor of 18 pT/√Hz, making them very sensitive to tiny magnetic field variations. Dopant spins in silicon also rank among the most coherent solid-state quantum systems, which makes this approach interesting for memory applications (Broome et al. 2018; Wyrick et al. 2019; Chatterjee et al. 2020).

There are still some concerns about this type of qubit: it still needs to be operated at cryogenic temperatures, and there are limitations to current manufacturing capabilities. For example, because the placement of the phosphorus dopants is so critical, post-doping fabrication steps need to be temperature limited to avoid diffusion of those dopants. This includes necessary steps like Si overgrowth that can be challenging to conduct at low temperature. In addition, HDL is direct-write, and though it has interesting advantages detailed on the previous slide, it is slow. This method will need to be sped up (e.g., by using parallelized SPM probes) or a substitute found.

Finally, inspection of integrated devices containing such qubits is currently difficult. Better metrology tools will be needed to confirm that qubits are present and of adequate quality and that they are integrated with the main structure. Ideally, such metrology would also be possible to do in an automated or in-line way.

Case Study: Fabrication Precision and Yield

52

Now that we have discussed some methods of fabricating different types of quantum systems with precision, we will describe a short case study investigating the relationships between fabrication precision and yield.

Case Study: Fabrication Precision and Yield for Direct-Write Approaches

- The goal: Produce an $N \times N$ array of qubits on a two-dimensional area using a direct write fabrication process.
- Variables:
  - *q* - Likelihood of forming exactly one* qubit in a given write attempt
  - *r* - Difference in position of a written qubit relative to desired write location
  - Acceptable write precision when $r < z*\sigma$, where σ is the standard deviation of the fabrication technique's positional placement and we assume that the write technique exhibits normally-distributed positional accuracy

$$P(0 \text{ failures in } N^2 \text{ attempts}) = (q(1 - 2 \times CDF(-z\sigma)))^{N^2}$$

CDF = Cumulative Distribution Function (normal distribution)

*Some physical qubit fabrication approaches merely require that at least one qubit is formed at each location

IDA 53

Consider a process in which we wish to produce an $N \times N$ array of qubits on a 2D area using a direct-write fabrication method. There are a number of variables that we must consider when trying to understand what the yield of the fabrication process will be:

- Product tolerances—what defines a successful result?
- The number of "failed" qubits we can tolerate.
- The positional tolerance the qubits must satisfy.

What characteristics of our starting materials and processing steps determine the likelihood that we will successfully create each qubit?

- Likelihood of forming exactly one qubit in the write location (as opposed to zero or more than one). Note, however, that some physical qubit-fabrication approaches merely require that *at least one* qubit is formed at a given address. For this example, however, we will require exactly one qubit to form.
- Difference in position of a written qubit relative to desired write location, defined as r.

These values will also depend on other variables, such as:

- The starting purity of the substrate or local variation in substrate properties. For forming NV color centers, this will affect the likelihood of forming exactly one qubit in the write location.
- If an annealing step is involved, then annealing time or temperature could affect the migration of a written "defect" from the write location or the likelihood of formation of the desired species in the first place.

Here we present a simple example based on four variables. We require that there can be no failures in the $N \times N$ grid of qubits for the product to be deemed acceptable. The probability of 0 failures in an $N \times N$ grid of cubits will be given by the binomial distribution where p denotes the probability of success at each position, under the assumption (a good assumption, for direct write) that each write's success or failure is independent of the success or failure of the other writes:

$$P(0 \text{ failures in } N^2 \text{ attempts}) = p^{N^2}$$

We define positional tolerance in terms of a *z*-value relative to the precision of the fabrication technique. Let the technique's positional precision (defined as the distance *r* between the actual qubit position and the target position) be defined by a normal distribution with mean 0 and standard deviation σ. Note that *r* is defined as $|\rho|$ as drawn from this distribution, since *r* is always non-negative. The positional tolerance of the product will be described by *z*, where *z* represents the multiples of σ that can be tolerated. So, assuming a qubit is formed successfully, we need to know the likelihood that it is also formed within the appropriate tolerance range. In other words, we need to know the probability that the distance *r* between the qubit location and the target location is less than $z\sigma$.

- The probability of forming a qubit at all for a given write is given by *q*.
- The probability that a qubit formed is within the permitted tolerance of the write target is given by $P(r < z\sigma)$, which is determined using the cumulative distribution function of the normal distribution, keeping in mind the role of absolute value in defining *r*:

$$P(r < z\sigma) = q*(\mathrm{CDF}(z\sigma) - \mathrm{CDF}(-z\sigma)) = q(1-2*\mathrm{CDF}(-z\sigma))$$

So, for a given write position, the probability of *successfully writing a qubit within tolerance* is given by:

$$p = P(\text{qubit formed}) * P(r < z\sigma \mid \text{qubit formed}) = q * (1 - 2 \times CDF(-z\sigma))$$

Therefore:

$$P(0 \text{ failures in } N\text{^}2 \text{ attempts}) = p^{N^2} = (q * (1 - 2 \times CDF(-z\sigma))^{N^2}$$

Case Study: Fabrication Precision and Yield for Direct-Write Approaches

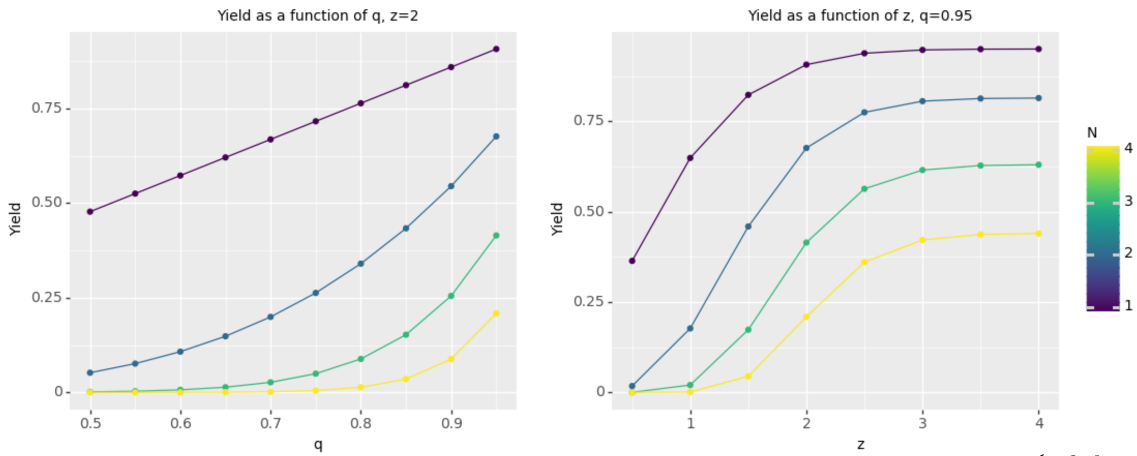

q = probability of forming exactly 1 qubit in one attempt ($0 \le q \le 1$)

z = permissible positional tolerance in units of method accuracy standard deviation

Can be recast in terms of annealing time and temperature for annealing-based methods

$$P(0 \text{ failures in } N^2 \text{ attempts}) = (q(1 - 2 \times CDF(-z\sigma)))^{N^2}$$

Increased *q* and *z* permit improved yield. Increased array size decreases yield.

IDA | 54

We can produce simple figures showing the probability of success in an *N*×*N* grid as a function of *N*, *z*, and *q*. These figures show that for large *N*, it becomes increasingly essential that *q* is as close to 1 as possible and *z* is as large as possible. To have a perfectly successful array of qubits, we need the formation of the qubits to be reliable and within tolerance. The possible yield quickly reaches a plateau as a function of *z* for fixed *q*: 95% reliability of forming each qubit is only 44% yield when the goal is to make 16 qubits.

This means that direct-write techniques will only be successful for large arrays of quantum dots if they can (1) detect failed writes and correct them and (2) ensure that annealing and other post-processing steps do not allow qubits to migrate outside the permitted tolerance range.

Effect of the Annealing Time and Temperature

Assume: $\sigma \propto \sqrt{Dt}$ $D \propto \sqrt{e^{-E_a/kT}}$ (Arrhenius dependence of D on T)

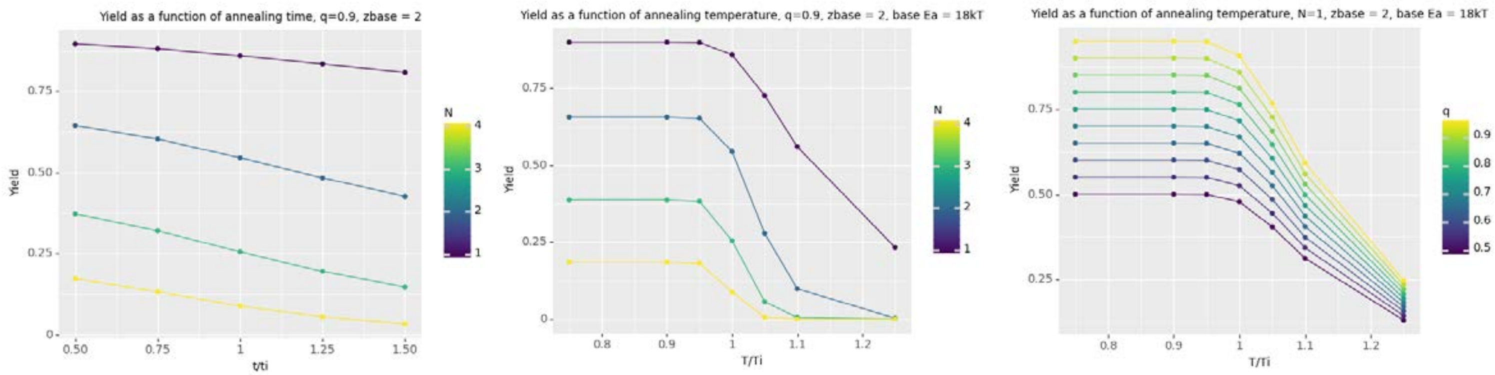

q = probability of forming exactly 1 NV in one attempt
zbase = permissible positional tolerance for $T = T_i$ and $t = t_i$
D = Diffusion coefficient
T = Annealing temperature
t = annealing time
σ = fabrication technique's positional precision
Subscript i denotes reference point for time and temperature

***T* and *t* give coarse and fine control of yield, within limits.**
This example does not account for the effect of *T* and *t* on *q*.

IDA 55

Let us consider next the effect of annealing time and temperature on these yields in processes that use an annealing step to cause a written defect to migrate to a location that will form the desired quantum state. We will use the concept of the "diffusion length" to understand the effect of time and temperature on the yield of the process.

The diffusion length of a mass-transport process is typically proportional to $\sqrt{(Dt)}$, where D is the diffusion coefficient (units of length^2/time) and t is time. Depending on the initial and boundary conditions, various coefficients may be applied to this diffusion length to define the typical distance that a species will move over time t. In the context of this example, we will not select any particular coefficient, but instead consider scaling laws.

Let us assume that the standard deviation σ of precision for a given annealing step is proportional to the diffusion length and that σ is therefore proportional to the square root of annealing time. Moreover, the temperature affects σ, because the diffusion coefficient will typically have an Arrhenius dependence on temperature.

As we have noted, a critical parameter in determining the yield of a given method is $P(r < z\sigma)$. More accurately, there is a fixed diffusion distance R that is the threshold of tolerance for the device. So, we can also write $P(r < R)$ and see that $R = z\sigma$, meaning that $z = R/\sigma$. In this case, both z and σ are functions of t and T. Since σ is proportional to $\sqrt{t}$ and $e^{-Ea/2kT}$, then z is inversely proportional to those quantities.

So, let us consider a process where we start with a value of z equal to 2 (process positional precision standard deviation σ is 1/2 of the required tolerance bound R). If we double our annealing time, then our diffusion length will increase by a factor of 1.4, which will in turn decrease the permissible value of z to 1.4, or 71% of its original value.

If instead we cut our diffusion time in half, then the value of z will increase by 40% to 2.8.

The dependence on temperature is more complicated. A typical activation energy for near-surface diffusion of vacancies in diamond may be estimated at 2 eV, or about 18 kT at 1000 °C (annealing temperature used in Hadden et al. 2018). Decreasing the annealing temperature by 10% causes the permissible value of z to increase by a factor of 2.46. Increasing the annealing temperature by 10%, in contrast, moves the permissible z to 40% of its original value. These small analyses show how sensitive the yield of these processes may be to the choice of t and T. In general, sensitivity to temperature fluctuations will be greater than sensitivity to time fluctuations.

The plots on this chart illustrate these dependencies. They show that time gives finer control over precision, while temperature gives more coarse control. They also show the importance of q and N in limiting the ultimate yield result. In particular, decreasing T only helps up to the point when q takes over in dominating the failure rate (the limit of p as z approaches infinity is q).

Note, however, that adjusting annealing time and temperature will likely affect the value of q as well. Increasing either variable could increase the likelihood of forming NVs using the femtosecond laser-writing method, but whether that translates to an increase or decrease in q will depend on the initial concentration of nitrogen in the sample. If there is a high concentration of nitrogen, then q may decrease because of the possibility of multiple-NV formation (recall that we want to form *exactly one* NV per write). In contrast, if there is a low nitrogen concentration, increased annealing time or temperature could increase the value of q.

Direct-Write Precise Qubit Array Formation: Practical Yield Examples

Method	Estimated *q*	Estimated *σ*	Application tolerance, *R*	Expected yield for 5×5 array	Reference
NV written by fs laser, quantum-grade diamond	0.31 ± 0.09	0.2 – 0.85 µm	1 µm	10^{-13}-10^{-16}	Hadden et al. (2018)
NV written by fs laser, optical-grade diamond	0.6 ± 0.2	~100 nm	1 µm	10^{-6}	Bharadwaj et al. (2019)
NV written by fs laser, optical-grade diamond, laser-induced diffusion	0.96	50 nm	1 µm	0.36	Bharadwaj et al. (2019)
HDL, P doping in Si	> 0.95	Unclear, estimate ~0.1 nm	0.5 nm	0.28	Randall et al. (2020); Broome et al. (2018)

Untenable

Workable, but still not great…

IDA 56

Let us consider actual values from published literature. We will focus on two direct-write methods of qubit formation with different applications. The first is femtosecond-laser writing of NV in diamond near prefabricated waveguides (also written using the femtosecond-laser method). We will explore a few modifications of this technique. Then we will discuss hydrogen-depassivation lithography, which can be used to write single P dopants with nanometer-scale precision in Si.

Hadden et al (2018) studied the use of femtosecond-laser writing to create waveguides and nitrogen vacancies in diamond. They used an annealing time of 3 hours and an annealing temperature of 1000 °C, with a 5 ppb nitrogen-content "quantum-grade" diamond target. Following Orwa et al. (2012), the Arrhenius coefficient for vacancy diffusion near a diamond surface is $3.6*10^{-6}$ cm^2/s, and activation energies for vacancy diffusion in diamond have been reported ranging from 1.7 to 4 eV. Vacancy diffusion is generally highest near the surface of diamond. We can therefore estimate an upper bound on the diffusion coefficient by using an activation energy of 1.7 eV. With 1.7 eV, the diffusion coefficient at 1000 °C should be about $6.7*10^{-13}$ cm^2/s, producing a diffusion length in 3 hours of approximately $8.5*10^{-5}$ cm, or 0.85 μm. With an activation energy of 2 eV, the diffusion length is ~0.2 μm. The defects created in these samples are at a depth of ~25 μm, which could be considered near-bulk; however, the actual precision of the technique appears to be on the order of hundreds of nanometers, suggesting that the activation energy for diffusion here is closer to the low end of the range, from 1.7–2 eV.

Hadden et al. (2018) achieved "single NV formation probability of 31 +/- 9%," or $q = 0.31$. They also seemed to consider 1 μm to be an adequate positional tolerance for their application of aligning NV within 13 μm waveguides. This is 1.2× the diffusion length estimated using 1.7 eV, and 5 times that estimated with 2 eV.

Bharadwaj et al. (2019) reviewed femtosecond-laser fabrication of NV centers, including a chart showing the likelihood of single NV formation as a function of laser pulse energy in optical-grade (high nitrogen concentration) diamond. This showed a peak of $q = 0.6$ at a pulse energy of 26 nJ in the example referenced and a spatial confinement <1 μm^2. Because of the higher density of nitrogen in optical-grade diamond, it is likely possible to tune annealing parameters to decrease the actual σ for this method. We estimate that σ can be decreased to on the order of ~100 nm. In optical-grade diamond, there are between 20,000 and 200,000 nitrogen atoms per cubic micrometer, which translates to ~20–30 nm between N atoms. However, the starting position of the vacancy will have some randomness relative to the intended focal point of the laser beam.

One method to improve the spatial confinement of this method is laser-induced vacancy diffusion, rather than thermal annealing. In this method, vacancy diffusion is induced by using a train of low-energy (19 nJ) femtosecond-laser pulses that guide diffusion within the focal volume of interest until a vacancy forms. This method was shown to yield single NV centers with a q of 96% and 50 nm positioning accuracy. There is a time and instrumentation trade-off here—live monitoring of each individual NV with fluorescence emission is necessary to determine when to cut off the diffusion pulses—but this also helps ensure that only single NVs are formed at each site (giving high q). Also, although each write step takes longer, the multi-hour annealing step at high temperature is avoided. For a very large array of vacancies, that may not save time, but avoiding high-temperature annealing could allow a greater variety of upstream structures to be fabricated that might otherwise be damaged by high-temperature exposure.

Contrast these numbers with the values we might see for hydrogen depassivation lithography, or HDL. In HDL on 2×1 surface reconstructed Si, the spot size is sub-nanometer (~0.4 nm), and the pixel write zone is ~0.77 nm^2 (Randall et al. 2020). Writing anywhere in that zone should ensure that the eventual dopant position is at the target lattice site. Challenges in dopant placement arise in the form of thermal drift and creep hysteresis that can affect the exact positional accuracy, but there is some tolerance to slight probe positioning errors that makes it easy to ensure single chemisorption of PH_3 at each write position. Therefore, with this method z is governed by the instrument's vibrational and thermal isolation, calibration, and fiduciary marks used to ensure correct positioning. The method also has the ability to detect and correct write failures using an in situ imaging mode. This translates to a high value of expected q. With high q and high z, this method has the potential for very high yield. The application for this type of lithography is coupled-donor systems that need to be a very precise distance apart; therefore, the tolerance R for dopant placement is only about ±0.5 nm (Broome et al. 2018).

The table contrasts the expected yield of these four methods for direct-writing qubits based on our four-parameter model. The yield for a 5×5 array is at best 36% (for femtosecond-laser NV formation in optical-grade diamond with laser-induced diffusion). Some improvement in σ for the techniques may be possible through optimizing annealing time and temperature or improved control over substrate composition, but q is actually dominating the yield for all these examples. Improvements in q are managed through use of active monitoring of qubit formation and error correction (if the first write fails, try again). Also, if the application allows multiple color centers at a given location (instead of exactly one), this can increase q. This shows the importance of optimizing q and σ to make even a small array of qubits by direct-write methods. A yield of 36% might be acceptable for certain price points, but a yield of 10^{-6} certainly will not be.

This analysis shows that the σ of the fabrication method sets the type of device fabrication that it can be used for. The femtosecond-laser technique with laser-induced diffusion is fine for aligning NV with micrometer-scale optical features like waveguides and could even be used to make arrays of NVs for certain types of sensors (where aggregate signal collection is desired), but this method cannot fabricate multiple qubits with nanometer-scale positional precision that are capable of controlled quantum interactions needed for quantum computing.

Finally, this analysis shows the potential for improvement that a given fabrication process can have, even before transitioning from academia to industry. The progression of three methods using femtosecond-laser pulses shows many orders of magnitude improvement in estimated yield. Industry development of this method could increase these yields further, for example, by optimizing laser-induced diffusion or substrate parameters and automating certain steps. Publication of yield and precision outcomes from various fabrication approaches also contributes to our understanding of how realistic certain goals are with respect to quantum computing. Yields like 0.36 and 0.28 for 25 physical qubits as shown on this chart are not nearly sufficient to produce the large numbers of logical qubits (each of which contains 1000–100,000 physical qubits, depending on physical qubit quality, as explained earlier) required for useful quantum computing.

NV Arrays and Manufacturing Precision: Sensing vs. Computing

Sensing

- Goal: form as many NV as possible in the ROI (the “address”) without permitting NV interaction
  - Annealing-based approaches acceptable
  - Control NV density through substrate N level
- Manage uncertainty in fabrication outcome via post-fabrication calibration

Computing

- Goal: form one or a few NV as close as possible to the center of the ROI (the “address”)
  - Annealing-based approaches can only be used with caution
  - Control NV position and density via precise femtosecond-laser methods
- Manage uncertainty in fabrication via *redundancy* and *error correction*

The same waveguide fabrication approaches may be used in either case!

ROI = Region of Interest

IDA 57

This chart contrasts the goals of sensing vs. computing in terms of fabrication precision for NV arrays. An understanding of permissible failure rates is needed for each application. For quantum information processing, qubits need to be formed reliably at each addressed site where they are expected to be. For quantum sensors, some number of missing qubits in the final product might be acceptable, so long as the sensor baseline signal is appropriately calibrated.

In fact, for quantum sensing applications, having individual or small numbers of qubits at each addressed position may not be the goal. Instead, the goal may be to have a high density of NV centers in the path of a waveguide that can be used to collect signal from those centers. In this context, there is an optimal density of NV that should be sought—the density that maximizes signal while preventing interaction among the NV centers. This optimal density has been estimated by Taylor et al. (2008) as being between 10^{15} and 10^{17} NV/cm^3. In other words, when the NV centers are at an average distance of 20–100 nm apart. Ensuring that NV density remains close to, but less than, this threshold, can be done through control of the initial *N* content of the diamond sample. Also, because producing many NV in one photonically addressed site is the goal here, a few adaptations of the fabrication methods outlined on the prior chart may be warranted:

- Apply the laser pulses to the full region of interest at each address.
- Adjust laser power to encourage formation of multiple vacancies in the site of interest without excessively damaging (or amorphizing) the crystal.
- Standard annealing approaches are likely acceptable because the goal is just to form as many NV as possible in the region of interest
- Calibrate the final sensitivity of the device based on the density of NV produced in the collection region for each address.

In the nomenclature of our four-variable framework, this means that the sensor application has a value of q that is really defined by the probability of forming at least some number of vacancies (rather than exactly one) at the addressed site, and the value of z is quite high.

Note that both sensing and computing can use the same waveguide-fabrication method, but the required precision on the NV placement determines which fabrication parameters are appropriate and what kinds of annealing steps may be permissible. But the femtosecond-laser fabrication method is flexible enough to be used for multiple purposes (waveguides and color center formation, for this example), and thus improving this technology will likely benefit both the sensing and computing application.

Enabling Scale-Up

IDA | 58

Now that we have discussed the case study of fabrication yield and precision, we will transition to considering issues of scale-up for fabricating arrays of quantum sensors or qubits.

Tennant's Law for Direct-Write Lithography

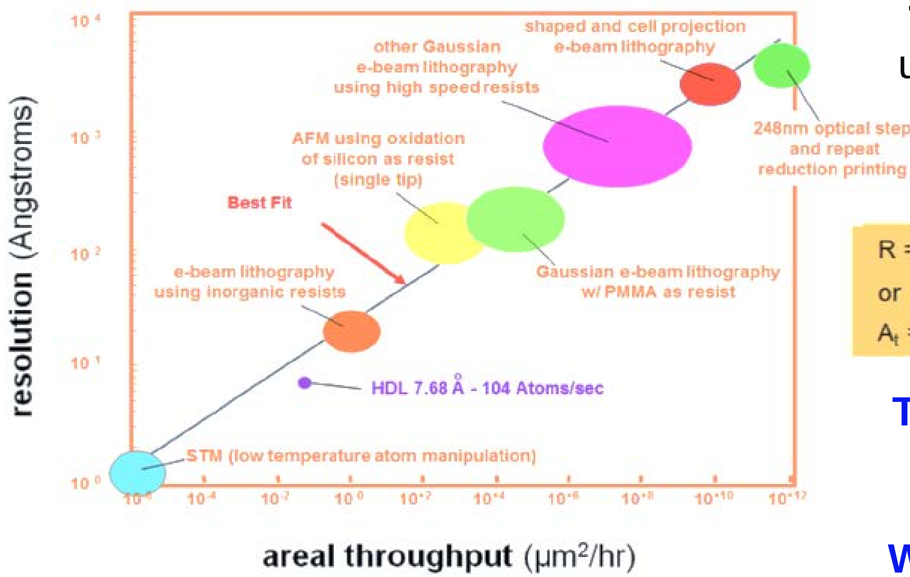

Tennant's Law: Area printed per unit time is proportional to the *fifth power* of resolution

$R = 23\ A_t^{0.2}$

or

$A_t = (R/23)^5$

Tennant's Law = Terrible scaling for mass production!

We need faster ways to fabricate dense arrays of physical qubits.

Sources:
Randall et al. (2019)
Tennant (1999)

IDA 59

An important scaling law that should be considered for direct-write applications is Tennant's law, which states that the areal throughput of a direct-write fabrication method is proportional to the fifth power of its resolution. This unfortunate scaling has been observed from direct-write lithography methods. We can make a few comments on Tennant's law as applied to the NV center array and HDL-fabricated quantum systems described in the preceding example.

First, for HDL, there is a fixed distance (13–14 nm) required for the coupled-quantum system application. This distance gives the optimal balance between allowing isolation of the qubit and enabling entanglement. The "resolution" for this type of system would really be related to how densely the addressing technology associated with each qubit can be placed on the chip while ensuring that the qubits are not destroyed by subsequent processing steps.

Alternatives to Direct-Write Methods

- Multiple-beam writing
  - Difficult engineering problem
- Mask-based lithography
  - Special methods required for ~10 nm scale resolution
  - Combined with directed assembly?
- Nanoimprint lithography
  - Gentle compared to e-beam lithography
  - Stamp must be highly reusable

Nanoimprint lithography

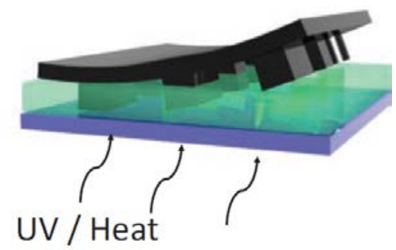

Electrophoretic Deposition

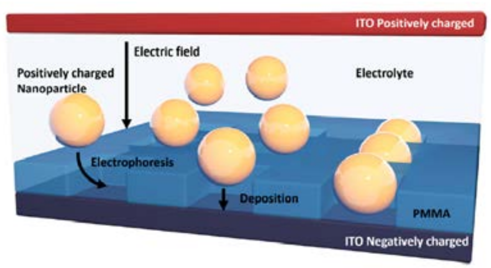

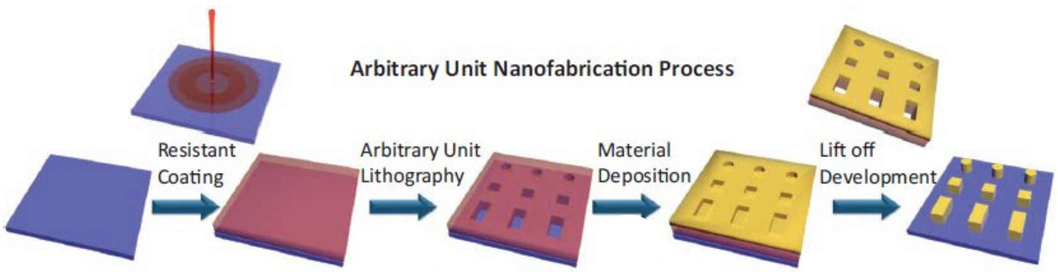

Sources:
Zhang, Kinnear, and Mulvaney (2020)
Zhang et al. (2018)

IDA | 60

There are a few possible solutions for dealing with Tennant's law: increasing the number of simultaneous write heads, using mask-based lithography instead of e-beam lithography (if resolution requirements allow), and using nanoimprint lithography with a highly reusable stamp.

Using multi-beam approaches to direct-write structures is a difficult engineering challenge, but is theoretically feasible for HDL using MEMS-based scanners (Randall et al. 2018). Issues that remain to be resolved for HDL include misalignment of tips relative to each other, drift management, developing specialized microcontrollers to manage the MEMs scanner, and tip reliability and lifetime. A repeatable and reliable scanning-probe-tip manufacturing process would be needed to enable massively parallel HDL probe fabrication.

We are not aware of efforts to develop multi-beam femtosecond-laser equipment for fabricating quantum systems, but engineering challenges for enabling that would likely be less related to precise management of positioning and drift and more related to power and thermal management and the density of scanners that could be obtained. The femtosecond-laser approach has less strict requirements on resolution relative to HDL—the target resolution is tens of nanometers or even micrometers, depending on the application, rather than nanometer-scale. We do postulate that design of dedicated manufacturing machinery may be reasonable for producing chips based on arrays of physical qubits once a reliable, valuable chip design is established through prototyping with slower fabrication methods.

Mask-based lithography has much higher areal throughput than direct-write methods of comparable resolution, but is only useful if the resolution is permissible. Depending on the photoresist, mask-based lithography can obtain resolutions of tens of nanometers using techniques such as extreme UV lithography, immersion lithography, and multiple patterning. However, these advanced-resolution methods are often associated with expensive, specialized equipment that may be unavailable to many academic researchers.

One interesting approach worth further exploration is to combine directed-assembly methods with top-down lithography (Zhang et al. 2020). In this approach, a pattern is produced on a substrate using a method such as optical lithography, and then nanocrystals are deposited in the pattern based on a self-assembly method such as electrophoretic deposition.

Electrophoretic deposition is an interesting directed self-assembly method that relies on the interaction of electric-field gradients and nanocrystals in solvents of contrasting polarizability. Nanocrystals will be either repelled from or attracted to regions of high electric field gradient (e.g., sharp corners or edges of a pattern), depending on their polarizability (not their charge) relative to the solvent. Electrophoretic deposition has been demonstrated with high yields (above 99%) and resolution on the scale of tens of nanometers, although it does require a conducting template (Zhang et al. 2020).

With the directed-self-assembly method, nanocrystals can be fabricated with high precision using solution-based methods, then deposited on a pattern, rather than needing to be grown in place (a process that is much more restrictive on the potential composition and microstructure of the nanocrystal). If the deposited nanocrystals could act as physical qubits (e.g., if they are quantum dots), or if they could catalyze the formation of a physical qubit at their attachment site (e.g., through a charge or mass-transfer process), then this method could produce highly precise arrays of qubits without using a direct-write step. This type of approach is worth exploring further, including to determine ways to integrate the arrays with photonic or CMOS structures (e.g., through post-deposition overgrowth and patterning).

Another interesting option for obtaining high resolution without relying too much on direct-write is to use nanoimprint lithography. In nanoimprint lithography, a stamp is fabricated using a very-high-fidelity method such as e-beam lithography, and then the stamp is used to pattern photoresist masks. Nanoimprint lithography has been used to produce photonic structures (Bar-On et al. 2018), and it has even been adapted to roll-to-roll fabrication (Shneidman et al. 2018) for fabricating polymer photonic structures. Nanoimprint lithography can improve the quality of fabricated structures by avoiding substrate damage that sometimes accompanies high-energy techniques such as e-beam lithography, and it also allows a single direct-write mask to be reused multiple times, which increases the effective areal throughput of the direct-write step. However, to be effective at reducing the impact of slow direct-write mask-fabrication processes, the stamp may need to be reused many times—ideally the stamp should not wear out in less than the amount of time required to fabricate a new stamp! As a reference point for scaling, it takes about 5 hours to produce a 6 cm^2 region with ~50 nm features by e-beam lithography. The same area can be produced in seconds with nanoimprint lithography once the stamp is fabricated (Zhang et al. 2020). If we assume 5 seconds per imprint, that means that this stamp would need to be reused 3600 times to prevent a bottleneck. Alternatively, if we assume that the stamp needed is 1 cm^2 in area (the current maximum area of a high-quality CVD diamond substrate is only about 0.25 cm^2), then the stamp would need to be reused 600 times to prevent a bottleneck in fabrication.

These examples provide areas for further research. For example, designing methods of fabricating arrays of color centers or quantum dots that either completely avoid direct-write steps or increase the effective speed of those direct-write steps (e.g., through nanoimprint lithography or multiplexing) would be important advances in scaling up the number of qubits that can be reliably fabricated with high precision. Approaches that are also conducive to integration with photonic structures or CMOS structures would be particularly desirable.

Rent's Rule and Quantum Computing

- **Rent's rule:** scaling of interconnections and control lines with (qu)bits
- **Quantum volume:** Quantum computing requires both a large number of qubits *N* and high circuit depth *d*
  - Today's systems are limited in one or both of these axes
- **Extensibility:** Varies for different systems
  - For example, single dopants in Si vs. trapped ions

$$T = tg^p$$

T: # of control terminals; t: # of connections required for each internal component; g: # of internal components; p: Rent exponent

$$V_q = \min(N, d)^2$$

Quantum volume—describes usefulness of quantum chip

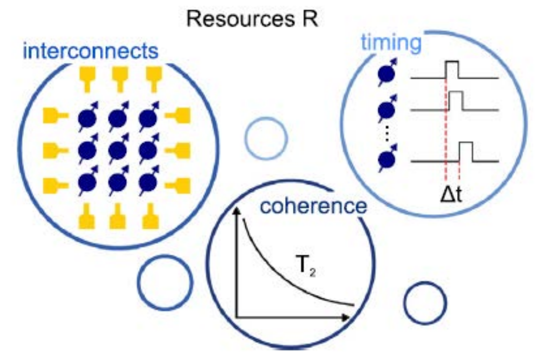

Source: Franke et al. (2019)

IDA | 61

In addition to Tennant's law, another important rule to consider in the fabrication of scaled-up quantum computers is "Rent's rule," which describes the relationship between the scaling of interconnections and control lines with the number of bits. Specifically, Rent's rule states that the total number of control terminals T scales with the number of internal components g to the power of the Rent exponent *p*, which accounts for the level of optimization of the system. Smaller values of *p* (less than 1) indicate more optimized systems.

Today, most quantum computers have linear scaling ($p = 1$). This is quite poor for scale-up, but it reduces the need for uniformity (reliability and precision) in manufacturing, which we have seen can be quite challenging for today's physical qubits. Overall, the usefulness of a quantum chip is limited by its quantum volume, which is defined by Franke et al. (2019) as the square of the minimum of the number of qubits and the "circuit depth." Circuit depth is the average number of operations that can be performed before an error will occur. Quantum computing today is limited in one of or both these axes. For example, decoherence times limit the circuit depth, while the area on a chip limits the number of qubits that can be used. Other limiting factors include available power for quantum error correction and cooling, interconnect bottlenecks, and issues with timing and delays in control lines. These concepts help us evaluate the potential of different types of qubits. For example, the single-dopant Si system can have a high density of qubits, but needs more work in terms of circuit depth. In contrast, superconducting qubits and trapped ions both have very large qubit sizes that keep *N* small. An interesting method of building circuit depth is the use of photonic links for interconnects. This option could be useful for working with color-center qubits like the NV, which can be integrated readily with photonics. This approach is being explored in the IARPA LogiQ program.

Heterogeneous Integration

- Improve system yield and reduce waste through parallel processing
- Take advantage of substrates and platforms optimized for different functions
  - Diamond for quantum memory
  - Aluminum nitride photonics
- Combine components using pick-and-place, layer lift-off and transfer, wafer bonding, etc.

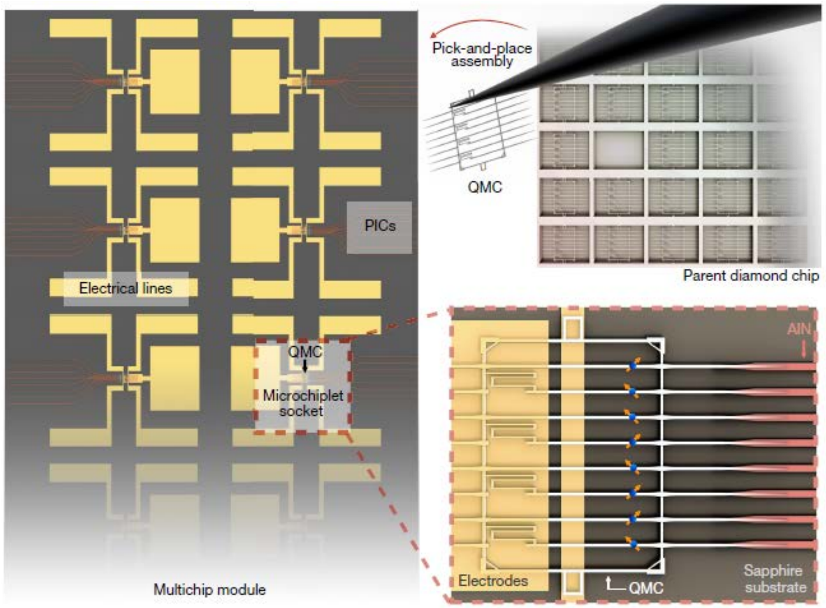

Wan et al. (2020)

Source: Elshaari et al. (2020).

Heterogeneous integration is an approach wherein components specialized for particular functions are brought together to facilitate an optimized working system. For example, in the context of quantum computing, consider a photonic chip that is integrated with a "quantum chip," such as an array of NV in diamond. Each of these components is fabricated using methods that work well for their specialized structures. The photonic chip can be fabricated using standard integrated photonics methods and substrates (e.g., aluminum nitride, silicon nitride, lithium niobate), and the quantum chip can be fabricated on a highly optimized (potentially very expensive) substrate (e.g., diamond). Then these components can be connected to form a complete system using methods like pick-and-place, wafer bonding, or layer lift-off and transfer.

Hybrid integration approaches have significant advantages for yield and waste reduction, as we saw in the case study on parallel vs. series atom chip fabrication (slides 38–39). In addition, hybrid integration builds on existing manufacturing optimization and capitalizes on the natural strengths and functions of component materials. This can improve system performance when the different components need such different and sometimes conflicting characteristics.

Examples of components that can be part of a hybrid quantum photonics system include photonic circuits (e.g., on substrates like $LiNbO_3$, aluminum nitride, or silicon nitride), quantum memory or photon sources (e.g., diamond color centers or III-V quantum dots), and single-photon detectors (e.g., superconducting nanowires). Photonic components can also be further split between substrates. For example, some substrates work better for low-loss photon transport, while others may be excellent for nonlinear or reconfigurable photonic elements (Elshaari et al. 2020).

One thing to keep in mind when reviewing potential hybrid-integration schemes is that *integrated* and *scalable* are not synonyms. Demonstrating that one component can be integrated with another type of component (e.g., CMOS electronics) can contribute to scalability, but it is not sufficient to guarantee it. For example, as we have discussed, fabrication methods that rely on direct-write steps such as e-beam lithography for every chip fabrication, or that rely on individualized error detection, correction, or adaptation that cannot be automated, are not scalable to million-qubit systems, even if the chips in question do integrate CMOS or photonic and quantum components.

Wan et al. (2020) reported one interesting example of heterogeneous integration in which aluminum nitride photonics chips and diamond-NV "quantum microchiplets" were integrated together to form up to 128-qubit systems. We explore the advantages of this "microchiplet approach" next.

Microchiplet Approach: Using Heterogeneous Integration to Solve Yield Issues

- Instead of making a large array with a high probability of at least one failed qubit fabrication attempt, make many small arrays ("microchiplets" or "tiles")
- Less wasted substrate area and time to achieve desired total number of qubits even though microchiplets use more area per qubit in the final product
- Makes sense when single-qubit yield is low—exact tipping point depends on the size of the area penalty for microchiplet qubits

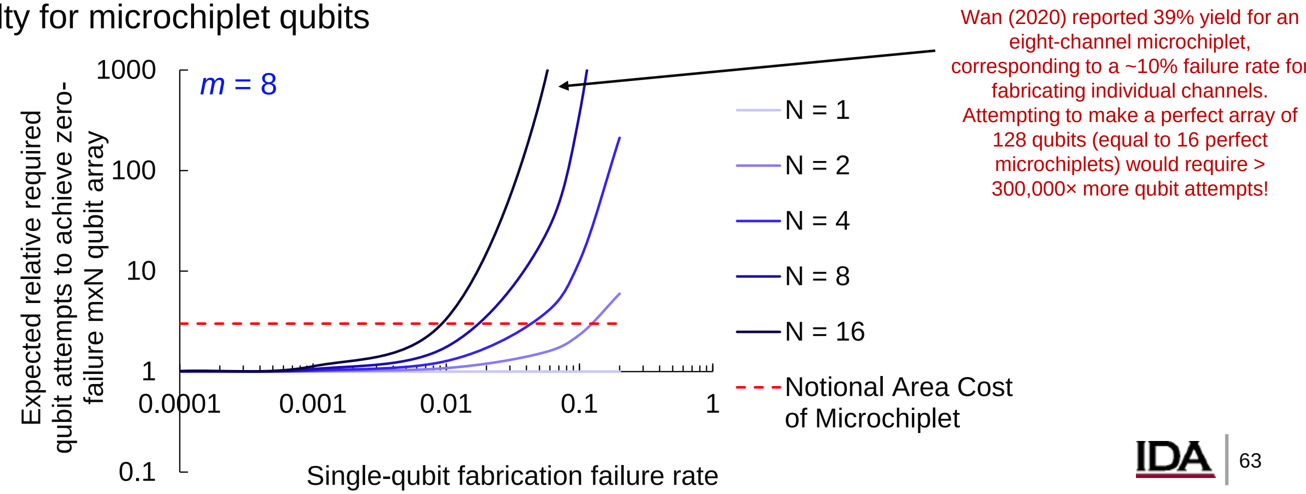

Source: Wan et al. (2020).

IDA | 63

In a "microchiplet approach," each "quantum microchiplet" contains a small number of qubits (8 or 16 in Wan et al. 2020), and the total large number of qubits is obtained by attaching many microchiplets to a prefabricated substrate that may contain electronic or photonic elements. Another way to think about this method is that the microchiplets are tiles in a mosaic that makes up the full quantum computing system. By using a microchiplet approach, the authors introduce some fault tolerance into their system fabrication, because they can choose to use only the microchiplets (tiles) that have all 8 or 16 desired color centers, rather than requiring fabrication of a single chip with no qubit fabrication failures in 128 attempts.

The drawback of the microchiplet approach is that it typically involves substantially more substrate area per qubit in the final product, because of the unused area at the edges of each microchiplet. But as shown in the chart, microchiplet methods can save significant resources (particularly, expensive substrates) when the ability to form perfect large arrays is limited by poor single-qubit yield. There is also the question of interconnecting the microchiplets at the signal level to achieve the necessary degree of functionality from the device.

The plot on this chart shows the ratio of the expected number of qubit attempts needed to achieve a perfect $8 \times N$ qubit array vs. the expected number of qubit attempts needed to obtain N perfect 8-qubit microchiplets as a function of the single-qubit fabrication failure rate. As shown in the chart, even if the area required per qubit in a microchiplet is much greater than the area/qubit in a larger array (represented by the red dashed line), the overall loss of materials and time is much less for the microchiplet approach for even modest numbers of total qubits (e.g., 32 or more), especially for today's typical single-qubit fabrication failure rates, which are rarely better than 1%, and worse than 10% for some approaches.

Indeed, in the Wan et al. (2020) example, the single-qubit fabrication failure rate appears to have been near 10%, because the reported eight-channel microchiplet yield was 39% (meaning they had at least one failure in 61% of their eight-channel microchiplets). If Wan et al. had attempted to fabricate a perfect 128-qubit array with their method, they would be expected to need 300,000 times as many qubit attempts than they in fact made. (With a 39% 8-qubit fabrication failure rate as reported in Wan et al.'s paper, and requiring 16 successful 8-qubit microchiplets per 128-qubit array, we calculate that 41 microchiplets were attempted, corresponding to 328 qubit attempts, to produce the 128-qubit system).

This analysis illustrates the value of the microchiplet approach. It also produces fairly straightforward scaling; that is, using the yields reported by Wan et al. (2020), this approach requires 1 / 0.39 = 2.56 as many qubit attempts as qubits that will appear in the final array.

High-Temperature Superconducting Nanowire Single Photon Detectors (SNSPDs)

- Many quantum-computing and quantum-sensing schemes need single-photon detectors
- SNSPDs are fast and have excellent quantum efficiency
- Integrating cryogenic and RT circuits is difficult
- Why not use high-temperature superconductors?
  - Usually ceramics: can be brittle and difficult to fabricate as wires. Also, composition stability can be a problem.
  - Some solutions: pulsed laser deposition, capping layers, selective epitaxy…

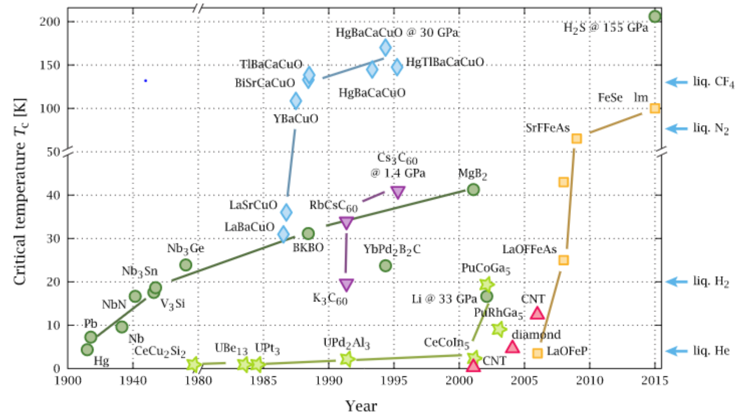

Superconductor Critical Temperatures. By P. J. Ray, own work, CC BY-SA 4.0, https://commons.wikimedia.org/w/index.php?curid=46193149.

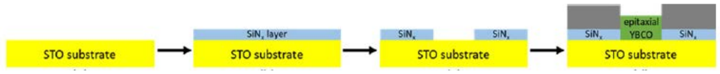

Xing et al. (2020).

Need: Research on HT-SNSPDs on quantum- and photonic-relevant structures.

Source: Elshaari et al. (2020).

IDA 64

One item that is also relevant to hybrid quantum systems is that of high-temperature superconducting nanowire single photon detectors (SNSPDs). Many quantum computing and quantum sensing schemes rely on single photon detectors. These are essential components for photonic supercomputing. The preferred type of single photon detector is the SNSPD, because it is fast and has excellent quantum efficiency. Unfortunately, metallic SNSPDs typically need to operate at cryogenic temperatures (millikelvins to a few kelvins). Cryogenic operation is expensive and takes up a lot of space, weight, and power. Also, the best electronic systems are optimized to work closer to room temperature, and integrating cryogenic and room-temperature circuits can be quite challenging (Elshaari et al. 2020). Therefore, a potential research goal to help enable higher temperature quantum sensing and computing, allowing us to take advantage of optimized microelectronics, is to try to raise the operating temperature of SNSPDs.

One possible option is to use high-temperature superconductors. For example, YBCO, which has a critical temperature of 85 K, has been used in some demonstrations to fabricate an SNSPD. Some of the challenges associated with high-temperature SNSPDs include their construction—they are typically composed of ceramic materials that can be very difficult to fabricate in nanowire form. Ceramics tend to be brittle, the precise composition of these materials can be difficult to obtain at very small (nanometer) scales, and follow-on fabrication steps (such as overgrowth) can further degrade their compositional stability. However, some research success has been demonstrated, for example, by using pulsed laser deposition with selective epitaxy to create the initial structure (pulsed laser deposition has excellent compositional tuning) or by using capping layers (Xing et al. 2020). We believe that further research into fabrication of HT-SNSPDs on quantum- and photonic-relevant structures (e.g., diamond, silicon nitride, aluminum nitride, $LiNBO_3$) would be of significant value and could be an important step in producing room-temperature quantum sensing and information processing systems.

Other General Factors to Consider for Yield Modeling

- Tendency of defects to cluster (defect distribution)
- Critical area—area where defects will produce die failure vs. area where defects don't matter to chip function
- Whether different processing steps and associated defects have the same critical areas and defect distributions
- Number of layers/processing steps
- Variation of processing steps, covariance of wafer and die quality

Reporting these factors assists evaluation of:
(a) Opportunities to improve fabrication methods
(b) Fault tolerance for mass production of component designs

Source: Kumar et al. (2006).

IDA 65

There are a number of additional factors that contribute to yield modeling that we did not explore in depth in this report. For example, yield modeling often includes a consideration of the distribution of likely defects and the relationship of that distribution to what are called "critical areas" on the chip design. Particles of dust may or may not disrupt the final circuit, depending on where they land. Some defects may only matter if they occur during certain manufacturing steps. In addition to this information, yield modeling often makes use of information about the number of layers or processing steps in the design, the variation of the outcomes of those steps, and the covariance of variables like wafer and die quality (e.g., wafer quality may refer to the purity of the substrate). We did not explore these details in depth in this report, but they are important to report in literature. For example, understanding where defects occur in fabrication processes helps target process improvements, while understanding which types of defects a component is susceptible to helps inform the potential for scale-up of that component. We would like to see more consideration and reporting of this type of information in literature on methods of fabricating integrated and monolithic quantum systems.

Outlook

IDA | 66

Fixed vs. Throughput Costs

$$\text{Spending} = C_{eq} + n_w c_w$$

Total spending is the cost of the equipment (fixed cost) + the cost per wafer manufactured * the number of wafers manufactured

$$\text{Throughput} = n_w Y_w d Y_d$$

Total throughput is the product of the number of wafers successfully manufactured (wafer yield * number of wafers attempted) and the number of successful devices (or chips) per wafer (device yield * devices/wafer).

$$c_d = \frac{\text{Spending}}{\text{Throughput}} = \frac{1}{Y_w d Y_d}\left(c_w + \frac{C_{eq}}{n_w}\right)$$

Cost per device decreases as more devices are produced (economies of scale)—as long as demand keeps up.

Demand limits throughput, which limits the permissible cost of equipment—quantum systems need reliable manufacturing methods with low fixed cost and high yield at relatively low throughput.

IDA | 67

Consider the role of throughput in the overall cost of manufacturing an integrated circuit. The reason that Si-based integrated circuits are so inexpensive is not actually that the manufacturing processes themselves are inherently inexpensive, it is because Si manufacturing has been engineered to produce devices with such high throughput and there is demand for that high volume of products (Baehr-Jones et al. 2012). Integrated circuit manufacturing relies on this economy of scale to keep the cost of individual chips low. Most of the cost for state-of-the-art semiconductor production is depreciation of the fabrication equipment (Armbruster et al. 2019).

This problem is easily understood in the framework of fixed and throughput costs. The amount of money spent by a company can be broken into two parts: fixed costs and costs incurred per manufactured unit. Fixed costs include items like manufacturing facilities, research and development, equipment, and acquiring patents on intellectual property, while throughput costs include items like materials, labor, and energy use. As more units are produced using fixed-cost equipment, the effective cost per unit decreases (until equipment depreciates and reduces yield or quality). Yield also plays an important role here, because throughput suffers when yields go down. So it may not be worth it to switch to a process that increases the density of devices if squeezing more devices into the wafer decreases the overall device yield (because the attempt at higher resolution reduces processing reliability). Also, if production outstrips demand, the effective cost per device will also increase because of unsold units.

The sweet spot, then, for quantum sensing and eventually quantum information processing is high-reliability manufacturing that has very low fixed costs and that achieves high yields at relatively low throughput. Manufacturing throughput is not as important for quantum systems, because the demand is absent. Therefore, manufacturers of quantum systems should try to capitalize on less expensive manufacturing methods or equipment that can be used for multiple purposes. This is one of the reasons that femtosecond-laser-based fabrication is so attractive—this equipment can be used to produce photonics as well as induce color centers in diamond, without the need for a clean room. Methods like this with potential multifunctional value should be developed further for their application to quantum systems. Similarly, relying on heterogeneous integration will be an important strategy for manufacturing quantum information processing systems. Because demand for these devices is likely to remain limited, the key to lowering their cost will be to capitalize on those technologies that have been developed and optimized for each component of the system, rather than seeking a specialized monolithic approach.

Creating the kind of demand that exists today for integrated circuits for quantum computing chips would first require the existence of devices that can connect a huge number of qubits into a reasonable packaging. Finding ways to decrease the cost and scale of packaging and interconnects for these devices will be an important investment in enabling this technology. Even so, it will be some time before throughput costs can reasonably be expected to dominate the cost of manufacturing quantum information processors.

References

Baehr-Jones et al. (2012).

Armbruster et al. (2019).

Opportunities for Further research

- Advanced processing with non-Si substrates
  - Epitaxy, highly anisotropic etching, lithography, planarization, 3D structure fabrication
  - Chemically and isotopically pure substrates (e.g., diamond, SiC) with increased area
- In-line measurement/testing/monitoring of photonic and quantum circuits and elements
- Tools for heterogeneous integration
  - Lift-off and layer transfer (e.g., with 2-D material-assisted or geometrically defined epitaxy)
  - Wafer bonding, alignment, and interconnection
  - High-temperature superconducting single-photon detectors
- Decreased reliance on direct-write approaches
  - Nanoimprint lithography with highly reusable stamps
  - Directed assembly with projection lithography
- Fabrication approaches with multifunctional potential (e.g., femtosecond laser)
- Increase reporting of manufacturing-relevant parameters in literature
  - Speed, yield, quality
  - Distribution of defects, types of defects
  - Critical areas for defects in device design

This slide summarizes some of the areas for further research for quantum sensors and information processors. First, to enable quantum sensors such as atom chips and NV-based gyroscopes, more research is needed on fabrication methods using the substrates relevant to these types of systems. In particular, substrates of interest include those that can directly host color centers (e.g., diamond, silicon carbide) or other types of qubits and substrates useful for linear and nonlinear photonic elements (e.g., $LiNbO_3$, aluminum nitride, silicon nitride). The types of processing that are needed include advanced methods of film growth (especially epitaxy), anisotropic etching, lithography, planarization, and 3D structure fabrication (e.g., with femtosecond-laser approaches). In the area of film growth, work is needed to allow stable, small scale, repeatable manufacturing of unusual materials (such as ferroelectrics for magneto-optical traps or high-temperature superconducting materials for photon detection) on these substrates. Highly anisotropic etching is useful not only for atom chips (e.g., to facilitate vias, interconnects, and vacuum chambers) but also for producing precisely patterned traps for quantum elements placed through directed-assembly methods.

Also, the substrates that will be hosting sensitive quantum systems (e.g., color centers) need to be engineered to be produced at larger scale with high chemical and isotopic purity. In the case of diamond specifically, the goal is increased area, low strain, high-quality surfaces, low ^{13}C concentration (although that can be managed through signal-processing strategies), and composition biased toward high NV- yield relative to NV concentration. Some potential strategies to lower the cost of diamond components include lift-off and layer transfer, geometrically defined epitaxy, and 2D material-assisted epitaxy.

Another important area for further research is in-line measurement, testing, and monitoring of photonic and quantum circuits and elements. We need automated ways to test details, such as:

- How many color centers, if any, have been produced at the desired location?
- What are the characteristic frequencies of those color centers?
- What are the electro-optic noise figures and nonlinearities in this photonic component?

In addition, quantum sensors and quantum information systems will need to take advantage of heterogeneous integration. Quantum sensors need to include miniaturized vacuum and laser components that can be readily connected to the actual sensing component. Potential strategies include lift-off and layer-transfer methods (for example, using 2D material-assisted or geometrically defined epitaxy and automated pick and place), wafer-bonding and alignment methods, and developing higher temperature superconducting single photon detectors on relevant substrates.

We would like to see the research community try to move away from relying on direct-write approaches to fabricating quantum sensors and information processors. We would like to see greater exploration of tools like nanoimprint lithography and directed assembly to facilitate precise, reliable placement of quantum dots, color centers, or other types of qubits in predetermined locations. Hydrogen depassivation lithography may see improvements through approaches like multiplexing, but opportunities to facilitate similar nanometer-scale precision with a reusable mask (e.g., a nanoimprint lithography stamp) would be of significant interest. Some ways to increase the reusability of nanoimprint lithography stamps include etching and patterning of stiff, hard materials (e.g., diamond) and coating with appropriate anti-stick, non-contaminating materials.

Furthermore, fabrication approaches that have the potential for multifunctionality (e.g., femtosecond-laser waveguide and color center fabrication) are deserving of further investment. These tools not only have the potential to allow multiple manufacturing steps to be done in the same system; they also allow quantum sensor manufacturing to capitalize on manufacturing improvements driven by demand for other products, such as integrated photonics.

Finally, we would like to see increased reporting in academic literature of parameters of importance for understanding the scale-up potential of fabrication methods. These include figures on speed, yield, and final quality of manufactured devices. Similarly, information about the distribution of defects caused by novel fabrication approaches, the types of defects encountered, and their potential impact on the success of the manufactured device is of interest.

Thoughts on Road-mapping

- Improved etching / patterning / implantation / growth / deposition / substrate purification / lift off / layer transfer / bonding / alignment methods for alternative substrates may be developed for sensors
- The first goal is just to make the devices, not necessarily inexpensively or at large scale
- The next goal is to make them densely, with addressable features—this is more of a quantum-computing goal
- Fabrication of quantum-computing systems will likely take advantage of the manufacturing advances from quantum sensing and work on the scale-up problem

IDA | 69

Finally, we close with some thoughts on road-mapping as applied to solid-state quantum technologies. Our analysis has seen that many of the fabrication tools and substrates of interest for quantum sensors will also be of interest for quantum computing. Therefore, improvements in the processing of those substrates or the application of those tools that may be developed for sensors can be adopted for information processors. The approach to improved manufacturing is expected to proceed in a few stages. First, determine how to make a given device. Then figure out how to make that device more compact, lower cost, and with higher precision. Devices made in proximity or at high density will be more relevant to quantum computing. Therefore, although large-scale quantum computing is still far from being realized, many of the manufacturing advances being made today can be expected to be of value to that technology later.

References

Achard, J., V. Jacques, and A. Tallaire. 2020. "Chemical Vapour Deposition Diamond Single Crystals with Nitrogen-Vacancy Centres: A Review of Material Synthesis and Technology for Quantum Sensing Applications." *Journal of Physics D: Applied Physics* 53, no. 31: 313001.

Acosta, Victor Marcel. 2011. "Optical Magnetometry with Nitrogen-Vacancy Centers in Diamond." PhD diss., UC Berkeley.

Acosta, Victor, and Philip Hemmer. 2013. "Nitrogen-Vacancy Centers: Physics and Applications." *MRS Bulletin* 38, no. 2: 127–30.

Ajoy, Ashok, and Paola Cappellaro. 2012. "Stable Three-Axis Nuclear-Spin Gyroscope in Diamond." *Physical Review A* 86, no. 6: 062104.

Armbruster, Alexander A., J. W. Bailey, G. R. Bliss, M. Breen, A. DiAngelo, M. L. Dominguez, T. P. Frazier, et al. 2019. "Analysis of Options to Enhance Domestic Microelectronics Manufacturing" IDA Document D-10591. Alexandria, VA: Institute for Defense Analyses.

Arute, Frank, Kunal Arya, Ryan Babbush, Dave Bacon, Joseph C. Bardin, Rami Barends, Rupak Biswas et al. 2019. "Quantum Supremacy Using a Programmable Superconducting Processor." *Nature* 574, no. 7779: 505–10.

Awschalom, David D., Ronald Hanson, Jörg Wrachtrup, and Brian B. Zhou. 2018. "Quantum Technologies with Optically Interfaced Solid-State Spins." *Nature Photonics* 12, no. 9: 516–27.

Baehr-Jones, Tom, Thierry Pinguet, Patrick Lo Guo-Qiang, Steven Danziger, Dennis Prather, and Michael Hochberg. 2012. "Myths and Rumours of Silicon Photonics." *Nature Photonics* 6, no. 4: 206–8.

Bar-On, O., P. Brenner, T. Siegle, R. Gvishi, H. Kalt, U. Lemmer and J. Sheuer. 2018. "High Quality 3D Photonics using Nano Imprint Lithography of Fast Sol-gel Materials." *Sci Rep* 8, 7833 (2018). https://doi.org/10.1038/s41598-018-26261-3.

Barry, John F., Jennifer M. Schloss, Erik Bauch, Matthew J. Turner, Connor A. Hart, Linh M. Pham, and Ronald L. Walsworth. 2020. "Sensitivity Optimization for NV-diamond Magnetometry." *Reviews of Modern Physics* 92, no. 1: 015004.

Bharadwaj, Vibhav, Ottavia Jedrkiewicz, J. P. Hadden, Belén Sotillo, María Ramos Vázquez, Paola Dentella, Toney T. Fernandez et al. 2019. “Femtosecond Laser Written Photonic and Microfluidic Circuits in Diamond.” *Journal of Physics: Photonics* 1, no. 2: 022001.

Blatt, Rainer, and David Wineland. 2008. “Entangled States of Trapped Atomic Ions.” *Nature* 453, no. 7198: 1008–15.

Broome, M. A., S. K. Gorman, M. G. House, S. J. Hile, J. G. Keizer, D. Keith, C. D. Hill et al. 2018. “Two-Electron Spin Correlations in Precision Placed Donors in Silicon.” *Nature Communications* 9, no. 1: 1–7.

Chatterjee, Anasua, Paul Stevenson, Silvano De Franceschi, Andrea Morello, Nathalie de Leon, and Ferdinand Kuemmeth. 2020. “Semiconductor Qubits in Practice.” *arXiv preprint arXiv:2005.06564*.

Chen, Yun-Jhih, Azure Hansen, Gregory W. Hoth, Eugene Ivanov, Bruno Pelle, John Kitching, and Elizabeth A. Donley. 2018. “Multi-axis Atom Interferometer Gyroscope with a Single Source of Atoms.” *arXiv preprint arXiv:1812.00106*.

Childress, Lilian, and Ronald Hanson. 2013. “Diamond NV Centers for Quantum Computing and Quantum Networks.” *MRS Bulletin* 38, no. 2: 134–38.

Childs, Andrew M., and Wim Van Dam. 2010. “Quantum Algorithms for Algebraic Problems.” *Reviews of Modern Physics* 82, no. 1: 1. https://doi.org/10.1103/RevModPhys.82.1.

Chuang, Ho-Chiao, Hsiang-Fu Li, Yun-Siang Lin, Yu-Hsin Lin, and Chi-Sheng Huang. 2013. “The Development of an Atom Chip with through Silicon Vias for an Ultra-high-vacuum Cell.” *Journal of Micromechanics and Microengineering* 23, no. 8: 085004.

Clarke, John, and Frank K. Wilhelm. 2008. “Superconducting Quantum Bits.” *Nature* 453, no. 7198: 1031–42.

Degen, Christian L., F. Reinhard, and Paola Cappellaro. 2017. “Quantum Sensing.” *Reviews of Modern Physics* 89, no. 3: 035002.

Durfee, D. S., Y. K. Shaham, and M. A. Kasevich. 2006. “Long-Term Stability of an Area-Reversible Atom-Interferometer Sagnac Gyroscope.” *Physical Review Letters* 97, no. 24: 240801.

DSB. “Applications of Quantum Technologies: Executive Summary.” 2019. Office of the Under Secretary of Defense for Research and Engineering, Defense Science Board, October 2019.

Dzurak, A. S., L. C. L. Hollenberg, D. N. Jamieson, F. E. Stanley, C. Yang, T. M. Buhler, V. Chan et al. 2003. “Charge-Based Silicon Quantum Computer Architectures Using Controlled Single-Ion Implantation.” *arXiv preprint cond-mat/0306265*. Harvard.

Elshaari, Ali W., Wolfram Pernice, Kartik Srinivasan, Oliver Benson, and Val Zwiller. 2020. “Hybrid Integrated Quantum Photonic Circuits.” *Nature Photonics*: 1–14.

Elster, A. D. 2020. “Relative Field Strength.” *Questions and Answers in MRI*. Elster LLC. Accessed December 4, 2020. mriquestions.com/how-strong-is-30t.html.

Fagaly, R. L. 2006. “Superconducting Quantum Interference Device Instruments and Applications.” *Review of Scientific Instruments* 77, no. 10: 101101.

Folman, Ron, Phillipp Treutlein, and Jörg Schmiedmayer, *Atom Chip Fabrication*, 2010. In *Atom Chips*, edited by J. Reichel and V. Vuletić, Chapter 3. Wiley-VCH, Weinheim.

Franke, David P., James S. Clarke, Lieven MK Vandersypen, and Menno Veldhorst. 2019. “Rent’s Rule and Extensibility in Quantum Computing.” *Microprocessors and Microsystems* 67:1–7.

Garrido-Alzar, Carlos L. 2019. “Compact Chip-Scale Guided Cold Atom Gyrometers for Inertial Navigation: Enabling Technologies and Design Study.” *AVS Quantum Science* 1, no. 1: 014702.

Gustavson. 2000. “Precision Rotation Sensing Using Atom Interferometry.” PhD diss., Stanford University.

Gustavson, T. L., A. Landragin, and M. A. Kasevich. 2000. “Rotation Sensing with a Dual Atom-Interferometer Sagnac Gyroscope.” *Classical and Quantum Gravity* 17, no. 12: 2385.

Hadden, J. P., V. Bharadwaj, B. Sotillo, S. Rampini, R. Osellame, J. D. Witmer, H. Jayakumar et al. 2018. “Integrated Waveguides and Deterministically Positioned Nitrogen Vacancy Centers in Diamond Created by Femtosecond Laser Writing.” *Optics Letters* 43, no. 15: 3586–89.

Haque, Ariful, and Sharaf Sumaiya. 2017. “An Overview on the Formation and Processing of Nitrogen-Vacancy Photonic Centers in Diamond by Ion Implantation.” *Journal of Manufacturing and Materials Processing* 1, no. 1: 6.

Honeywell. 2020. GG1302AN. https://aerospace.honeywell.com/en/learn/products/sensors/gg1320an-digital-ring-laser-gyroscope.

Intel Newsroom. 2018. “2018 CES: Intel Advances Quantum and Neuromorphic Computing Research. January 8, 2018. https://newsroom.intel.com/news/intel-advances-quantum-neuromorphic-computing-research/.

Joneckis, Lance G., Steven Waruhiu, John C. Biddle, Olivia S. Sun, and Leonard J. Buckley. 2019. “Overview of the Status of Quantum Science and Technology and Recommendations for the DoD.” IDA Document D-10709. Alexandria: VA: Institute for Defense Analyses.

Keil, Mark, Omer Amit, Shuyu Zhou, David Groswasser, Yonathan Japha, and Ron Folman. 2016. “Fifteen Years of Cold Matter on the Atom Chip: Promise, Realizations, and Prospects.” *Journal of modern optics* 63, no. 18: 1840–85.

Kitching, John. 2018. “Chip-Scale Atomic Devices.” *Applied Physics Reviews* 5, no. 3: 031302.

Korkishko, Yu N., V. A. Fedorov, V. E. Prilutskiy, V. G. Ponomarev, I. V. Fedorov, S. M. Kostritskii, I. V. Morev et al. 2018. “High-Precision Inertial Measurement Unit IMU-5000.” In *2018 IEEE International Symposium on Inertial Sensors and Systems* (*INERTIAL*), 1–4.

Kumar, N., K. Kennedy, K. Gildersleeve, R. Abelson, C. M. Mastrangelo, and D. C. Montgomery. 2006. “A Review of Yield Modelling Techniques for Semiconductor Manufacturing.” *International Journal of Production Research* 44, no. 23: 5019–36.

Ladd, Thaddeus D., Fedor Jelezko, Raymond Laflamme, Yasunobu Nakamura, Christopher Monroe, and Jeremy Lloyd OâBrien. 2010. “Quantum Computers.” *Nature* 464, no. 7285: 45. https://doi.org/10.1038/nature08812.

Le Sage, D., L. M. Pham, N. Bar-Gill, C. Belthangady, M. D. Lukin, A. Yacoby, and R. L. Walsworth. 2012. *Phys. Rev. B* 85, 121202(R).

Liu et al. 2015. “The Fabrication and Characterization of Nano-SQUIDs Based on Nb Thin Films,” *Physica C* 515:36–40.

Menéndez, Ramón José Pérez. 2019. “IFOG and IORG Gyros: A Study of Comparative Performance.” In *Gyroscopes-Principles and Applications*. IntechOpen.

Montanaro, Ashley. 2016. “Quantum Algorithms: An Overview.” *NPJ Quantum Information* 2: 15023. https://doi.org/10.1038/npjqi.2015.23.

Napolitano, Fabien. 2010. “Fiber-Optic Gyroscopes Key Technological Advantages,” 1-8.

National Academies of Sciences, Engineering, and Medicine. 2019. *Quantum Computing: Progress and Prospects*. Washington, DC: The National Academies Press. https://doi.org/10.17226/25196.

Nielsen, Michael A., and Isaac L. Chuang. 2010. “Quantum Computation and Quantum Information.” In *Quantum Computation and Quantum Information*, edited by Michael A. Nielsen, Isaac L. Chuang. Cambridge, UK: Cambridge University Press. https://doi.org/10.1017/CBO9780511976667.

Noor, Radwan M., and Andrei M. Shkel. 2018. “MEMS Components for NMR Atomic Sensors.” *Journal of Microelectromechanical Systems* 27, no. 6: 1148–59.

NREL. 2020. “Best Research Cell Efficiency Chart.” National Renewable Energy Research Laboratory. Accessed November 10, 2020. https://www.nrel.gov/pv/cell-efficiency.html.

O'brien, Jeremy L., Akira Furusawa, and Jelena Vučković. 2009. "Photonic Quantum Technologies." *Nature Photonics* 3, no. 12: 687–95.

Orwa, J. O., K. Ganesan, J. Newnham, C. Santori, P. Barclay, K. M. C. Fu, R. G. Beausoleil et al. 2012. "An Upper Limit on the Lateral Vacancy Diffusion Length in Diamond." *Diamond and Related Materials* 24: 6–10.

Photovoltaics Report. Fraunhofer Institute for Solar Energy Systems, ISE, June 23, 2020.

Passaro, Vittorio, Antonello Cuccovillo, Lorenzo Vaiani, Martino De Carlo, and Carlo Edoardo Campanella. 2017. "Gyroscope Technology and Applications: A Review in the Industrial Perspective." *Sensors* 17, no. 10: 2284.

Paturel, Y., J. Honthaas, H. Lefèvre, and F. Napolitano. 2014. "One Nautical Mile Per Month FOG-based Strapdown Inertial Navigation System: A Dream Already within Reach?" *Gyroscopy and Navigation* 5, no. 1: 1–8.

Preskill, John. 2018. "Quantum Computing in the NISQ Era and Beyond." *Quantum* 2:79. https://doi.org/10.22331/q-2018-08-06-79.

Qiang, Xiaogang, Xiaoqi Zhou, Jianwei Wang, Callum M. Wilkes, Thomas Loke, Sean O'Gara, Laurent Kling et al. 2018. "Large-Scale Silicon Quantum Photonics Implementing Arbitrary Two-Qubit Processing." *Nature Photonics* 12, no. 9: 534–39.

Ragg, Simon, Chiara Decaroli, Thomas Lutz, and Jonathan P. Home. 2019. "Segmented Ion-Trap Fabrication Using High Precision Stacked Wafers." *Review of Scientific Instruments* 90, no. 10: 103203.

Randall, John N., James HG Owen, Joseph Lake, Rahul Saini, Ehud Fuchs, Mohammad Mahdavi, SO Reza Moheimani, and Benjamin Carrion Schaefer. 2018. "Highly Parallel Scanning Tunneling Microscope Based Hydrogen Depassivation Lithography." *Journal of Vacuum Science & Technology B, Nanotechnology and Microelectronics: Materials, Processing, Measurement, and Phenomena* 36, no. 6: 06JL05.

Randall, John N., James HG Owen, Joseph Lake, and Ehud Fuchs. 2019. "Next Generation of Extreme-Resolution Electron Beam Lithography." *Journal of Vacuum Science & Technology B, Nanotechnology and Microelectronics: Materials, Processing, Measurement, and Phenomena* 37, no. 6: 061605.

Randall, J. N., J. H. G. Owen, E. Fuchs, R. Saini, R. Santini, and S. O. R. Moheimani. 2020. "Atomically Precise Digital e-Beam Lithography." In *Novel Patterning Technologies for Semiconductors, MEMS/NEMS and MOEMS 2020* 11324:113240X. International Society for Optics and Photonics.

Robbes, D. 2006. "Highly Sensitive Magnetometers," *Sensors and Actuators A* 129:86–93.

Romaszko, Zak David, Seokjun Hong, Martin Siegele, Reuben Kahan Puddy, Foni Raphaël Lebrun-Gallagher, Sebastian Weidt, and Winfried Karl Hensinger. 2020. "Engineering of Microfabricated Ion Traps and Integration of Advanced on-Chip Features." *Nature Reviews Physics*: 1–15.

Rudolph, Terry. 2017. "Why I Am Optimistic about the Silicon-Photonic Route to Quantum Computing." *APL Photonics* 2, no. 3: 030901.

Schmelz, Matthias, and Ronny Stolz. 2017. "Superconducting Quantum Interference Device (SQUID) Magnetometers." In *High Sensitivity Magnetometers*, 279–311. Springer, Cham.

Schwindt, Peter D. D., Brad Lindseth, Svenja Knappe, Vishal Shah, John Kitching, and Li-Anne Liew. 2007. "Chip-Scale Atomic Magnetometer with Improved Sensitivity by Use of the M x Technique." *Applied physics letters* 90, no. 8: 081102.

Shneidman, Anna V., Kaitlyn P. Becker, Michael A. Lukas, Nicholas Torgerson, Cheng Wang, Orad Reshef, Michael J. Burek, Kateri Paul, Joseph McLellan, and Marko Lončar. 2018. "All-Polymer Integrated Optical Resonators by Roll-to-Roll Nanoimprint Lithography." *Acs Photonics* 5, no. 5: 1839–45.

Sipahigil, Alp, Ruffin E. Evans, Denis D. Sukachev, Michael J. Burek, Johannes Borregaard, Mihir K. Bhaskar, Christian T. Nguyen et al. 2016. "An Integrated Diamond Nanophotonics Platform for Quantum-Optical Networks." *Science* 354, no. 6314: 847–50.

Taylor, J. M., Paola Cappellaro, L. Childress, Liang Jiang, Dmitry Budker, P. R. Hemmer, Amir Yacoby, R. Walsworth, and M. D. Lukin. 2008. "High-Sensitivity Diamond Magnetometer with Nanoscale Resolution." *Nature Physics* 4, no. 10: 810–16.

Tennant, Donald M. "Limits of Conventional Lithography." 1999. In *Nanotechnology*, 161–205. Springer, New York, NY.

Van Toan, Nguyen, Naoki Inomata, Nguyen Huu Trung, and Takahito Ono. 2018. "Knudsen Pump Produced via Silicon Deep RIE, Thermal Oxidation, and Anodic Bonding Processes for on-Chip Vacuum Pumping." *Journal of Micromechanics and Microengineering* 28, no. 5: 055001.

Veldhorst, Menno, C. H. Yang, J. C. C. Hwang, W. Huang, J. P. Dehollain, J. T. Muhonen, S. Simmons et al. 2015. "A Two-Qubit Logic Gate in Silicon." *Nature* 526, no. 7573: 410–14.

Walker, Thad G., and Michael S. Larsen.2016. "Spin-Exchange-Pumped NMR Gyros." In *Advances in Atomic, Molecular, and Optical Physics* 65:373–401. Academic Press.

Wan, N. H., T. J. Lu, K. C. Chen, M. P. Walsh, M. E. Trusheim, L. De Santis, E. A. Bersin, et al. 2020. "Large-Scale Integration of Artificial Atoms in Hybrid Photonic Circuits." *Nature* 583 (7815): 226–31.

Weis, Antoine, Georg Bison, and Zoran D. Grujić. 2017. "Magnetic Resonance Based Atomic Magnetometers." In *High Sensitivity Magnetometers*, 361–424. Springer, Cham.

Wolf, Thomas, Philipp Neumann, Kazuo Nakamura, Hitoshi Sumiya, Takeshi Ohshima, Junichi Isoya, and Jörg Wrachtrup. 2015. "Subpicotesla Diamond Magnetometry." *Physical Review X* 5, no. 4: 041001.

Wu, Rongbo, Jintian Lin, Min Wang, Zhiwei Fang, Wei Chu, Jianhao Zhang, Junxia Zhou, and Ya Cheng. 2019. "Fabrication of a Multifunctional Photonic Integrated Chip on Lithium Niobate on Insulator Using Femtosecond Laser-Assisted Chemomechanical Polish." *Optics Letters* 44, no. 19: 4698-4701.

Wyrick, Jonathan, Xiqiao Wang, Ranjit V. Kashid, Pradeep Namboodiri, Scott W. Schmucker, Joseph A. Hagmann, Keyi Liu et al. 2019. "Atom-by-Atom Fabrication of Single and Few Dopant Quantum Devices." *Advanced Functional Materials* 29, no. 52: 1903475.

Xing, X., K. Balasubramanian, S. Bouscher, O. Zohar, Y. Nitzav, A. Kanigel, and A. Hayat. 2020. "Photoresponse above 85 K of Selective Epitaxy Grown High-Tc Superconducting Microwires." *Applied Physics Letters* 117, no. 3: 032602.

Zhang, Heyou, Calum Kinnear, and Paul Mulvaney. 2020. "Fabrication of Single-Nanocrystal Arrays." *Advanced Materials* 32, no. 18: 1904551.

Zhang, Heyou, Jasper Cadusch, Calum Kinnear, Timothy James, Ann Roberts, and Paul Mulvaney. 2018. "Direct Assembly of Large Area Nanoparticle Arrays." *ACS Nano* 12, no. 8: 7529–537.

REPORT DOCUMENTATION PAGE

Form Approved
OMB No. 0704-0188

1. REPORT DATE: December 2020

2. REPORT TYPE: FINAL

3. DATES COVERED *(From–To)*

4. TITLE AND SUBTITLE

Manufacturing for Quantum Systems (Presentation)

5a. CONTRACT NUMBER: HQ0034-14-D-0001

5b. GRANT NUMBER

5c. PROGRAM ELEMENT NUMBER

6. AUTHOR(S)

Swallow, Jessica G.
Joneckis, Lance G.

5d. PROJECT NUMBER: CRP 2258

5e. TASK NUMBER

5f. WORK UNIT NUMBER

7. PERFORMING ORGANIZATION NAME(S) AND ADDRESS(ES)

Institute for Defense Analyses
Systems and Analyses Center
4850 Mark Center Drive
Alexandria, VA 22311-1882

8. PERFORMING ORGANIZATION REPORT NUMBER

IDA Document NS D-20438

9. SPONSORING / MONITORING AGENCY NAME(S) AND ADDRESS(ES)

Institute for Defense Analyses
Systems and Analyses Center
4850 Mark Center Drive
Alexandria, VA 22311-1882

10. SPONSOR/MONITOR'S ACRONYM(S)

IDA

11. SPONSOR/MONITOR'S REPORT NUMBER(S)

12. DISTRIBUTION/AVAILABILITY STATEMENT

Approved for public release; distribution is unlimited (30 March 2021).

13. SUPPLEMENTARY NOTES

14. ABSTRACT

The goals of this central research project were to (1) understand manufacturing and fabrication challenges, including for supporting technologies, limiting the performance of a few representative quantum systems of interest to DoD, (2) link manufacturing approaches to potential manufacturing yield and reliability characteristics, and (3) identify potential areas for DoD-supported research in quantum manufacturing. This work aims to identify research areas that will not only impact the manufacturability of quantum sensors today, but also increase the viability of scaled-up quantum computing in the future. Doing so helps the DoD focus resources, accelerate the development of quantum technology, and connect quantum technology to DoD applications and capabilities of interest, such as position, navigation, and timing. Because of limited resources, we focused our scope to a few representative options from a variety of possible quantum sensing and computing platforms. Specifically, we focused our analysis on atom chips, nitrogen vacancy (NV) color centers in diamond, and precisely-placed phosphorus dopants in silicon. We recommend several areas for further research, including advanced processing with non-silicon substrates, in-line measurement, monitoring, and testing tools for photonic and quantum circuits and elements, approaches to enable heterogeneous integration (e.g., lift-off and layer transfer, wafer bonding, high temperature superconducting single photon detectors), methods to decrease reliance on direct-write approaches, and adaptation of fabrication approaches with multifunctional potential. We also note the need for increased reporting of manufacturing-relevant parameters in literature, such as speed, yield, and defect types, distributions, and effects on functional structures. Advancements in manufacturing and fabrication of quantum sensors and their supporting technologies will not only advance these technologies towards commercial availability, but also support future scale-up of solid state quantum computing architectures.

15. SUBJECT TERMS

Atom Chips; Gyroscopes; Manufacturing; Materials Processing; Nitrogen Vacancy; Quantum Computing; Quantum Sensing

16. SECURITY CLASSIFICATION OF:			17. LIMITATION OF ABSTRACT	18. NUMBER OF PAGES	19a. NAME OF RESPONSIBLE PERSON
a. REPORT	b. ABSTRACT	c. THIS PAGE			Buckley, Leonard J.
Uncl.	Uncl.	Uncl.	SAR	151	19b. TELEPHONE NUMBER *(include area code)* (703) 578-2800

Standard Form 298 (Rev. 8-98)
Prescribed by ANSI Std. 39.18